Electronic Supporting Information

For

A New ONO^{3-} Trianionic Pincer Ligand with Intermediate Flexibility and its Tungsten Alkylidene and Alkylidyne Complexes

*Sudarsan VenkatRamani, Ion Ghiviriga, Khalil A. Abboud, Adam S. Veige **

Department of Chemistry, Center for Catalysis, University of Florida
P.O. Box 117200, Gainesville, FL, 32611.

veige@chem.ufl.edu

Table of Contents

Experimental Section

General Considerations

Unless specified otherwise, all manipulations were performed under an inert atmosphere using standard Schlenk or glove-box techniques. Glassware was oven dried before use. Pentane, hexane, toluene, diethyl ether (Et_2O), tetrahydrofuran (THF), benzene (C_6H_6) were dried using a GlassContours drying column and stored over 4 Å molecular sieves. Benzene-d_6 (Cambridge Isotopes) was dried over sodium-benzophenone ketyl, distilled and stored over 4 Å molecular sieves. Toluene-d_8 (Cambridge Isotopes) was dried over CaH_2; vacuum transferred and stored over 4 Å molecular sieves. THF-d_8 (Cambridge Isotopes) was used as received. (^{t}BuO)$_3$W≡C^{t}Bu[1], 2-amino-4,6-di-tert-butylphenol[2-5], 3,5-di-tert-butyl-2-hydroxybenzaldehyde[6-8], 2,4-di-tert-butyl-6-((3,5-di-tert-butyl-2-hydroxybenzylidene)amino)phenol[9-13], and $Ph_3P{=}CH_2$[14] were prepared according to published procedures. All other reagents were purchased from commercial vendors and used without further purification. ^{1}H, ^{13}C{^{1}H}, and 2D NMR spectra were obtained on an Inova 500 MHz, and ^{31}P{^{1}H} was acquired on a Varian Mercury Broad Band 300 MHz, or Varian Mercury 300 MHz. The chemical shifts are reported in δ (ppm) and were referenced to the lock signal on the TMS scale for ^{1}H and ^{13}C NMR spectra, and neat NH_3 scale for ^{15}N NMR spectra. For ^{1}H and ^{13}C{^{1}H} NMR spectra, the residual solvent peak was used as an internal reference. Elemental analyses were performed at Complete Analysis Laboratory Inc., Parsippany, New Jersey.

DFT Calculations

Geometry optimization and single point analysis of **4a** were performed using spin-restricted density functional theory calculations, using a hybrid functional B3LYP[15, 16] and LANL2DZ[17]

basis as implemented in the Gaussian 09[18] program suite. The atomic coordinates from the crystal structure was used as an initial input for the geometry optimized structures. Molecular orbital pictures were generated from Gabedit[19] at their reported isovalues.

NMR spectroscopy characterization and method

NMR spectra were obtained on a Varian Mercury spectrometer operating at 300 MHz for ^{1}H, or a Varian Inova spectrometer operating at 500 MHz for ^{1}H. The chemical shifts are reported in δ (ppm) and were referenced to the lock signal on the TMS scale for ^{1}H and ^{13}C NMR spectra, neat H_3PO_4 scale for ^{31}P NMR spectra, and neat NH_3 scale for ^{15}N NMR spectra. Compounds **1**-**6** were characterized by ^{1}H, ^{13}C, and ^{15}N NMR. The chemical shifts are presented in **Table 1**. The assignments were made primarily based on the cross-peaks observed in the ^{1}H-^{13}C *g*HMBC spectra. ^{15}N NMR shifts were based on the cross-peaks observed in the ^{1}H-^{15}N *g*HMBC spectra. All spectra were obtained in C_6D_6 at ambient temperature, unless noted otherwise.

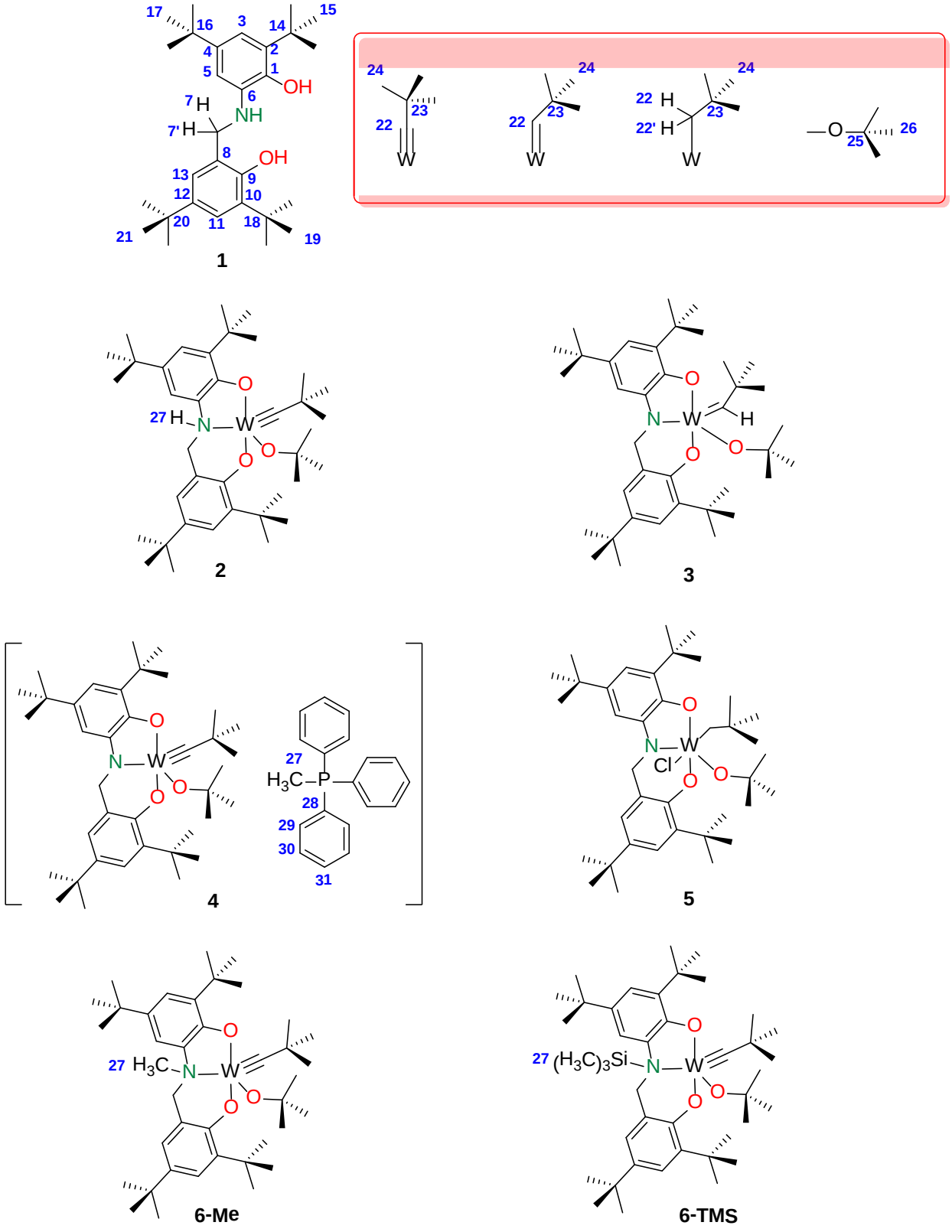

Figure S1. Labeling scheme for ^{1}H and ^{13}C NMR resonances of compounds **1** - **6**

Table S1. ^{1}H, $^{13}C\{^{1}H\}$,and ^{15}N NMR chemical shift data.

Compd.	1	2[a]	3	4[b]	5	6-Me	6-TMS
H3	7.06	7.39	7.28	6.81	6.73	7.39	7.29
H5	6.81	7.09	7.05	6.66	6.63	7.18	7.10
H7	3.87	4.97	5.45	5.36	6.61	5.48	5.49
H7'	3.87	4.78	5.06	5.03	6.27	4.77	5.25
H11	7.48	7.53	7.48	7.43	7.47	7.58	7.49
H13	6.92	7.04	7.20	7.25	7.20	7.14	7.14
H15	1.27	1.77	1.73	1.82	1.22	1.73	1.67
H17	1.38	1.37	1.43	1.44	1.24	1.31	1.32
H19	1.62	1.76	1.74	1.78	1.59	1.72	1.68
H21	1.36	1.36	1.32	1.38	1.53	1.35	1.31
H22	-	-	8.90	-	2.39	-	-
H22'	-		-	-	2.19	-	-
H24	-	0.82	0.68	1.13	0.94	0.78	0.76
H26	-	1.78	1.41	1.99	1.72	1.73	1.68
H27	-	2.79	-	-	-	2.04	0.01
C1	142.9	152.9	155.0	156.0	155.2	158.3	159.2
C2	143.1	136.4	134.9	131.2	146.7	136.8	135.9
C3	116.6	121.0	116.3	107.0	122.8	121.2	119.7
C4	135.6	138.9	141.8	137.3	149.4	140.5	139.5
C5	112.8	113.8	107.1	102.5	109.0	111.1	114.9
C6	135.9	135.8	146.0	153.1	145.9	144.8	141.4
C7	50.4	55.6	53.8	54.1	52.3	64.1	60.8
C8	122.9	121.7	128.4	129.4	127.9	121.6	124.5
C9	153.8	160.3	160.7	161.5	150.5	159.1	161.6
C10	136.2	137.4	135.0	136.6	137.1	138.3	137.5
C11	123.2	122.0	122.2	120.2	122.6	122.7	121.9
C12	141.3	140.5	142.1	138.4	134.8	141.6	141.4
C13	123.8	122.5	122.2	122.5	122.8	123.0	122.0
C14	34.3	34.9	34.6	34.8	34.4	35.1	34.9
C15	31.5	29.3	30.2	30.2	31.2	29.5	29.4
C16	34.4	34.3	34.6	34.6	34.5	34.4	34.2
C17	29.9	31.6	32.1	32.6	31.7	31.7	31.6
C18	35.0	35.2	35.1	35.7	35.0	35.4	35.3
C19	29.7	30.0	30.0	30.7	30.4	30.1	30.1
C20	34.1	34.1	34.2	34.1	34.5	34.1	34.1
C21	31.6	31.6	31.6	32.1	29.7	31.6	31.6
C22	-	288.5	255.6	290.5	93.2	288.7	289.0

C23	-	50.0	44.6	49.2	37.0	50.1	50.1
C24	-	33.2	33.7	35.2	34.4	32.9	33.1
C25	-	79.4	84.5	76.5	89.8	80.0	79.9
C26	-	33.1	30.8	34.1	29.8	33.0	32.9
C27	-	-	-	-	-	47.1	-0.6

N_{pincer}	50.0	48.1	260.6	129.8	299.8	48.9	*nm*

a measured in toluene-d_8 at – 30 °C; ***b*** $^{31}P\{^1H\}$ for **4** appears at 21.7 ppm in THF-d_8; $-CH_3$ of $\{MePPh_3\}^+$ resonates at 2.55 ppm in THF-d_8; $^{13}C\{^1H\}$ resonances for $-CH_3$ and $-C_6H_5$ groups of $\{MePPh_3\}^+$ cation are broadened and therefore not measured.

Synthesis of $[ON^{CH2}O]H_3$ (1)

In a well-ventilated fume hood, under ambient conditions 2,4-di-tert-butyl-6-((3,5-di-tert-butyl-2-hydroxybenzylidene)amino)phenol (6.57 g, 15.0 mmol) was suspended in 100 mL of ethanol (200 proof) and chilled using an ice-water bath. To this cold, rapidly stirring suspension, 2.27 g of $NaBH_4$ (60.0 mmol, 4 equiv.) was added using a spatula in portions (time interval of 10 - 15 seconds between the additions). By the end of the addition, the reaction mixture had turned color from yellow to deep red-orange. After 10 minutes of stirring at this temperature, the reaction mixture was refluxed under argon for 2 hours during when the color changed to deep purple. The reflux was stopped, the reaction mixture was allowed to reach ambient temperature, and then immediately quenched by addition of an excess of 1N HCl until fuming ceased. The reaction mixture changed from purple to off-white. Water was added to dilute the reaction mixture and then the organic phase was extracted three times with dichloromethane. The golden colored organic phase was dried using $MgSO_4$, filtered and the solvent was removed in vacuo. A single pentane trituration gave a cream colored solid (Yield = 4.99 g, 69.7%), identified as the hydrochloride salt, **1·HCl**.

The hydrochloride salt **1·HCl** (3.03 g, 6.36 mmol) was dissolved in 75 mL of methanol and a methanolic solution of NaOMe (0.351 g of $NaOMe_{(s)}$, 6.36 mmol) was added in drops using a pipette. The color changed from hazy yellow to a homogeneous yellow solution. After 45 minutes of stirring, the solvent was removed in vacuo, and extracted with acetonitrile. Filtration, in vacuo removal of solvent and pentane trituration afforded **1** as a pale-yellow solid which was further purified by recrystallizing from pentane. (Yield = 1.45 g, 51.8%)

^{1}H NMR (C_6D_6, 500 MHz): δ = 7.51 (d, 1H, $^4J_{HH}$ = 1.9 Hz, Ar-*H*), 7.10 (d, 1H, $^4J_{HH}$ = 1.9 Hz, Ar-*H*), 6.94 (d, 1H, $^4J_{HH}$ = 1.9 Hz, Ar-*H*), 6.83 (d, 1H, $^4J_{HH}$ = 1.9 Hz, Ar-*H*), 3.89 (s, 2H, C*H*$_2$),

1.65 (s, 9H, Ar-C(CH_3)$_3$), 1.40 (s, 9H, Ar-C(CH_3)$_3$), 1.39 (s, 9H, Ar-C(CH_3)$_3$), 1.29 (s, 9H, Ar-C(CH_3)$_3$) ppm.

^{13}C{^{1}H} (75 MHz, C_6D_6): δ = 154.2 (s, Ar), 143.5 (s, Ar), 143.3 (s, Ar), 141. 7 (s, Ar), 136.6 (s, Ar), 136.3 (s, Ar), 136.0 (s, Ar), 124.2 (s, Ar), 123.5 (s, Ar), 123.3 (s, Ar), 116.9 (s, Ar), 113.2 (s, Ar), 50.8 (s, -CH$_2$-), 35.4 (s, Ar-C(CH$_3$)$_3$), 34.8 (s, Ar-C(CH$_3$)$_3$), 34.7 (s, Ar-C(CH$_3$)$_3$), 34.5 (s, Ar-C(CH$_3$)$_3$), 32.0 (s, Ar-C(CH$_3$)$_3$), 31.9 (s, Ar-C(CH$_3$)$_3$), 30.2 (s, Ar-C(CH$_3$)$_3$), 30.1 (s, Ar-C(CH$_3$)$_3$) ppm.

^{15}N NMR (From ^{1}H-^{15}N *g*HMBC, 500 MHz, C_6D_6): δ = 50.0 ppm

HRMS (ESI-TOF) m/z: $[M+H]^+$ Calcd for $C_{29}H_{46}NO_2$ 440.3523; Found 440.3532

NMR Characterization of [ON^{CH2}O]H$_3$ (1)

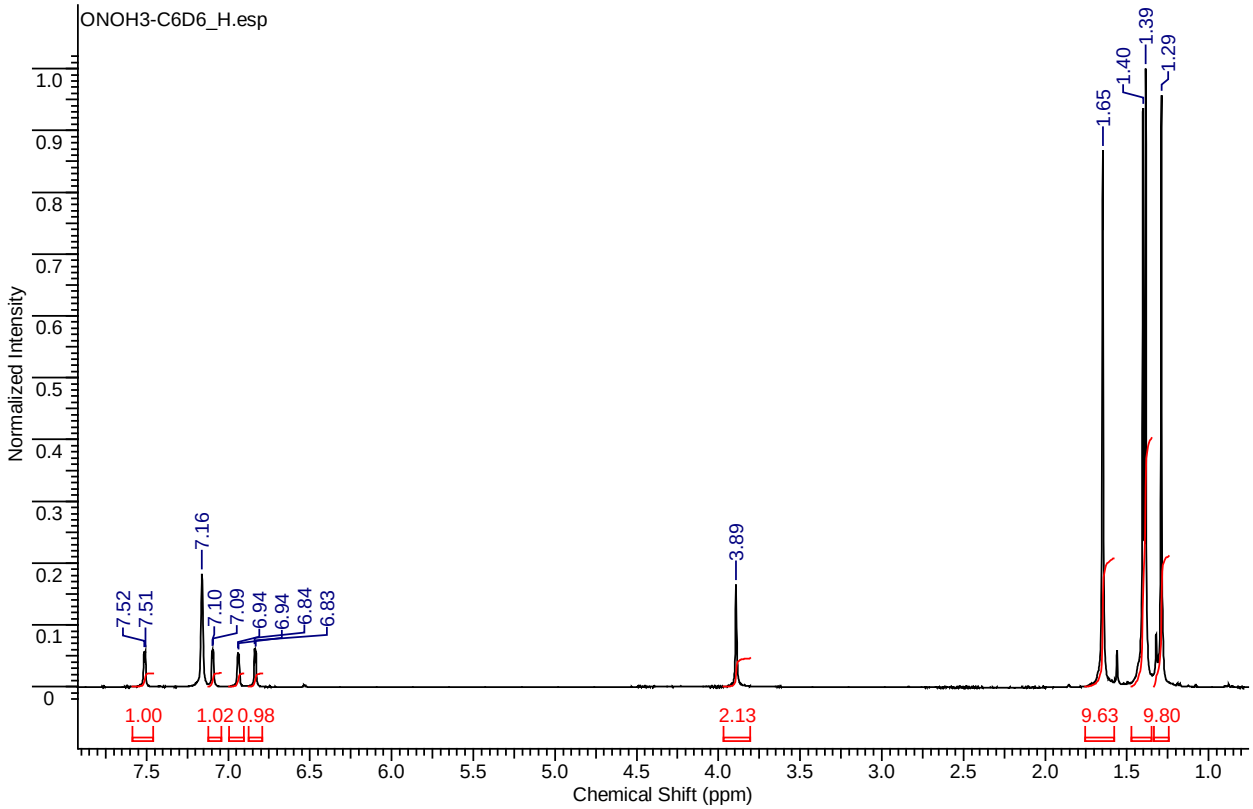

Figure S2. . ^{1}H NMR spectrum of **1** (C_6D_6, 300 MHz, 25 °C)

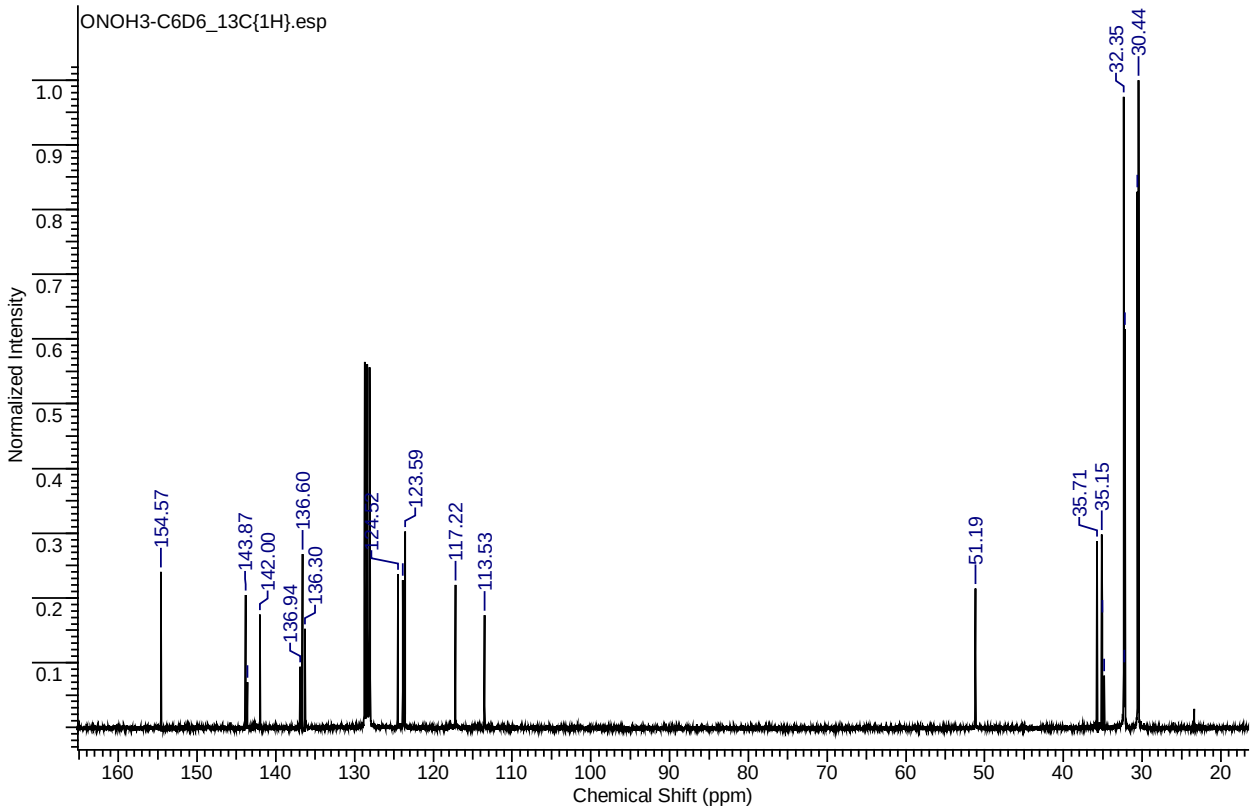

Figure S3. $^{13}C\{^{1}H\}$ NMR spectrum of **1** (C_6D_6, 75 MHz, 25 °C)

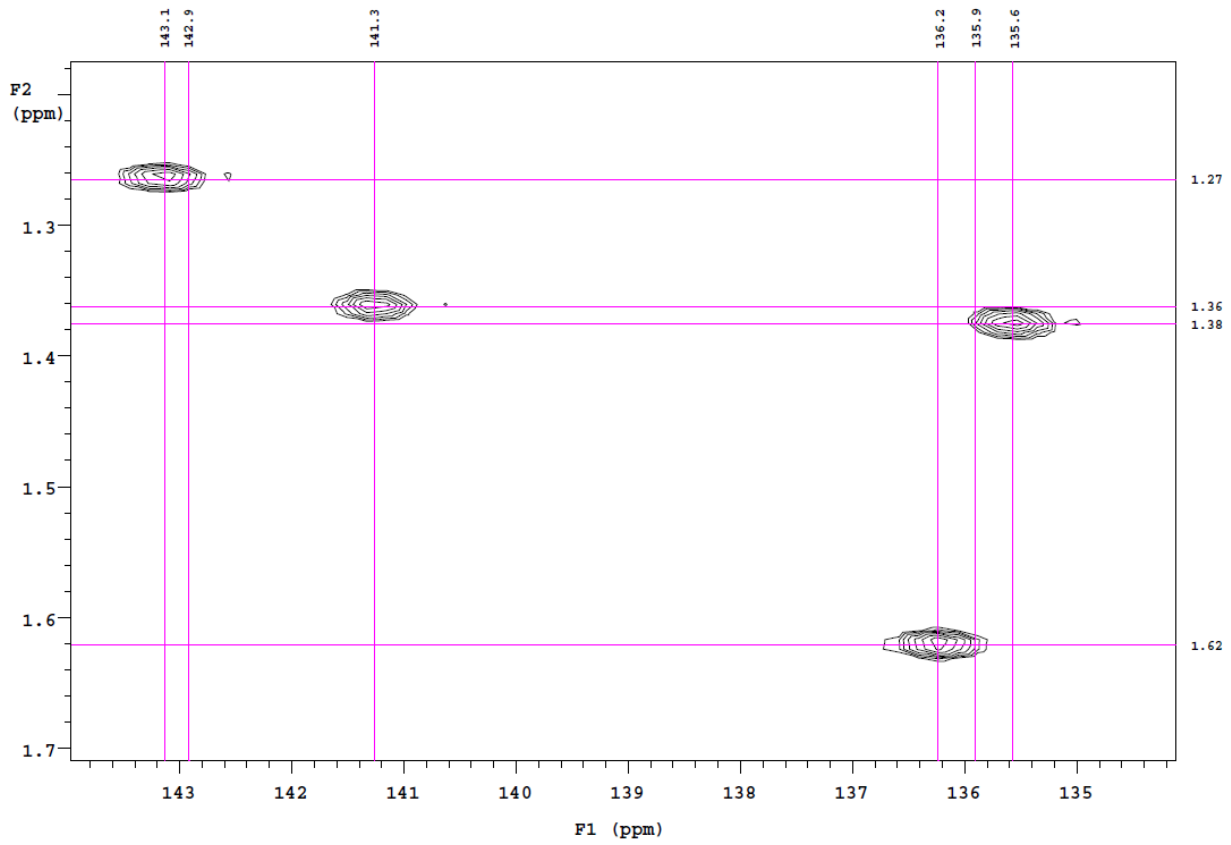

Figure S4. ^{1}H-^{13}C *g*HMBC spectrum of **1** (C_6D_6, 500 MHz, 25 °C)

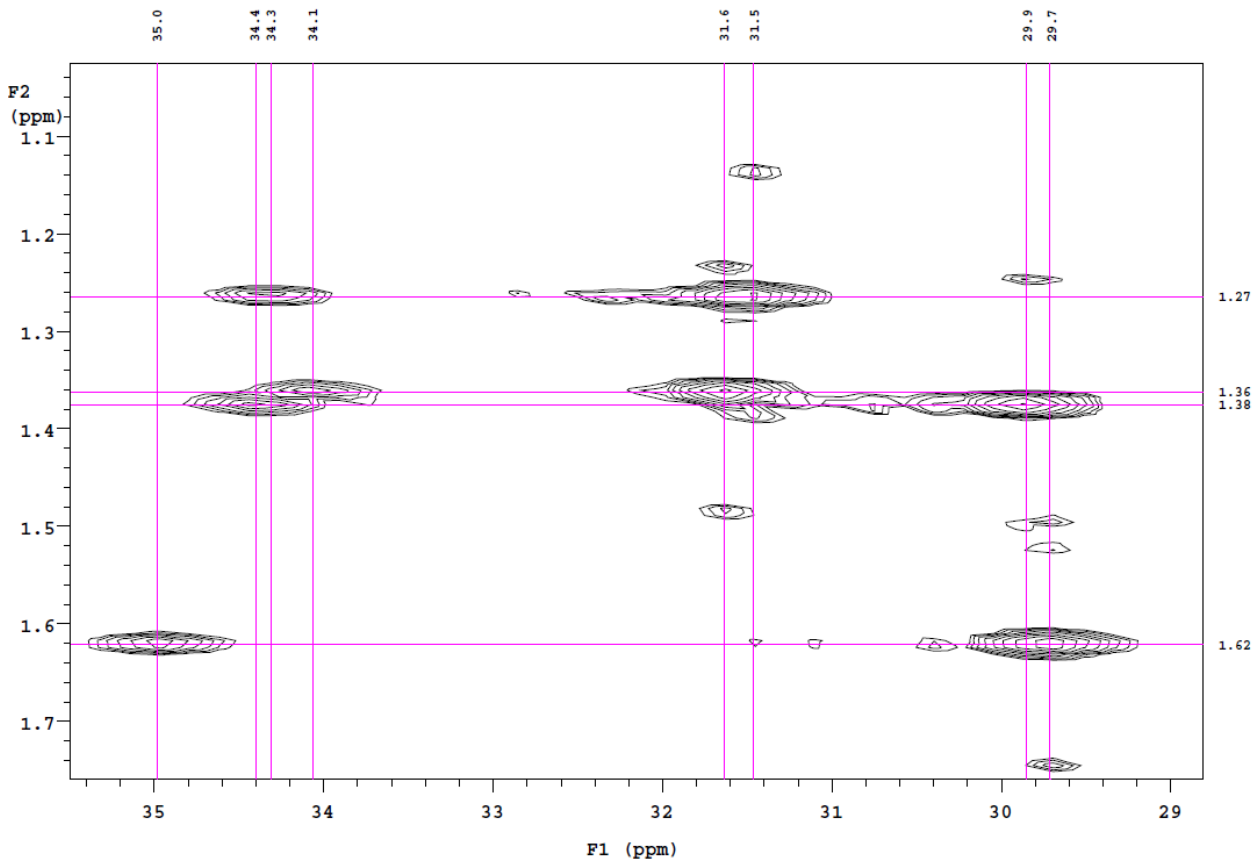

Figure S5. ^{1}H-^{13}C *g*HMBC spectrum of **1** (C_6D_6, 500 MHz, 25 °C)

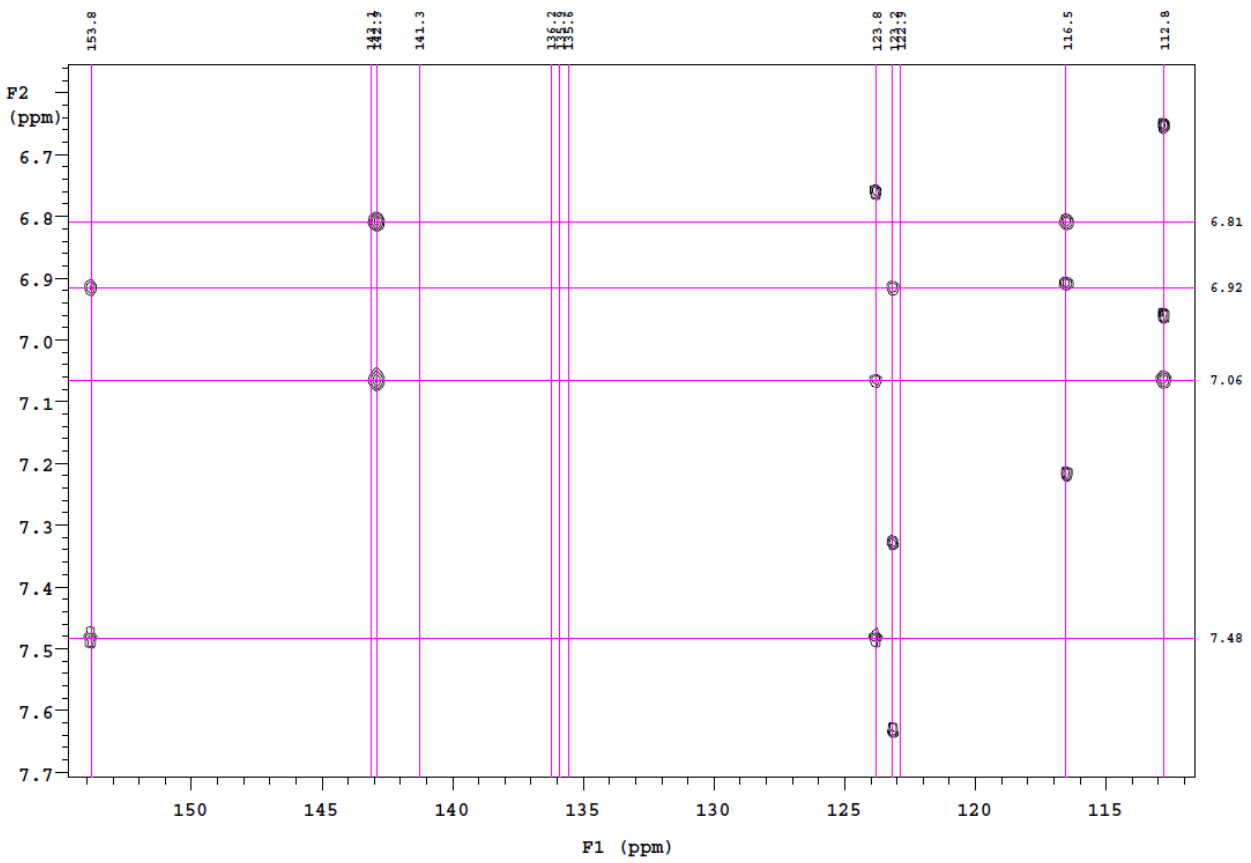

Figure S6. ^{1}H-^{13}C *g*HMBC spectrum of **1** (C_6D_6, 500 MHz, 25 °C)

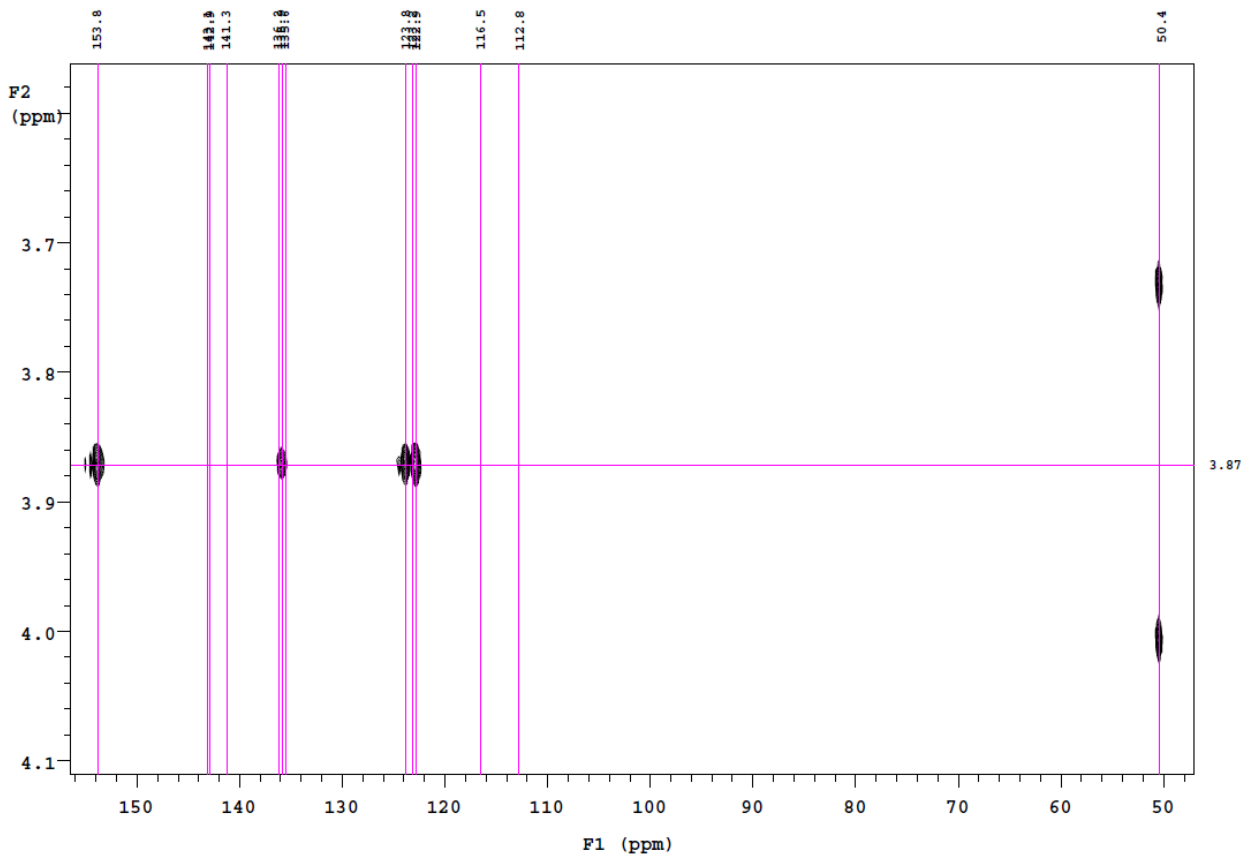

Figure S7. ^{1}H-^{13}C *g*HMBC spectrum of **1** (C_6D_6, 500 MHz, 25 °C)

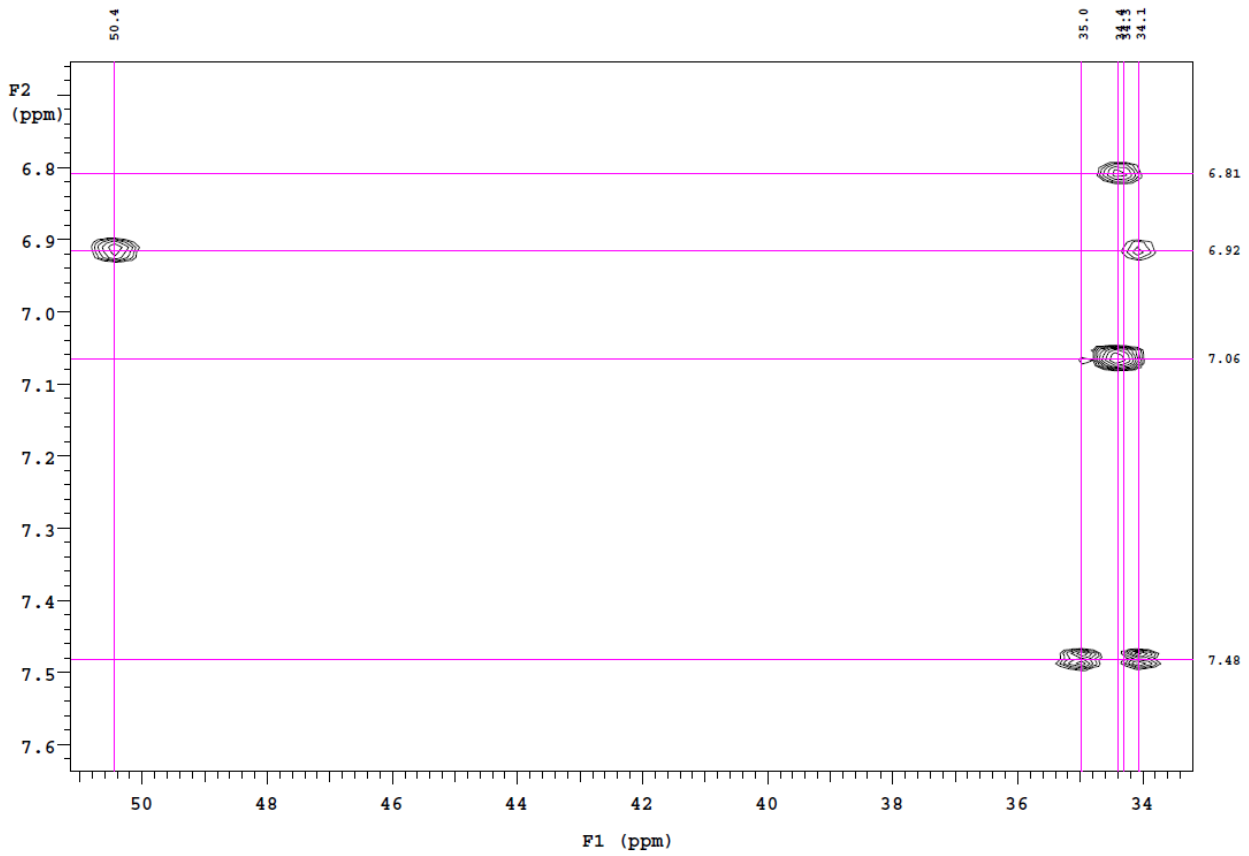

Figure S8. ^{1}H-^{13}C *g*HMBC spectrum of **1** (C_6D_6, 500 MHz, 25 °C)

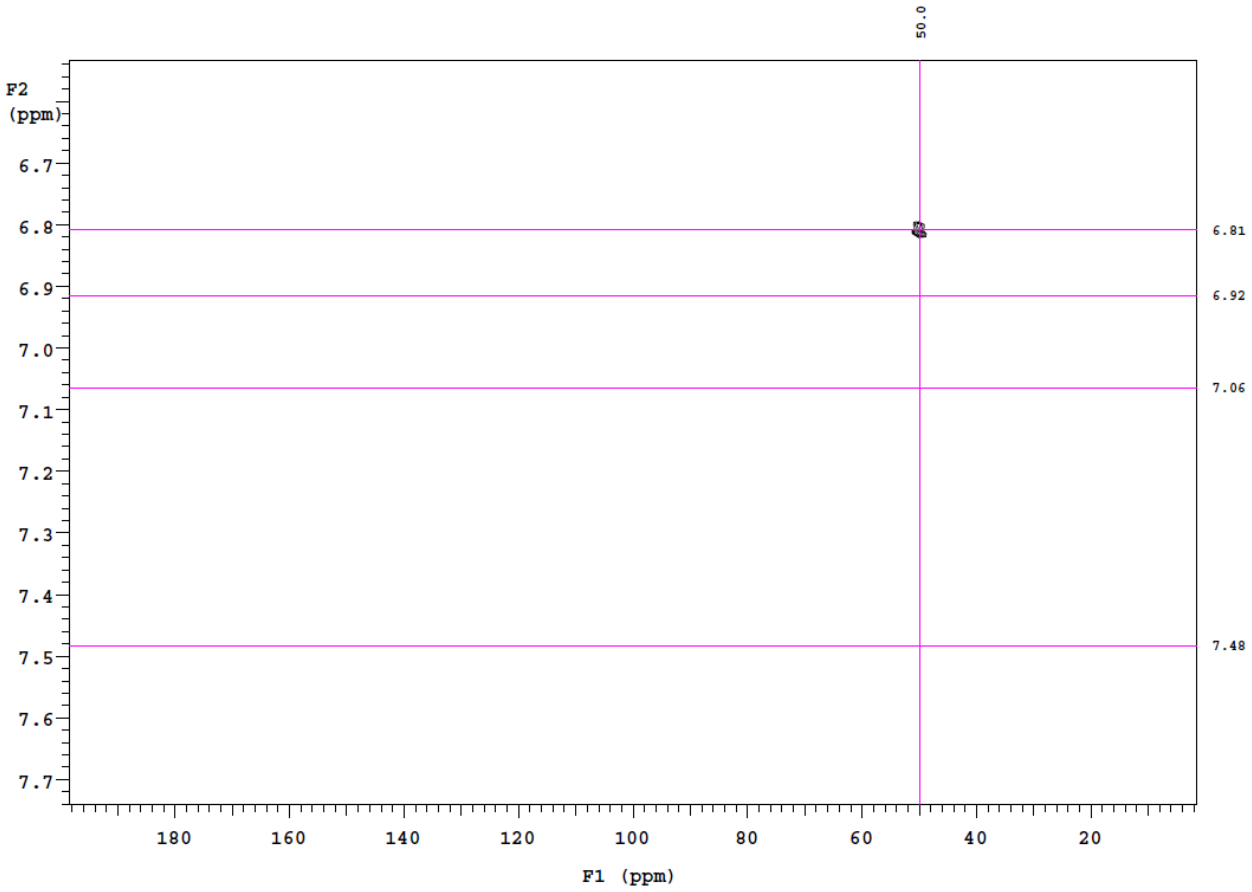

Figure S9. ^{1}H-^{15}N *g*HMBC spectrum of **1** (C_6D_6, 500 MHz, 25 °C)

HRMS Characterization of 1

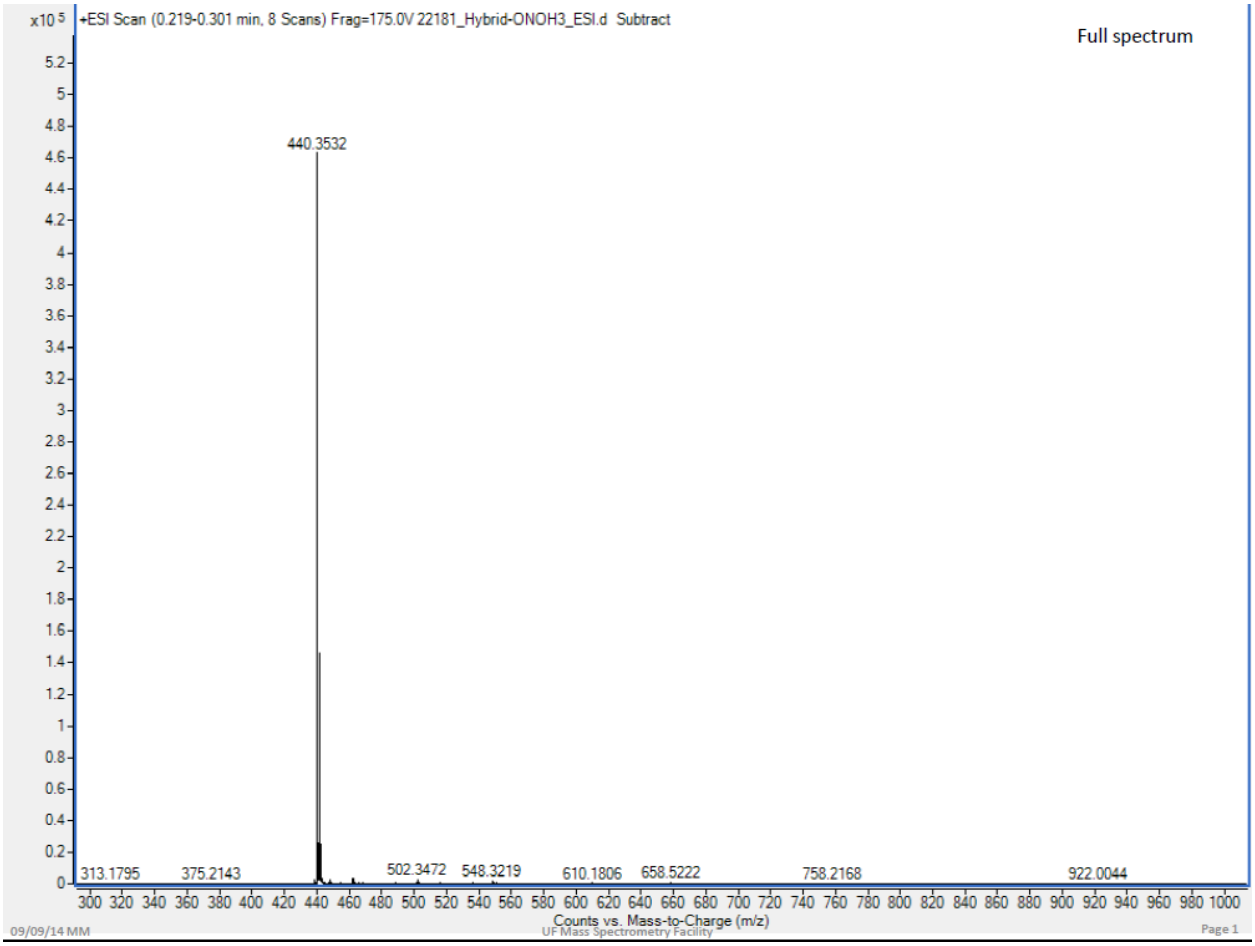

Figure S10. HRMS (ESI-TOF) of $[ON^{CH2}O]H_3$ (**1**); m/z: $[M+H]^+$ Calcd for $C_{29}H_{46}NO_2$ 440.3523; Found 440.3532

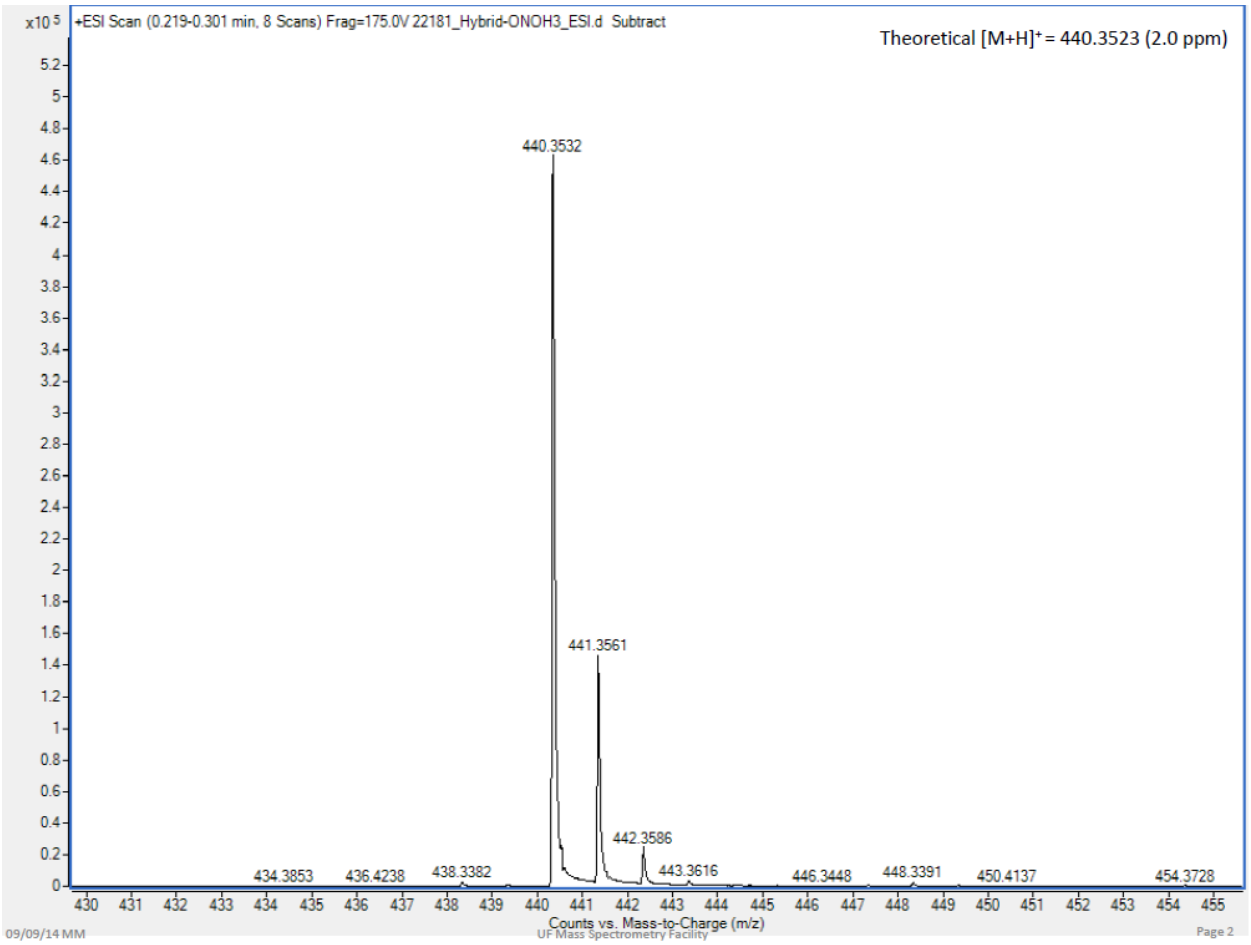

Figure S11. HRMS (ESI-TOF) of $[ON^{CH2}O]H_3$ (**1**); m/z: $[M+H]^+$ Calcd for $C_{29}H_{46}NO_2$ 440.3523; Found 440.3532

Synthesis of $[ONH^{CH2}O]W{\equiv}C^tBu(O^tBu)$ (2) and $[ON^{CH2}O]W{=}CH^tBu(O^tBu)$ (3)

In a glove box, a scintillation vial with **1** (100 mg, 0.227 mmol) in 2 mL of benzene was added to a benzene solution of $(^tBuO)_3W{\equiv}C^tBu$ (111 mg, 0.235 mmol, 1.03 equiv) at ambient temperature and allowed to stir. After 30 mins, all volatiles were evaporated under vacuum for 1 h. The resulting red-brown powder was dissolved in pentane and filtered through a Celite® plug. The red-brown powder was identified as $[ON\boldsymbol{H}^{CH2}O]W{\equiv}C^tBu(O^tBu)$ (**2**) using $^{13}C\{^1H\}$NMR spectroscopy. Warming a C_6D_6 solution of complex **2** to 70 °C facilitated proton migration from the amino backbone to

the alkylidyne fragment affording [ON^{CH2}O]W=C***H***^{t}Bu(O^{t}Bu) (**3**). (Total Yield = 119 mg, 68.6%)

[ON*H*^{CH2}O]W≡C^{t}Bu(O^{t}Bu) (2)

^{1}H NMR (C_7D_8, 500 MHz, − 30 °C): δ = 7.54 (d, 1H, $^{4}J_{HH}$ = 1.9 Hz, Ar-*H*), 7.40 (d, 1H, $^{4}J_{HH}$ = 1.9 Hz, Ar-*H*), 7.09 (d, 1H, $^{4}J_{HH}$ = 1.9 Hz, Ar-*H*), 7.04 (d, 1H, $^{4}J_{HH}$ = 1.9 Hz, Ar-*H*), 4.97 (dd, 1H, $^{2}J_{HH}$ = 14.0 Hz, $^{3}J_{HH}$ = 12.9 Hz, C*H*$_2$), 4.78 (dd, 1H, $^{2}J_{HH}$ = 14.0 Hz, $^{3}J_{HH}$ = 1.8 Hz, C*H*$_2$), 2.79 (br, 1H, N*H*), 1.78 (s, 9H, Ar-C(C*H*$_3$)$_3$), 1.77 (s, 9H, Ar-C(C*H*$_3$)$_3$), 1.76 (s, 9H, Ar-C(C*H*$_3$)$_3$), 1.37 (s, 9H, Ar-C(C*H*$_3$)$_3$), 1.36 (s, 9H, Ar-C(C*H*$_3$)$_3$), 0.82 (s, 9H, W≡C(C*H*$_3$)$_3$) ppm.

^{13}C NMR (indirect detection from ^{1}H-^{13}C *g*HMBC) (C_7D_8, 500 MHz, − 30 °C): δ = 288.5 (W≡*C*C(CH$_3$)$_3$), 160.3 (Ar-*C*), 159.2 (Ar-*C*), 140.5 (Ar-*C*), 138.9 (Ar-*C*), 137.4 (Ar-*C*), 136.4 (Ar-*C*), 135.8 (s, Ar-*C*), 122.5 (Ar-*C*), 122.0 (Ar-*C*), 121.7 (Ar-*C*), 121.0 (Ar-*C*), 113.8 (Ar-*C*), 79.4 (O*C*(CH$_3$)$_3$), 55.6 (*C*H$_2$), 50.0 (W≡C*C*(CH$_3$)$_3$), 35.2 (Ar-*C*(CH$_3$)$_3$), 34.9 (Ar-*C*(CH$_3$)$_3$), 34.3 (Ar-*C*(CH$_3$)$_3$), 34.1 (Ar-*C*(CH$_3$)$_3$), 33.2 (OC(*C*H$_3$)$_3$), 33.1 (W≡CC(*C*H$_3$)$_3$), 31.6 (Ar-C(*C*H$_3$)$_3$), 30.0 (Ar-C(*C*H$_3$)$_3$), 29.3 (s, Ar-C(*C*H$_3$)$_3$) ppm.

^{15}N NMR (From ^{1}H-^{15}N *g*HMBC, 500 MHz, C_7D_8, − 30 °C): δ = 48.1 ppm

Anal. Calcd. for $C_{38}H_{61}NO_3W$: C, 59.76%; H, 8.05%; N, 1.83%. Found: C, 59.70%; H, 7.92%; N, 2.04%

[ON^{CH2}O]W=C*H*^{t}Bu(O^{t}Bu) (3)

^{1}H NMR (C_6D_6, 500 MHz): δ = 8.90 (s, 1H, $^{2}J_{WH}$ = 15 Hz, W=C*H*(C(C*H*$_3$)$_3$)), 7.50 (d, 1H, $^{4}J_{HH}$ = 2.4 Hz, Ar-*H*), 7.30 (d, 1H, $^{4}J_{HH}$ = 2.4 Hz, Ar-*H*), 7.20 (d, 1H, $^{4}J_{HH}$ = 2.4 Hz, Ar-*H*), 7.07 (d, 1H, $^{4}J_{HH}$= 2.4 Hz, Ar-*H*), 5.44 (d, 1H, $^{2}J_{HH}$ = 16.7 Hz, C*H*$_2$), 5.08 (d, 1H, $^{2}J_{HH}$ = 16.7 Hz, CH$_2$), 1.75 (s, 9H, Ar-C(C*H*$_3$)$_3$), 1.74 (s, 9H, Ar-C(C*H*$_3$)$_3$), 1.45 (s, 9H, Ar-C(C*H*$_3$)$_3$)), 1.43 (s, 9H, -OC(C*H*$_3$)$_3$)), 1.34 (s, 9H, Ar-C(C*H*$_3$)$_3$)), 0.68 (s, 9H, W=CH(C(C*H*$_3$)$_3$)) ppm.

$^{13}C\{^{1}H\}$ NMR (C_6D_6, 125 MHz): δ = 255.6 (s, W=*C*HC$(CH_3)_3$)), 160.7 (s, Ar-*C*), 155.0 (s, Ar-*C*), 146.0 (s, Ar-*C*), 142.1 (s, Ar-*C*), 141.8 (s, Ar-*C*), 135.0 (s, Ar-*C*), 134.9 (s, Ar-*C*), 128.4 (s, Ar-*C*), 122.2 (s, Ar-*C*), 116.3 (s, Ar-*C*), 107.1 (s, Ar-*C*), 84.5 (s, -O*C*$(CH_3)_3$), 53.8 (s, *C*H_2), 44.6 (s, W=CH*C*$(CH_3)_3$), 35.1 (s, Ar-*C*$(CH_3)_3$), 34.6 (s, Ar-*C*$(CH_3)_3$), 34.2 (s, Ar-*C*$(CH_3)_3$), 33.7 (s, W=CHC(*C*$H_3)_3$), 32.1 (s, Ar-C(*C*$H_3)_3$), 31.6 (s, Ar-C(*C*$H_3)_3$), 30.8 (s, OC(*C*$H_3)_3$), 30.2 (s, Ar-C(*C*$H_3)_3$), 30.0 (s, Ar-C(*C*$H_3)_3$) ppm.

^{15}N NMR (From ^{1}H-^{15}N *g*HMBC, 500 MHz, C_6D_6): δ = 260.6 ppm

Anal. Calcd. for $C_{38}H_{61}NO_3W$: C, 59.76%; H, 8.05%; N, 1.83%. Found: C, 59.70%; H, 7.92%; N, 2.04%

NMR Characterization of [ON*H*^{CH2}O]W≡C^{t}Bu(O^{t}Bu) (2)

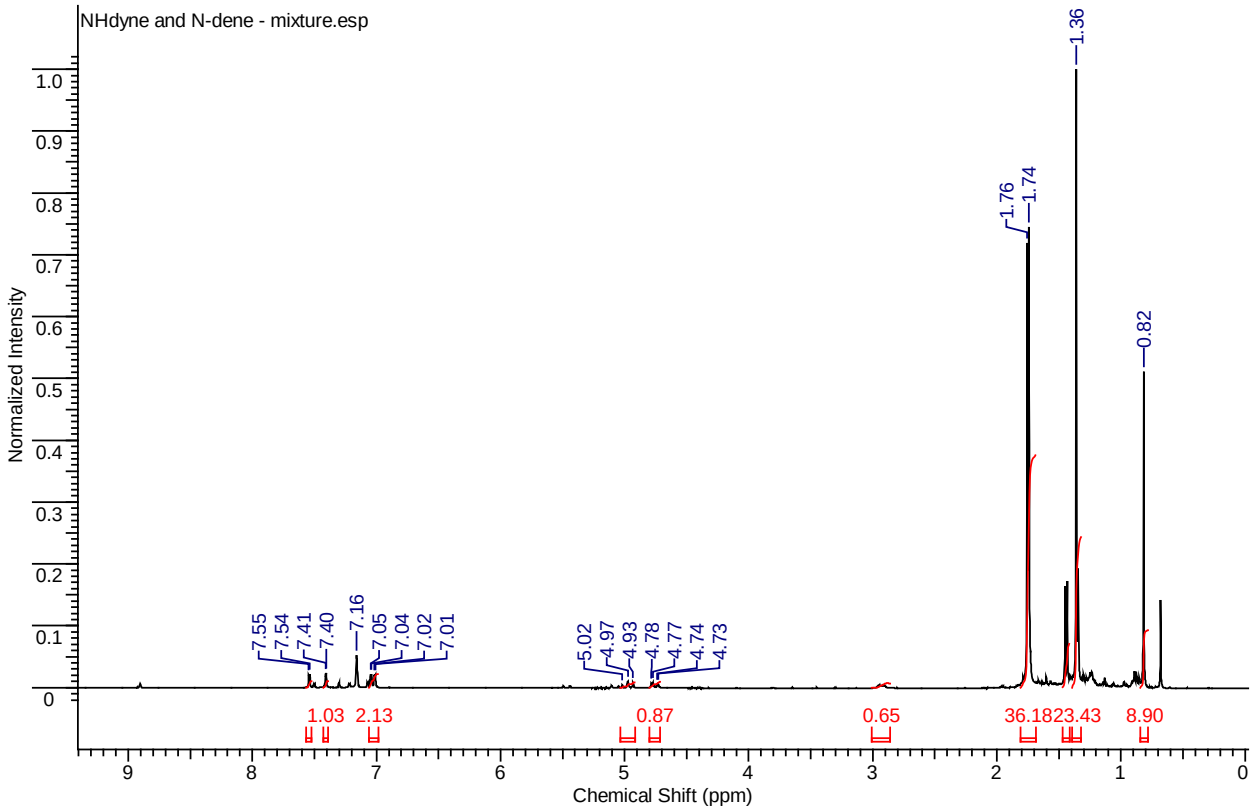

Figure S12. ^{1}H NMR spectrum of a mixture of [ON*H*^{CH2}O]W≡C^{t}Bu(O^{t}Bu) (**2**) and [ON^{CH2}O]W=C*H*^{t}Bu(O^{t}Bu) (**3**) (C_6D_6, 300 MHz, 25 °C). The highlighted peaks correspond to [ONH^{CH2}O]W≡C^{t}Bu(O^{t}Bu) (**2**). The minor peaks that have not been highlighted correspond to **3**.

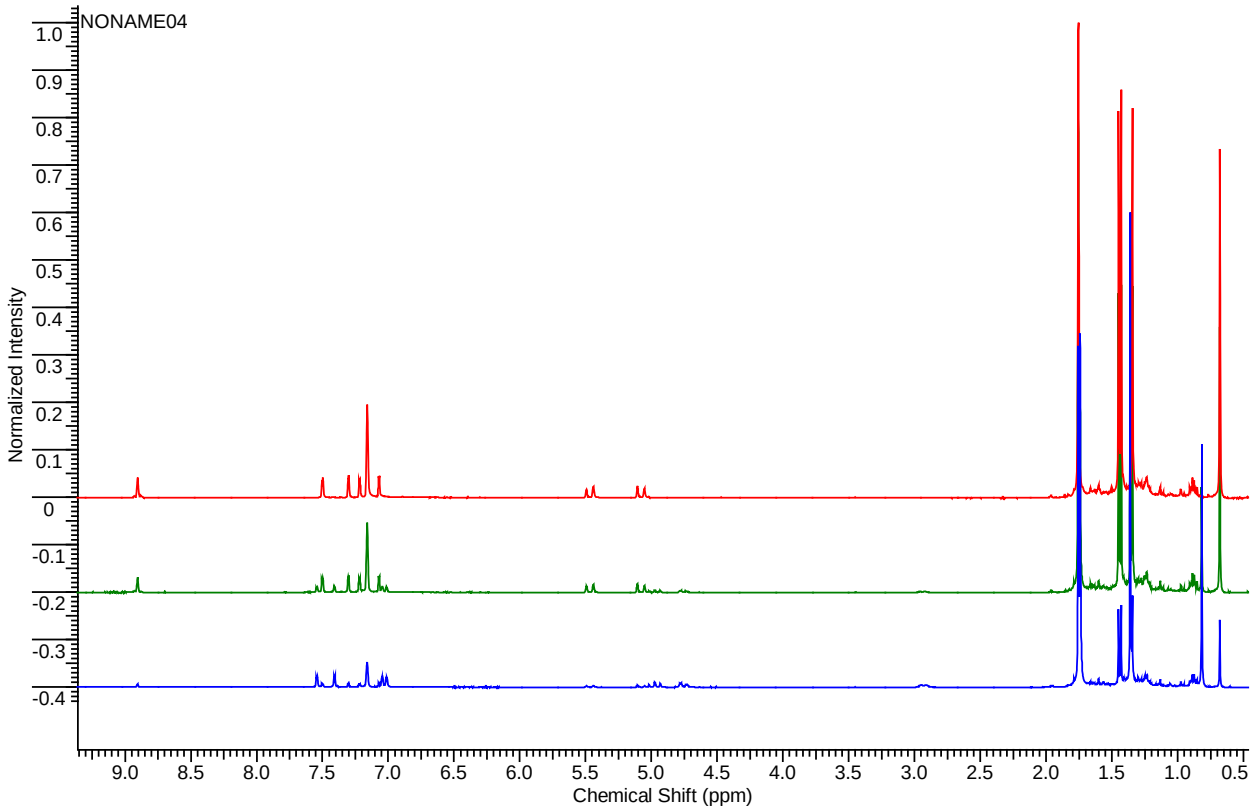

Figure S13. ^{1}H NMR spectrum showing the conversion of [ON^{CH2}*H*O]W≡C^{t}Bu(O^{t}Bu) (**2**) to [ON^{CH2}O]W=C*H*^{t}Bu(O^{t}Bu) (**3**) (C_6D_6, 300 MHz, 25 °C). The BLUE spectrum corresponds to [ON^{CH2}*H*O]W≡C^{t}Bu(O^{t}Bu) (**2**); the GREEN spectrum is after 1 day in C_6D_6 at 25 °C; the RED spectrum is after heating the complex in C_6D_6 to 70 °C for 90 minutes to ensure full conversion to **2**.

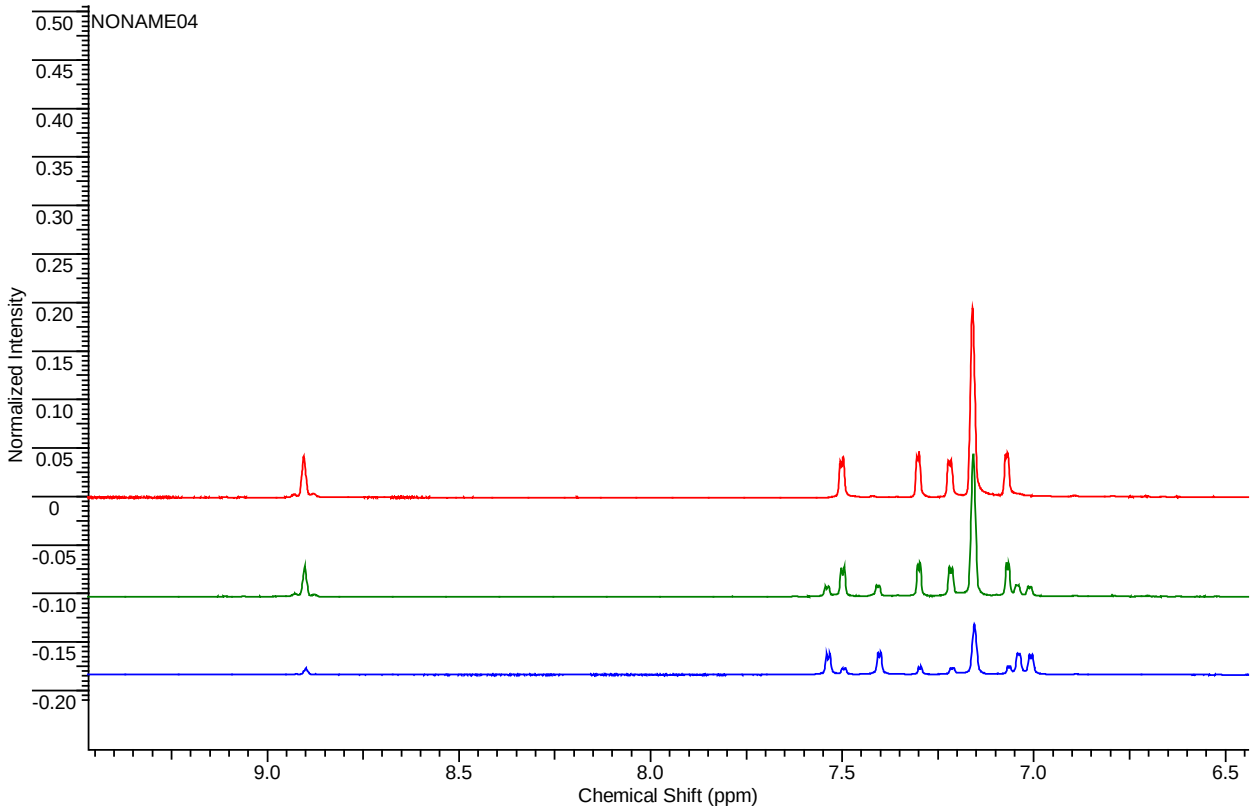

Figure S14. Conversion of [ON*H*^{CH2}O]W≡C^{t}Bu(O^{t}Bu) (**2**) to [ON^{CH2}O]W=C*H*^{t}Bu(O^{t}Bu) (**3**) – Zoom of the aromatic region (C_6D_6, 300 MHz, 25 °C). The BLUE spectrum corresponds to [ON*H*^{CH2}O]W≡C^{t}Bu(O^{t}Bu) (**2**); the GREEN spectrum is after 1 day in C_6D_6 at 25 °C; the RED spectrum is after heating the complex in C_6D_6 to 70 °C for 90 minutes to ensure full conversion to **3**.

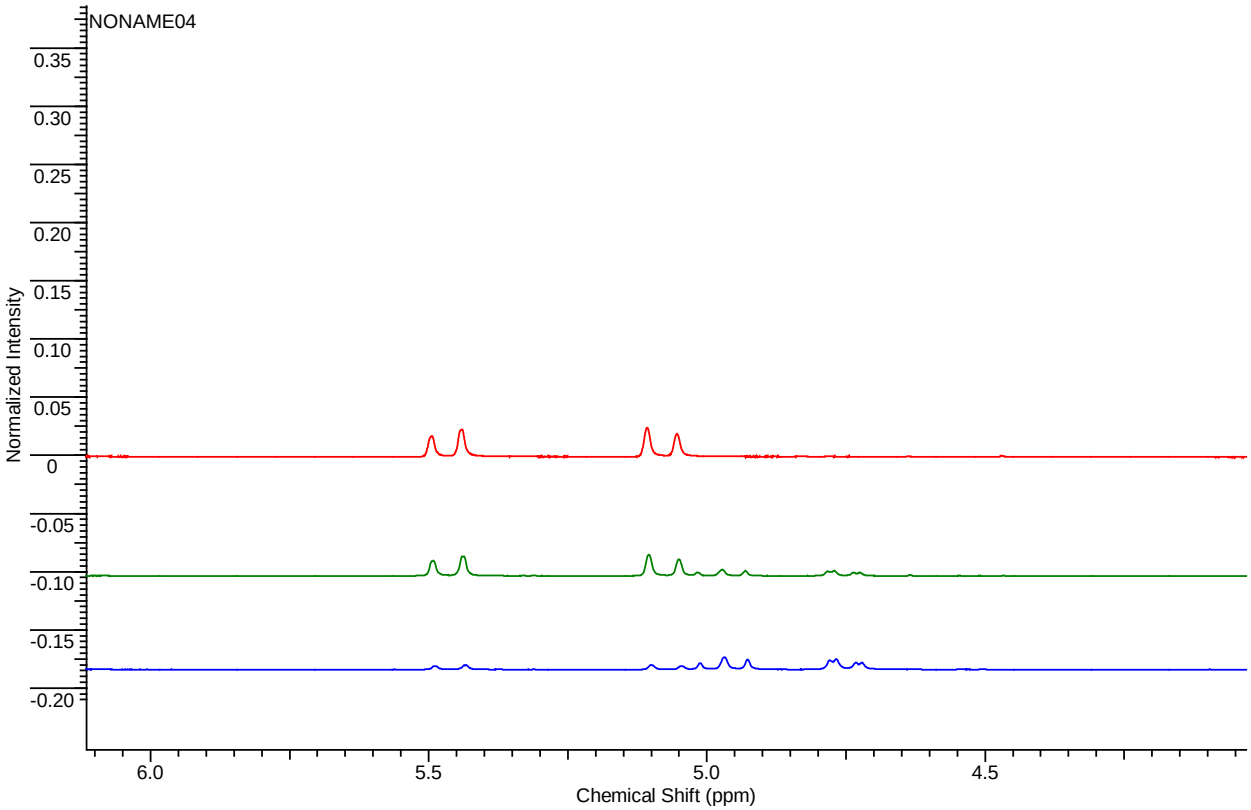

Figure S15. Conversion of [ON*H*^{CH2}O]W≡C^{t}Bu(O^{t}Bu) (**2**) to [ON^{CH2}O]W=C*H*^{t}Bu(O^{t}Bu) (**3**) – Zoom of the methylene region (C_6D_6, 300 MHz, 25 °C). The BLUE spectrum corresponds to [ON*H*^{CH2}O]W≡C^{t}Bu(O^{t}Bu) (**2**); the GREEN spectrum is after 1 day in C_6D_6 at 25 °C; the RED spectrum is after heating the complex in C_6D_6 to 70 °C for 90 minutes to ensure full conversion to **3**.

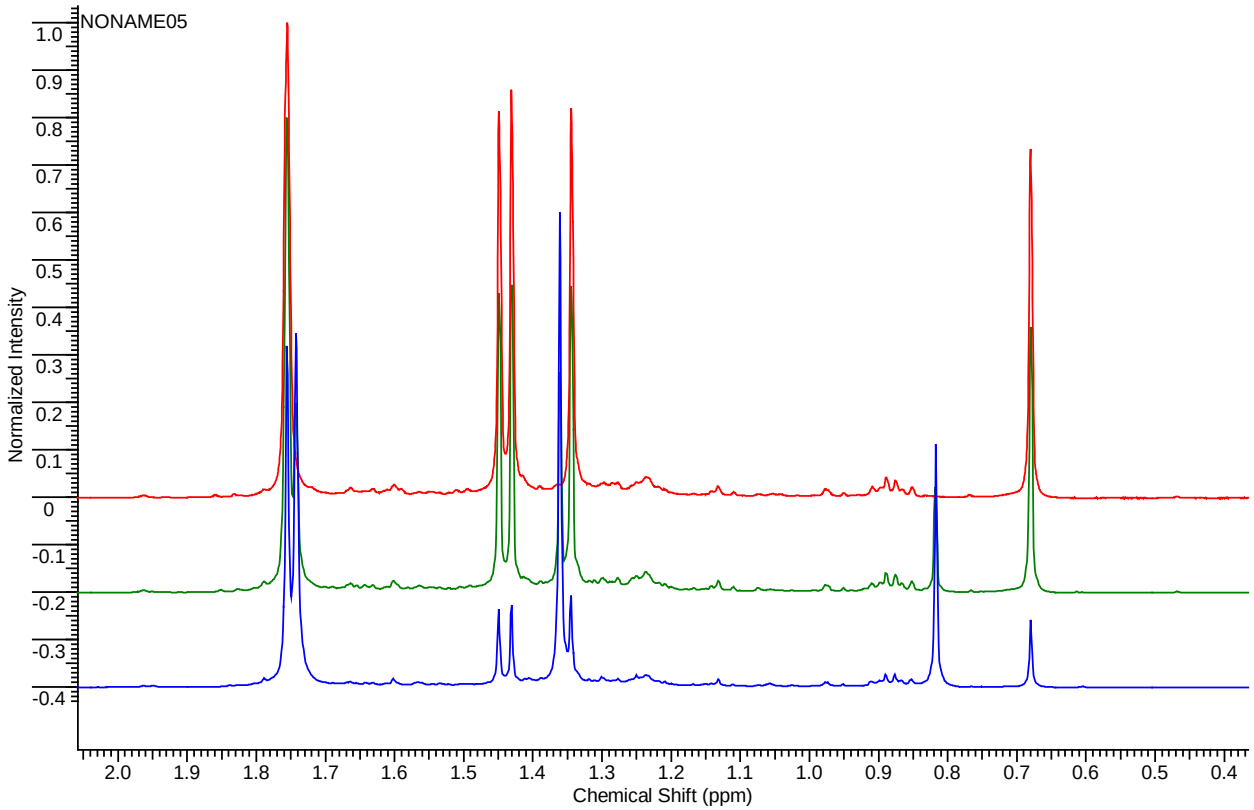

Figure S16. Conversion of [ON*H*^{CH2}O]W≡C^{t}Bu(O^{t}Bu) (**2**) to [ON^{CH2}O]W=C*H*^{t}Bu(O^{t}Bu) (**3**) – Zoom of the aliphatic region (C_6D_6, 300 MHz, 25 °C). The BLUE spectrum corresponds to [ON*H*^{CH2}O]W≡C^{t}Bu(O^{t}Bu) (**2**); the GREEN spectrum is after 1 day in C_6D_6 at 25 °C; the RED spectrum is after heating the complex in C_6D_6 to 70 °C for 90 minutes to ensure full conversion to **3**.

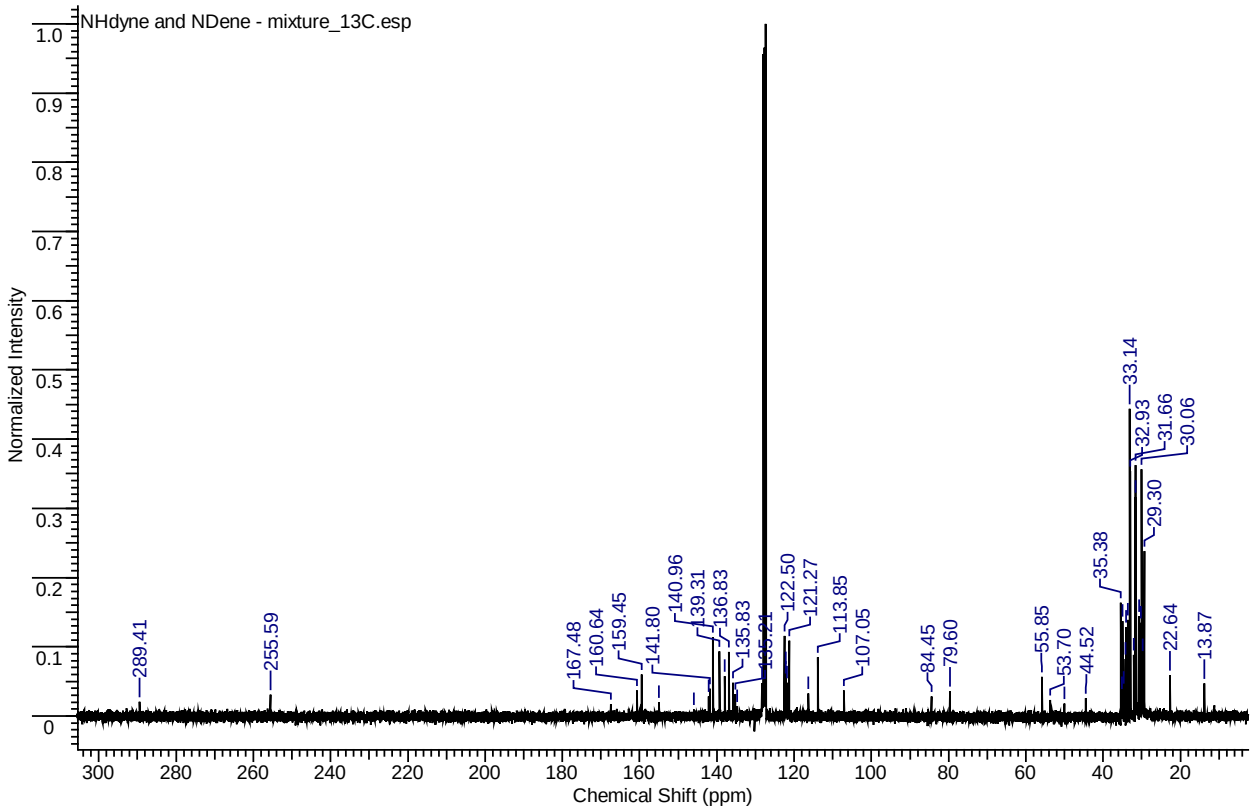

Figure S17. $^{13}C\{^{1}H\}$ NMR spectrum of the mixture of [ON*H*^{CH2}O]W≡C^{t}Bu(O^{t}Bu) (**2**) and [ON^{CH2}O]W=*C*H^{t}Bu(O^{t}Bu) (**3**) (C_6D_6, 75 MHz, 25 °C) [Note: W≡C^{t}Bu resonates at 289.4 ppm and W=CH^{t}Bu resonates at 255.6 ppm]

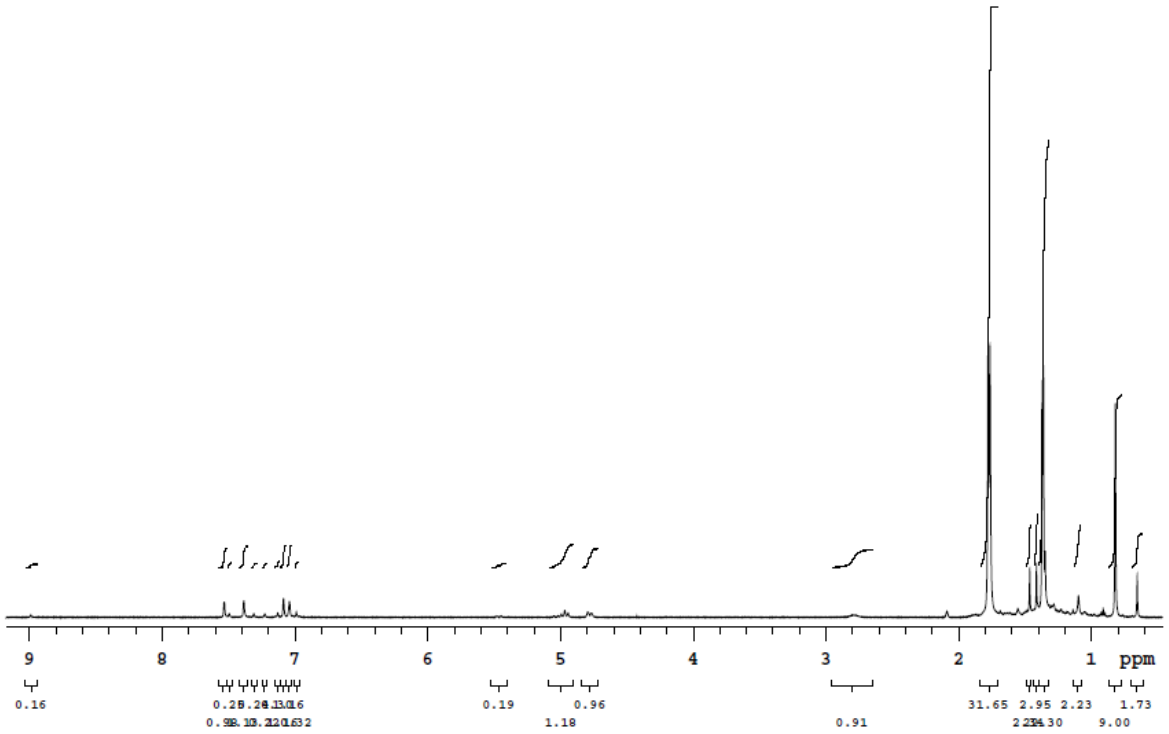

Figure S18. ^{1}H NMR spectrum of **2** (Toluene-d_8, 500 MHz, − 30 °C)

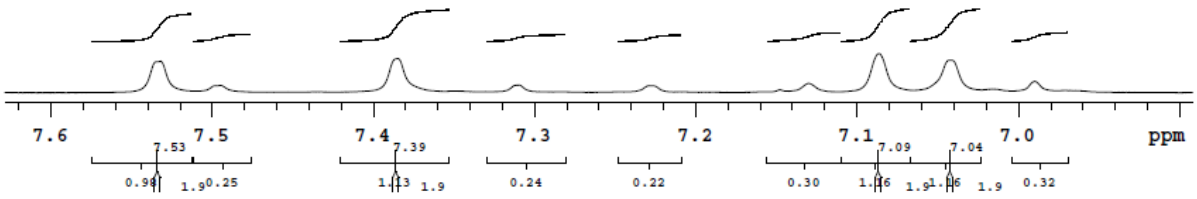

Figure S19. ^{1}H NMR spectrum of **2** - Expansion (Toluene-d_8, 500 MHz, − 30 °C)

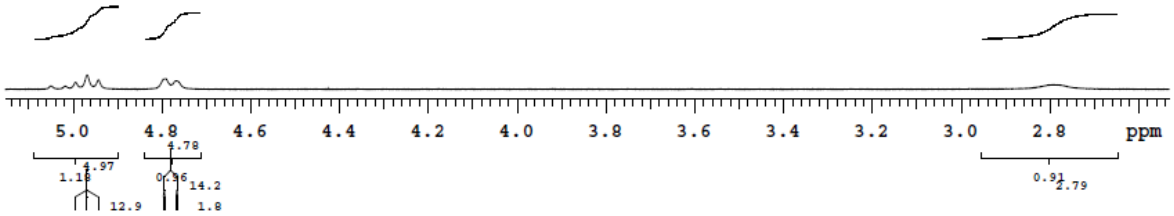

Figure S20. ^{1}H NMR spectrum of **2** - Expansion (Toluene-d_8, 500 MHz, − 30 °C)

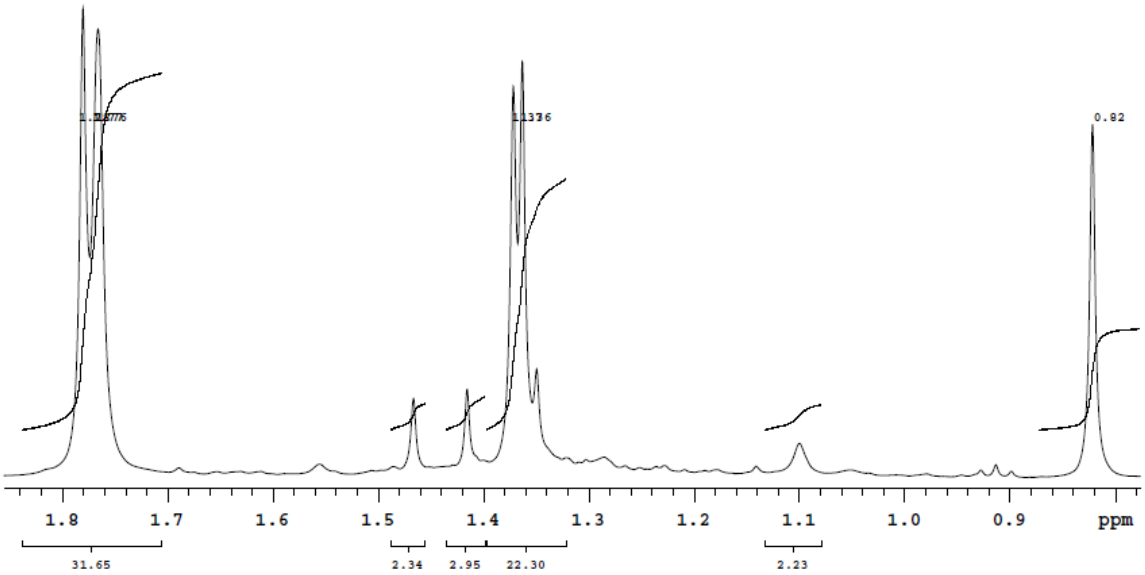

Figure S21. ^{1}H NMR spectrum of **2** - Expansion (Toluene-d_8, 500 MHz, − 30 °C)

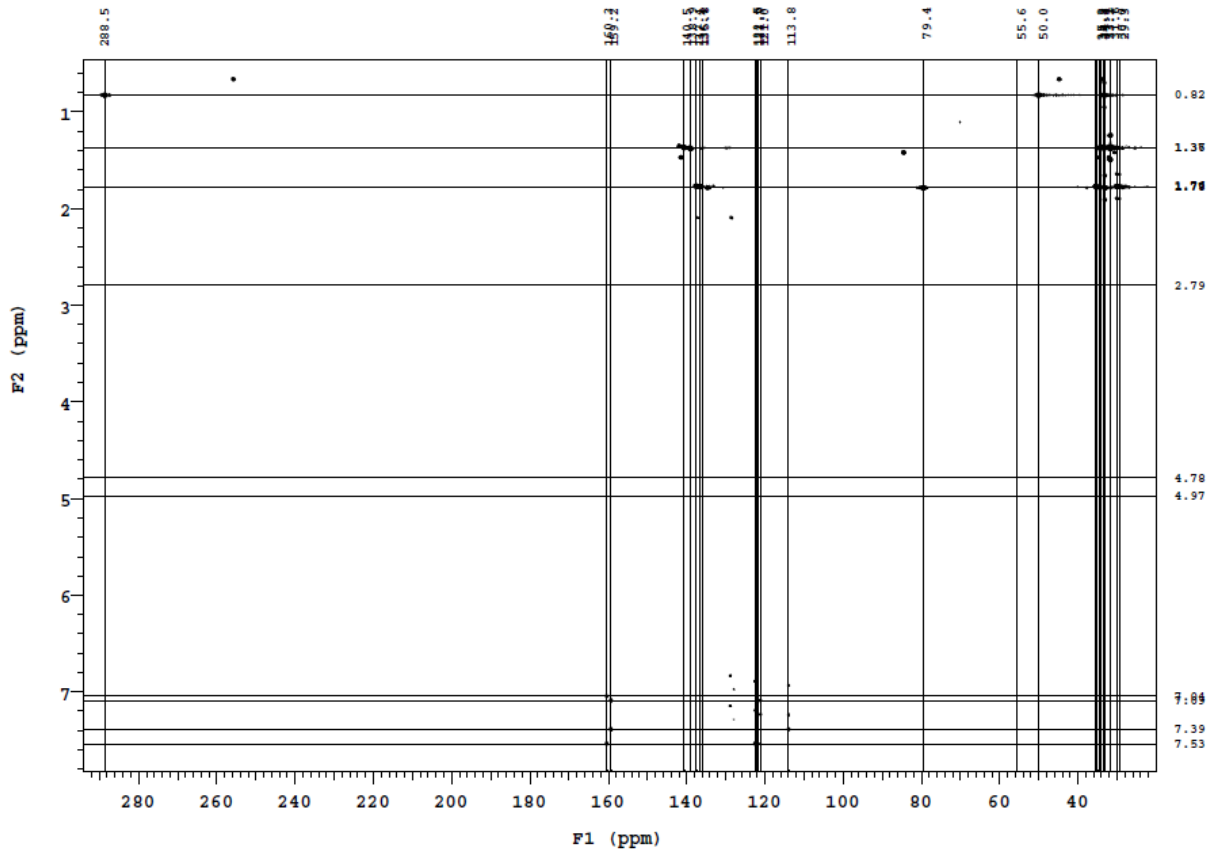

Figure S22. $^{1}H - {}^{13}C$ *g*HMBC spectrum of **2** (Toluene-d_8, 500 MHz, − 30 °C)

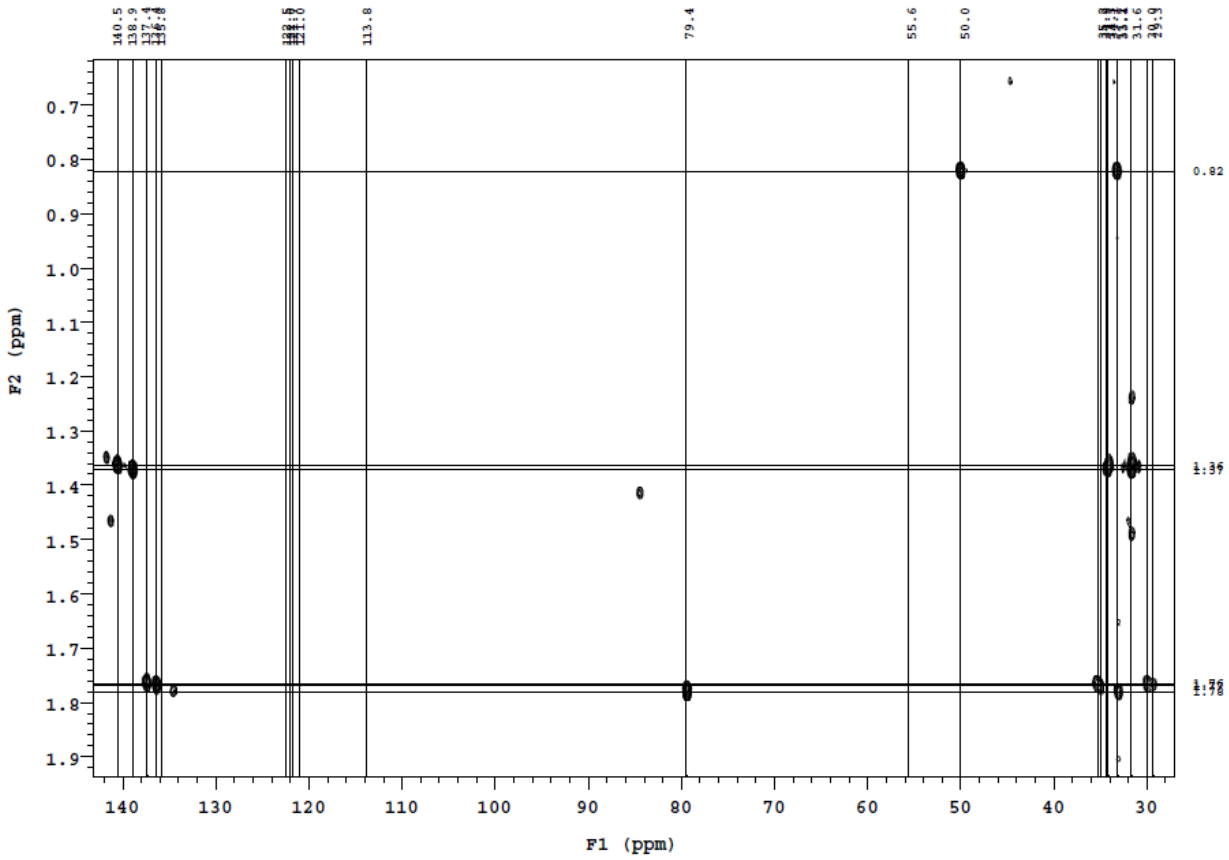

Figure S23. $^{1}H - {}^{13}C$ *g*HMBC spectrum of **2** (Toluene-d_8, 500 MHz, − 30 °C)

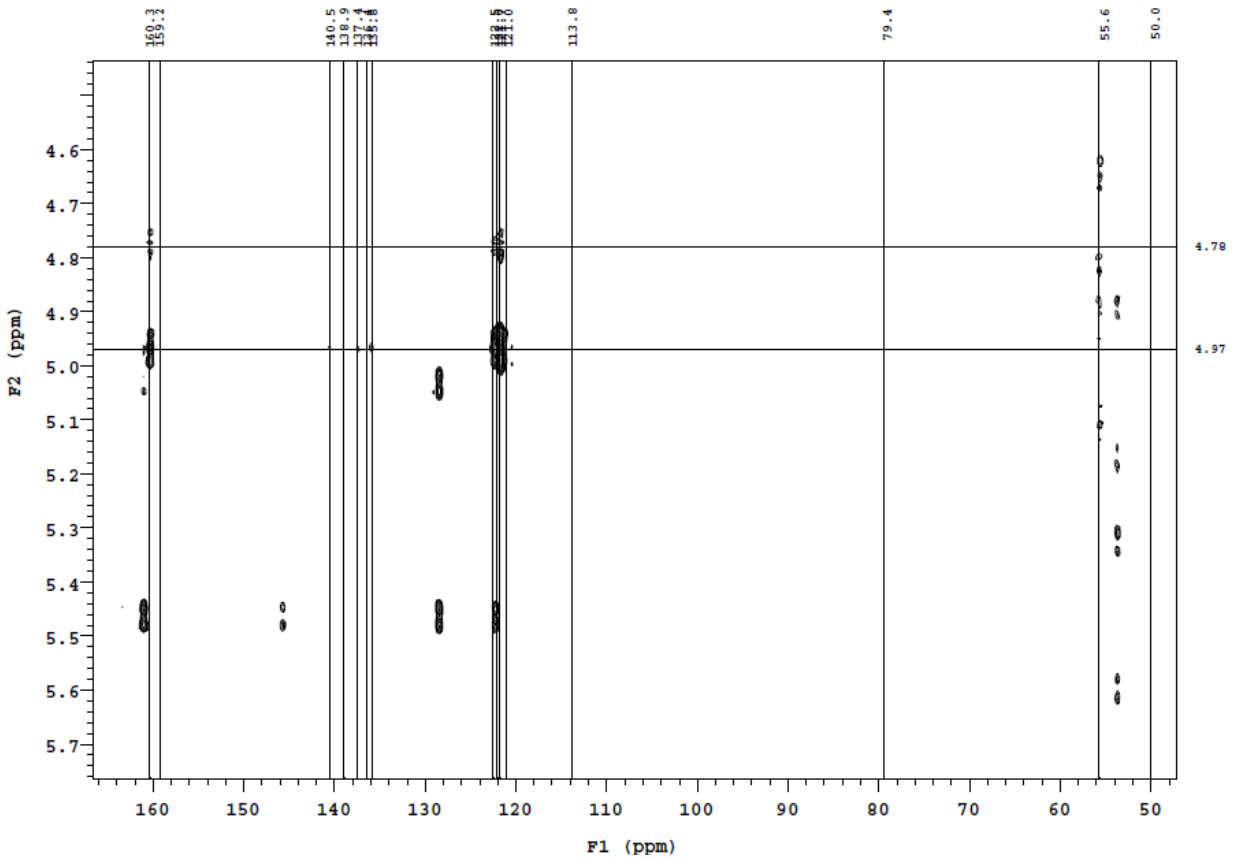

Figure S24. $^{1}H - {}^{13}C$ *g*HMBC spectrum of **2** (Toluene-d_8, 500 MHz, − 30 °C)

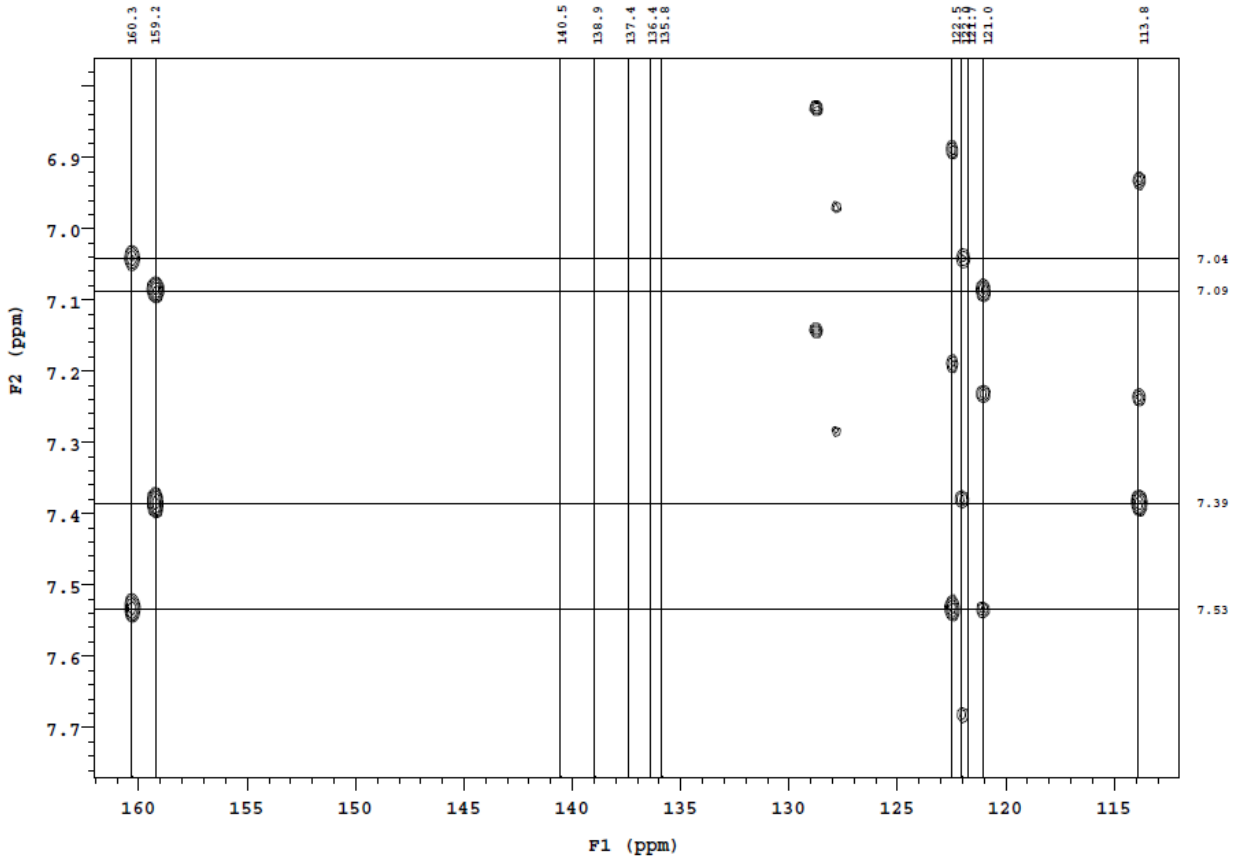

Figure S25. $^{1}H - {}^{13}C$ *g*HMBC spectrum of **2** (Toluene-d_8, 500 MHz, − 30 °C)

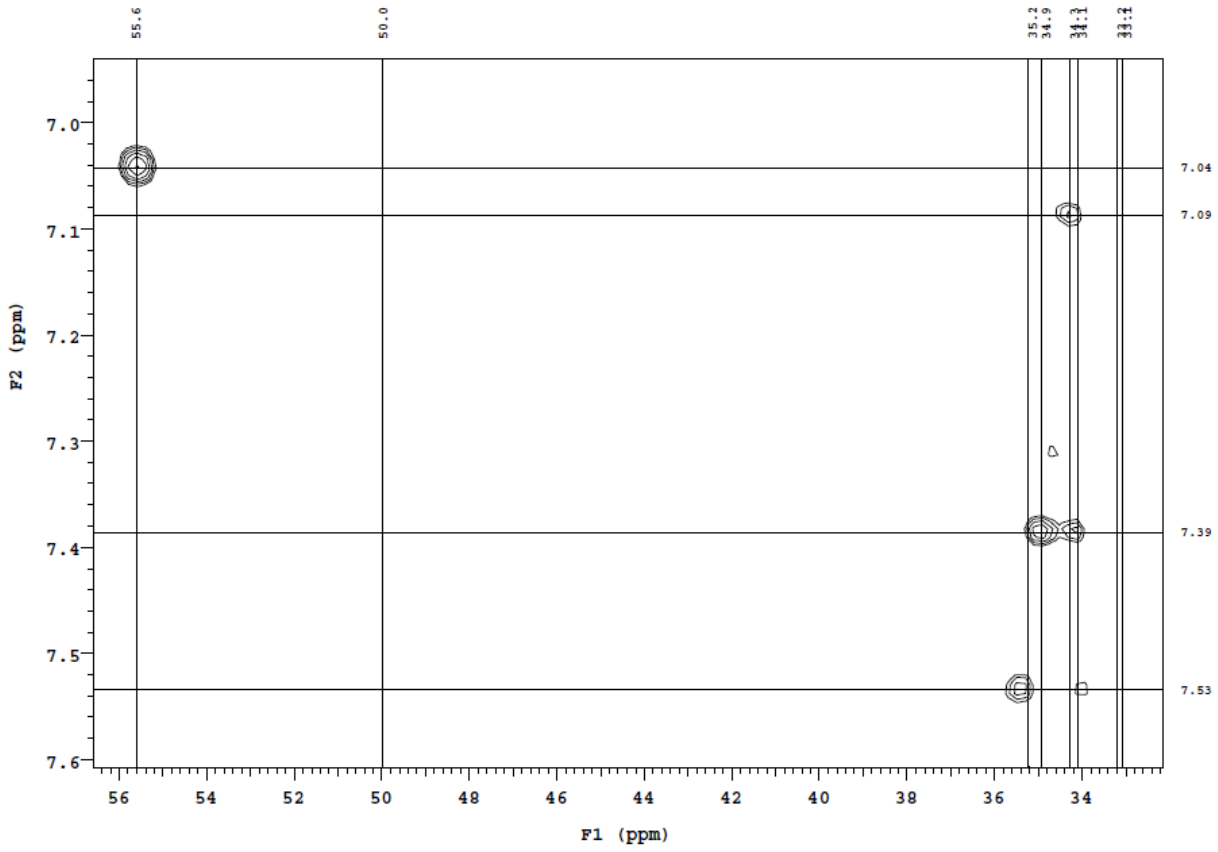

Figure S26. $^{1}H - {}^{13}C$ *g*HMBC spectrum of **2** (Toluene-d_8, 500 MHz, − 30 °C)

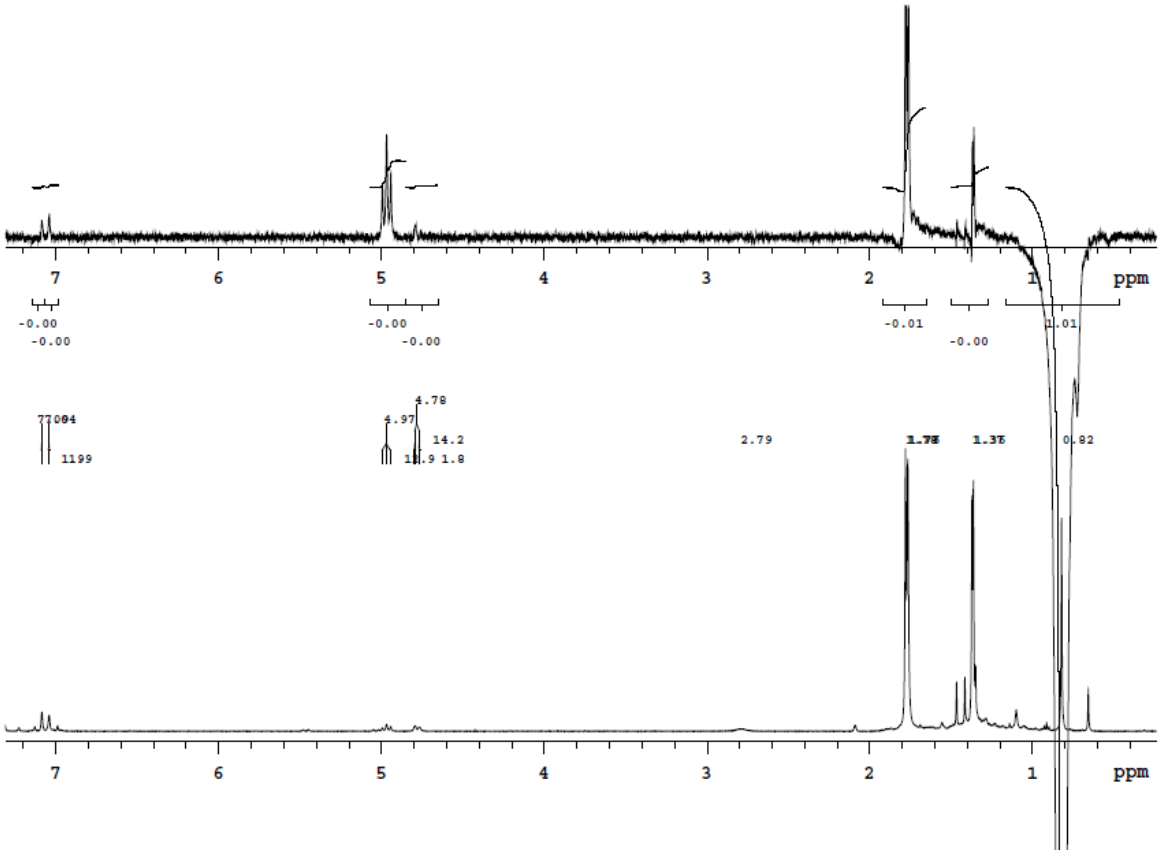

Figure S27. (Top) NOESY 1D spectrum of 2 with selective inversion at 0.82 ppm; (bottom) ^{1}H NMR spectrum of **2** (Toluene-d_8, 500 MHz, − 30 °C)

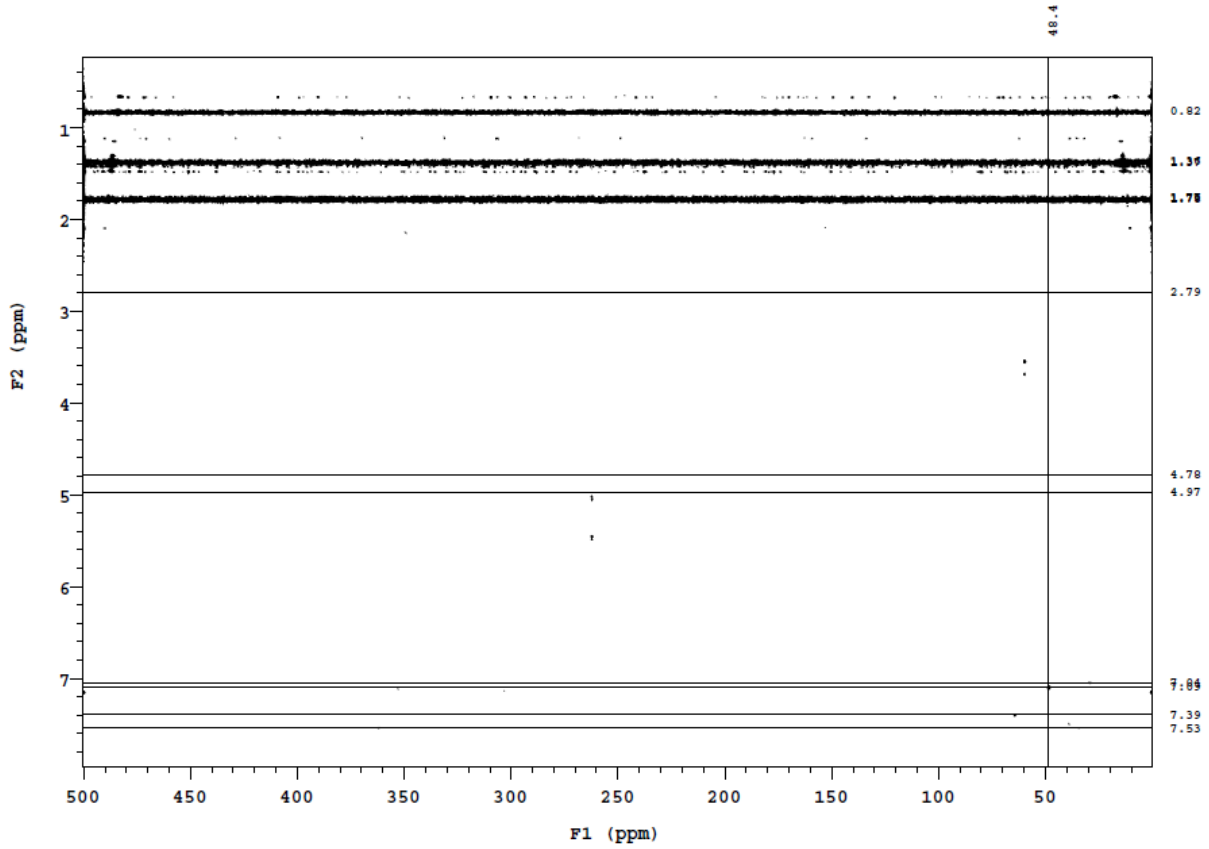

Figure S28. $^{1}H - {}^{15}N$ *g*HMBC spectrum of **2** (Toluene-d_8, 500 MHz, − 30 °C)

NMR characterization of [ON^{CH2}O]W=C*H*^{t}Bu(O^{t}Bu) (3)

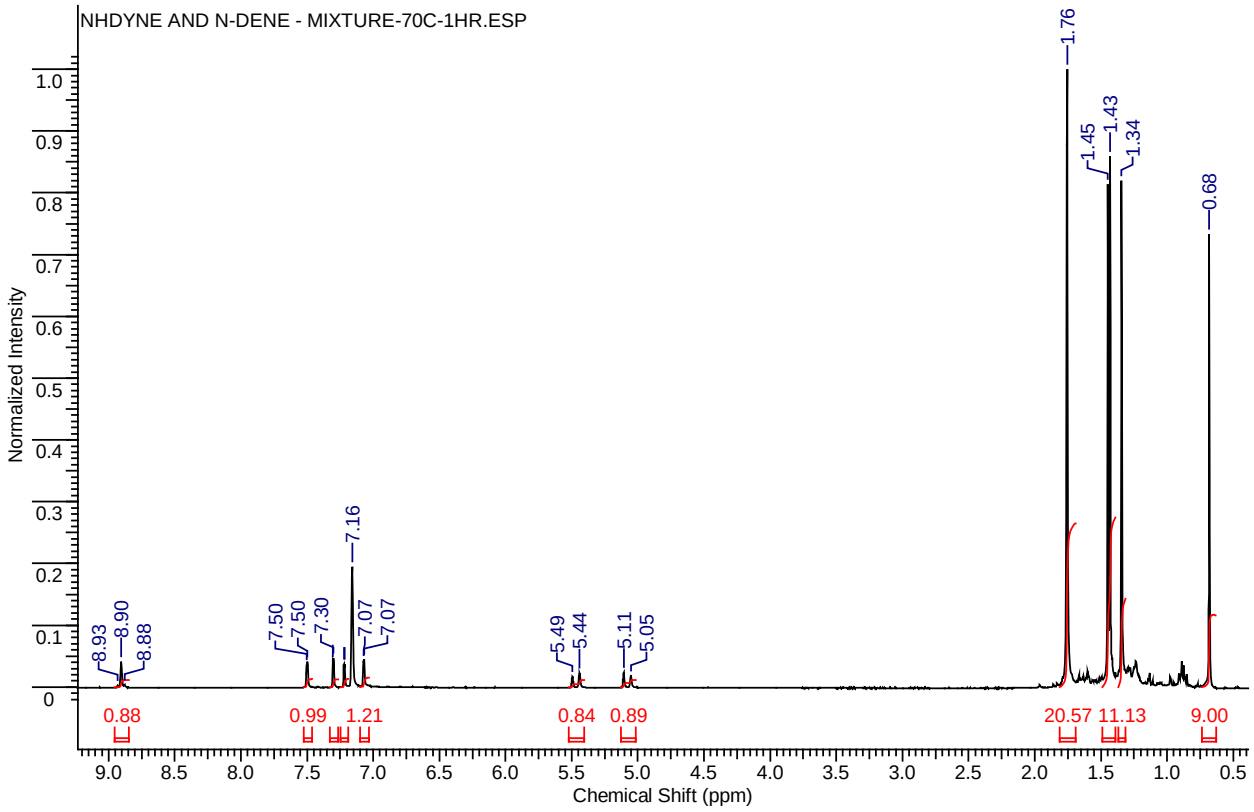

Figure S29. ^{1}H NMR spectrum of **3** (C_6D_6, 300 MHz, 25 °C)

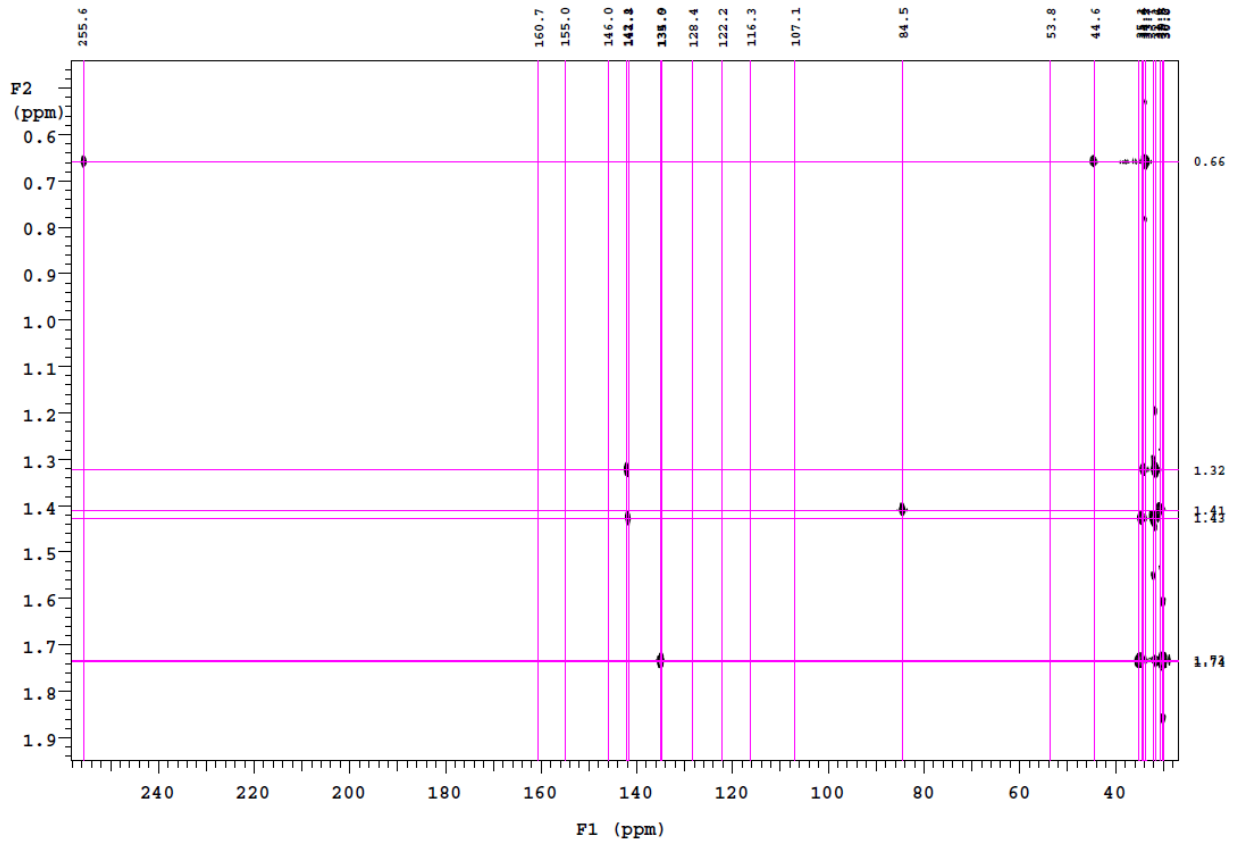

Figure S30. ^{1}H – ^{13}C *g*HMBC spectrum of **3** (500 MHz, C_6D_6, 25 °C)

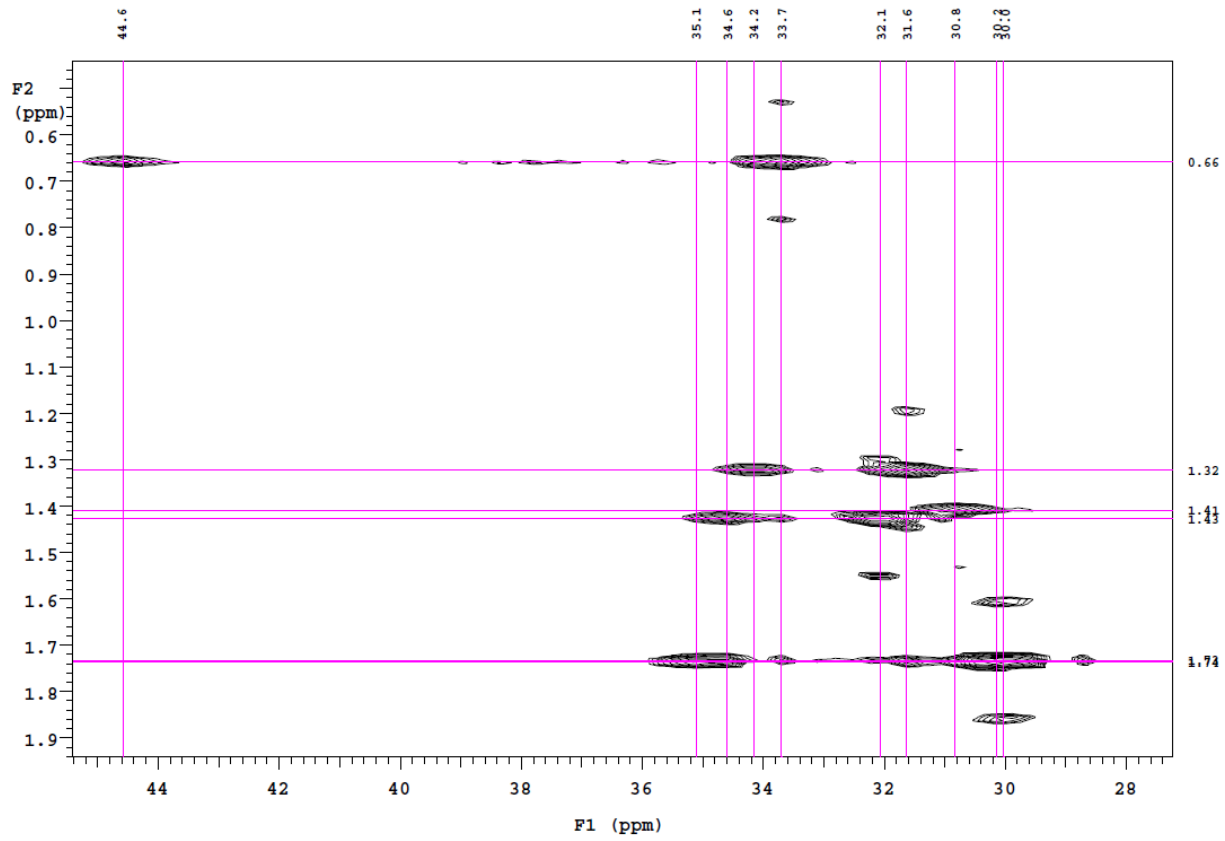

Figure S31. ^{1}H – ^{13}C *g*HMBC spectrum of **3** (500 MHz, C_6D_6, 25 °C)

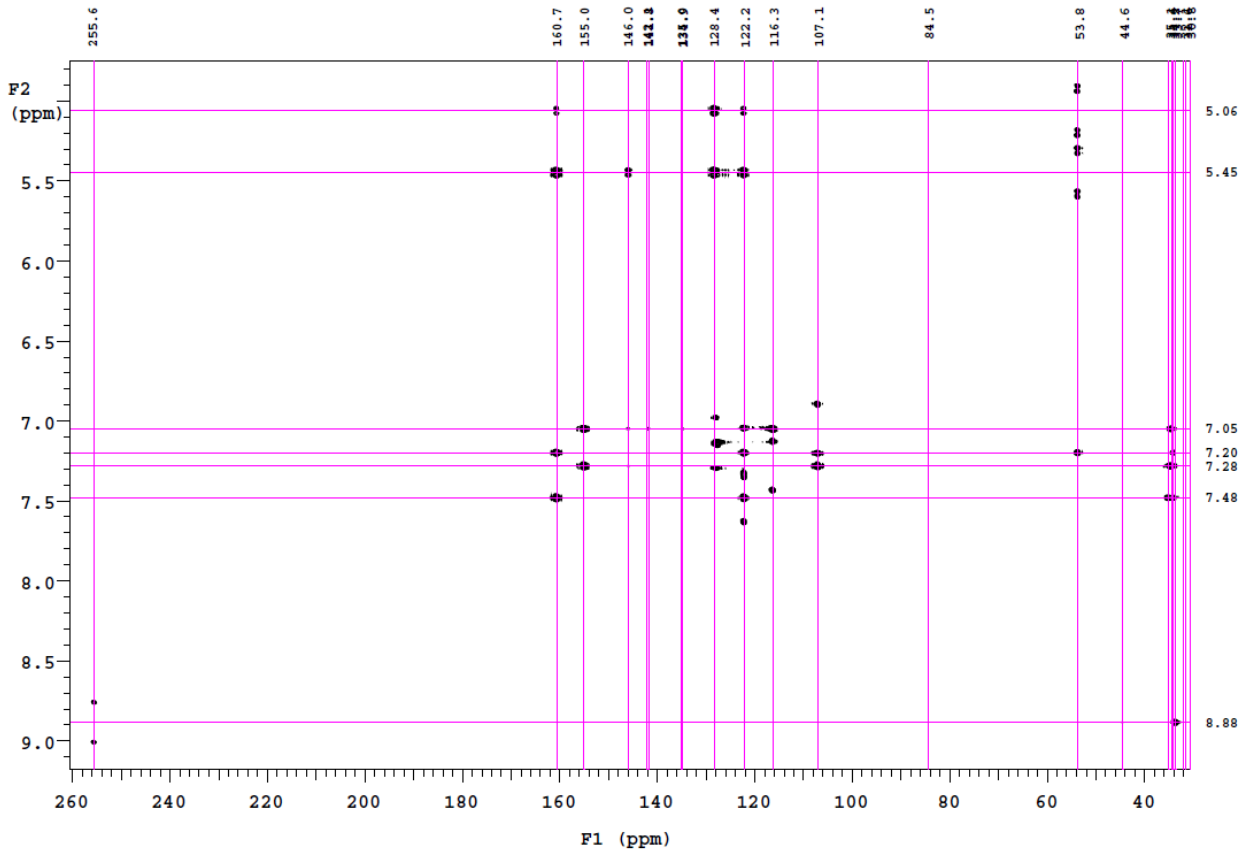

Figure S32. ^{1}H – ^{13}C *g*HMBC spectrum of **3** (500 MHz, C_6D_6, 25 °C)

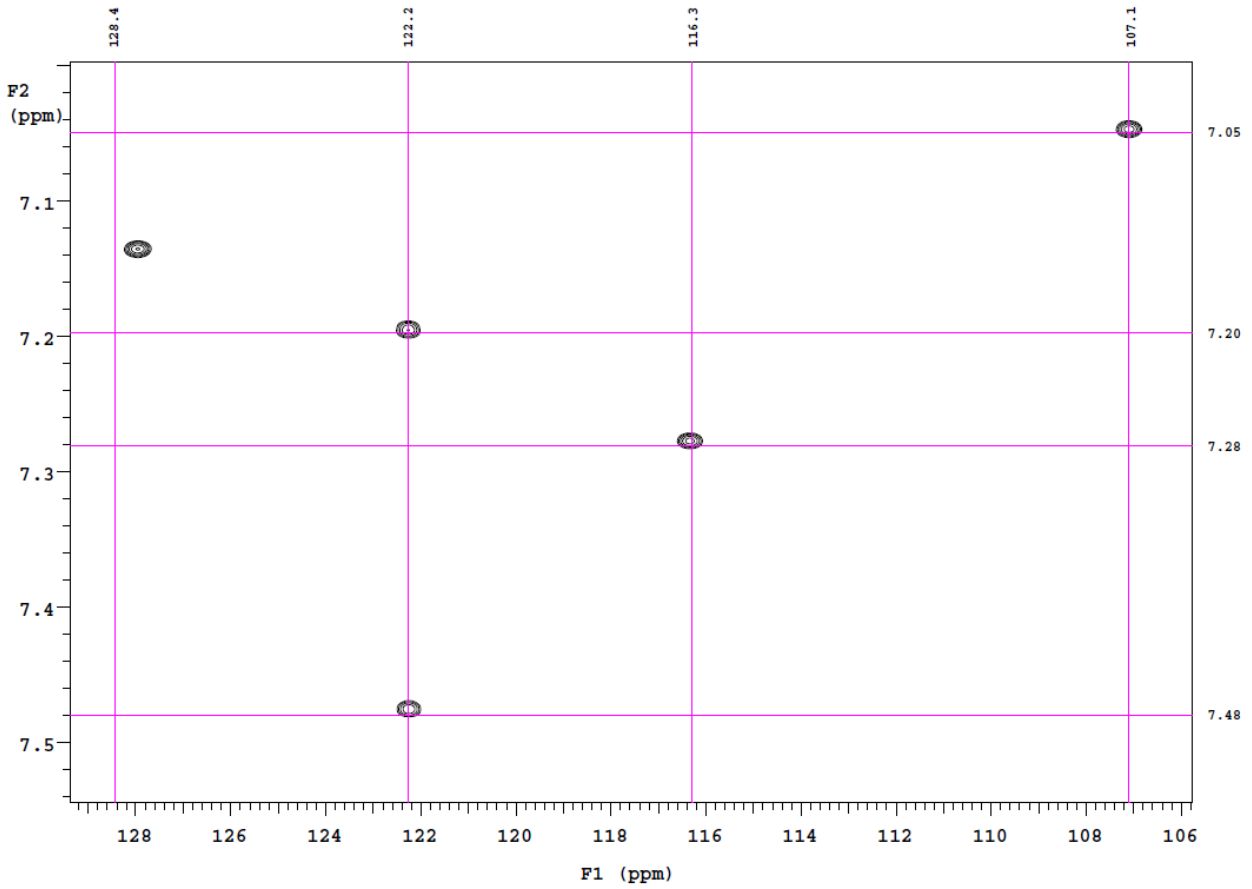

Figure S33. ^{1}H – ^{13}C *g*HSQC spectrum of **3** (500 MHz, C_6D_6, 25 °C)

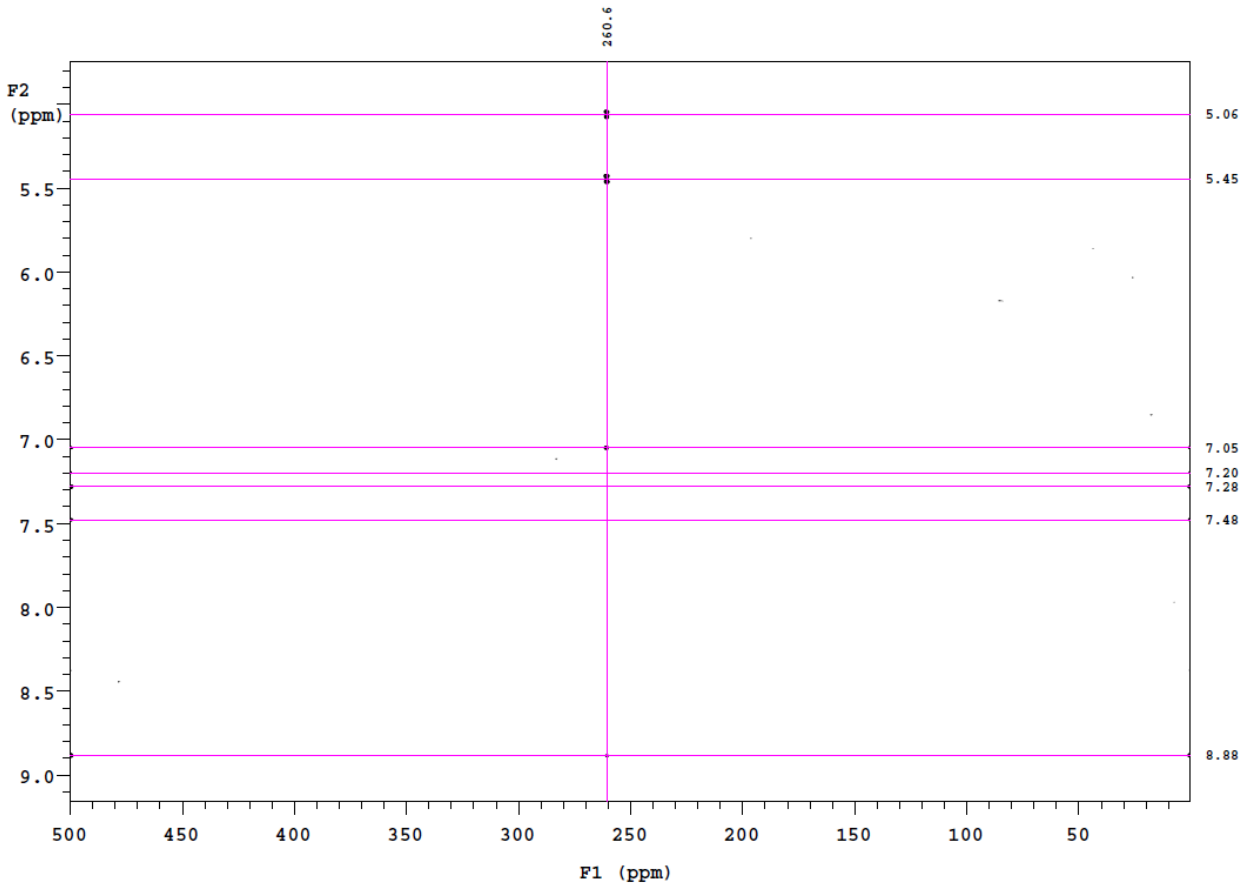

Figure S34. $^{1}H - {}^{15}N$ *g*HMBC spectrum of **3** (500 MHz, C_6D_6, 25 °C)

Synthesis of {MePPh$_3$}{[ON^{CH2}O]W≡C^{t}Bu(O^{t}Bu)} (4)

A pentane solution (5 mL) of **2** (173 mg, 0.227 mmol, 1.0 eq) was added in drops to the rapidly stirring pentane solution of $Ph_3P{=}CH_2$ (75 mg, 0.27 mmol, 1.2 eq); an immediate color change from yellow to orange was observed with the formation of a precipitate. The reaction mixture was stirred for 4 hours before being filtered through a medium porosity frit. The orange residue was washed with pentane (x3) and dried in vacuo to remove volatiles. (Yield = 226 mg, 96%) Crystals suitable for X-ray crystallography were grown from pentane diffusion into a concentrated THF solution of **4**.

Note: 2D NMR assignments were made using a benzene-d_6 solution of **4**. Additional 1D NMR experiments in THF-d_8 were performed to discern a few broad resonances. The methyl group

from $\underline{CH_3}PPh_3$ appears as a broad singlet in THF-d_8 (2.55 ppm); the $^{31}P\{^1H\}$ NMR spectrum of **4** which is extremely broad in C_6D_6 resolves as a sharp singlet in THF-d_8. The aromatic resonances for the phenyl groups in $CH_3P\underline{Ph_3}$ appear broad in both C_6D_6 and THF-d_8.

The resonances for **4** in THF-d_8 (for both ^1H and $^{13}C\{^1H\}$ NMR) essentially mirror the corresponding resonances in C_6D_6, making assignment rather straightforward.

^1H NMR (C_6D_6, 500 MHz, 25 °C): δ = 7.45 (d, 1H, $^3J_{HH}$ = 2.2 Hz, Ar-*H*), 7.27 (d, 1H, $^3J_{HH}$ = 2.2 Hz, Ar-*H*), 7.10 (br, 3H, Ar-*H*), 7.00 (br, 7H, Ar-*H*), 6.83 (d, 1H, $^3J_{HH}$ = 1.8 Hz), 6.68 (d, 1H, $^3J_{HH}$ = 1.8 Hz), 5.37 (d, 1H, $^2J_{HH}$ = 15.7 Hz), 5.1 (d, 1H, $^2J_{HH}$ = 15.7 Hz), 2.01 (s, 9H, OC(C*H*$_3$)$_3$), 1.84 (s, 9H, Ar-C(C*H*$_3$)$_3$), 1.80 (s, 9H, Ar-C(C*H*$_3$)$_3$), 1.46 (s, 9H, Ar-C(C*H*$_3$)$_3$), 1.39 (s, 9H, Ar-C(C*H*$_3$)$_3$), 1.15 (s, 9H, W≡C(C*H*$_3$)$_3$) ppm.

$^{13}C\{^1H\}$ NMR (C_6D_6, 125 MHz, 25 °C): δ = 290.6 (s, W≡*C*(C(CH$_3$)$_3$)), 161.5 (s, Ar-*C*), 156.0 (s, Ar-*C*), 153.1 (s, Ar-*C*), 138.4 (s, Ar-*C*), 137.3 (s, Ar-*C*), 136.6 (s, Ar-*C*), 134.3 (s, Ar-*C*), 132.4 (d, $^3J_{CP}$ = 10.9 Hz), 131.2 (s, Ar-*C*), 130.0 (d, $^3J_{CP}$ = 10.9 Hz), 129.4 (s, Ar-*C*), 122.4 (s, Ar-*C*), 120.1 (s, Ar-*C*), 118.7 (d, J_{CP} = 82.1 Hz), 107.0 (s, Ar-*C*), 102.6 (s, Ar-*C*), 76.5 (s, O*C*(CH$_3$)$_3$), 54.1 (s, *C*H$_2$), 49.1 (s, W≡C(*C*(CH$_3$)$_3$)), 35.7 (s, Ar-*C*(CH$_3$)$_3$), 35.2 (s, W≡C(C(*C*H$_3$)$_3$)), 34.8 (s, Ar-*C*(CH$_3$)$_3$), 34.6 (s, Ar-*C*(CH$_3$)$_3$), 34.1 (s, Ar-*C*(CH$_3$)$_3$), 34.1 (s, OC(*C*H$_3$)$_3$), 32.6 (s, Ar-C(*C*H$_3$)$_3$), 32.1 (s, Ar-C(*C*H$_3$)$_3$), 30.7 (s, Ar-C(*C*H$_3$)$_3$), 30.2 (s, Ar-C(*C*H$_3$)$_3$) ppm.

^{15}N NMR (From ^1H-^{15}N *g*HMBC, 500 MHz, C_6D_6): δ = 130.0 ppm

$^{31}P\{^1H\}$ NMR (121 MHz, C_6D_6): δ = 21.3 ppm (br)

^1H NMR (THF-d_8, 500 MHz, 25 °C): δ = 7.65 (br, 3H, Ar-*H*), 7.50 (br, 6H, Ar-*H*), 7.43 (br, 6H, Ar-*H*), 7.08 (br d, 1H, $^4J_{HH}$ = nm, Ar-*H*), 6.97 (br d, 1H, $^4J_{HH}$ = nm, Ar-*H*), 6.34 (br d, 1H, $^4J_{HH}$ = nm, Ar-*H*), 6.28 (br d, 1H, $^4J_{HH}$ = nm, Ar-*H*), 4.75 (d, 1H, $^2J_{HH}$ = 15.4 Hz, C*H*$_2$), 4.66 (d, 1H, $^2J_{HH}$ = 15.4 Hz, C*H*$_2$), 2.55 (br s, 3H, $^2J_{HP}$ = nm, C*H*$_3$PPh$_3$), 1.62 (s, 9H, OC(C*H*$_3$)$_3$), 1.44 (s, 9H,

Ar-C(CH_3)$_3$), 1.41 (s, 9H, Ar-C(CH_3)$_3$), 1.30 (s, 9H, Ar-C(CH_3)$_3$), 1.28 (s, 9H, Ar-C(CH_3)$_3$), 0.73 (s, 9H, W≡C(C(CH_3)$_3$)) ppm.

^{13}C{^{1}H} NMR (THF-d_8, 125 MHz, 25 °C): δ = 290.1 (s, W≡*C*(C(CH$_3$)$_3$)), 162.3 (s, Ar-*C*), 156.8 (s, Ar-*C*), 153.8 (s, Ar-*C*), 138.7 (s, Ar-*C*), 137.5 (s, Ar-*C*), 136.8 (s, Ar-*C*), 135.8 (s, Ar-*C*), 134.1 (d, $^3J_{CP}$ = 10.5 Hz), 131.3 (d, $^3J_{CP}$ = 12.6 Hz), 131.3 (s, Ar-*C*), 130.3 (s, Ar-*C*), 129.2 (s, Ar-*C*), 123.0 (s, Ar-*C*), 121.7 (d, J_{CP} = 88.2 Hz), 120.6 (s, Ar-*C*), 107.2 (s, Ar-*C*), 103.0 (s, Ar-*C*), 76.8 (s, O*C*(CH$_3$)$_3$), 54.5 (s, *C*H$_2$), 49.4 (s, W≡C(*C*(CH$_3$)$_3$)), 36.2 (s, Ar-*C*(CH$_3$)$_3$), 35.6 (s, W≡C(C(*C*H$_3$)$_3$)), 35.2 (s, Ar-*C*(CH$_3$)$_3$), 35.2 (s, Ar-*C*(CH$_3$)$_3$), 34.8 (s, Ar-*C*(CH$_3$)$_3$), 34.4 (s, OC(*C*H$_3$)$_3$), 33.2 (s, Ar-C(*C*H$_3$)$_3$), 32.7 (s, Ar-C(*C*H$_3$)$_3$), 31.3 (s, Ar-C(*C*H$_3$)$_3$), 30.6 (s, Ar-C(*C*H$_3$)$_3$) ppm.

^{31}P{^{1}H} NMR (121 MHz, C_6D_6): δ = 21.7 ppm

^{15}N NMR: δ = not measured

Anal. Calcd. for $C_{57}H_{78}NO_3PW$: C, 65.82%; H, 7.56%; N, 1.35%. Found: C, 65.69%; H, 7.34%; N, 1.57%.

NMR Characterization of {$MePPh_3$}{[$ON^{CH2}O$]W≡C^{t}Bu(O^{t}Bu)} (4)

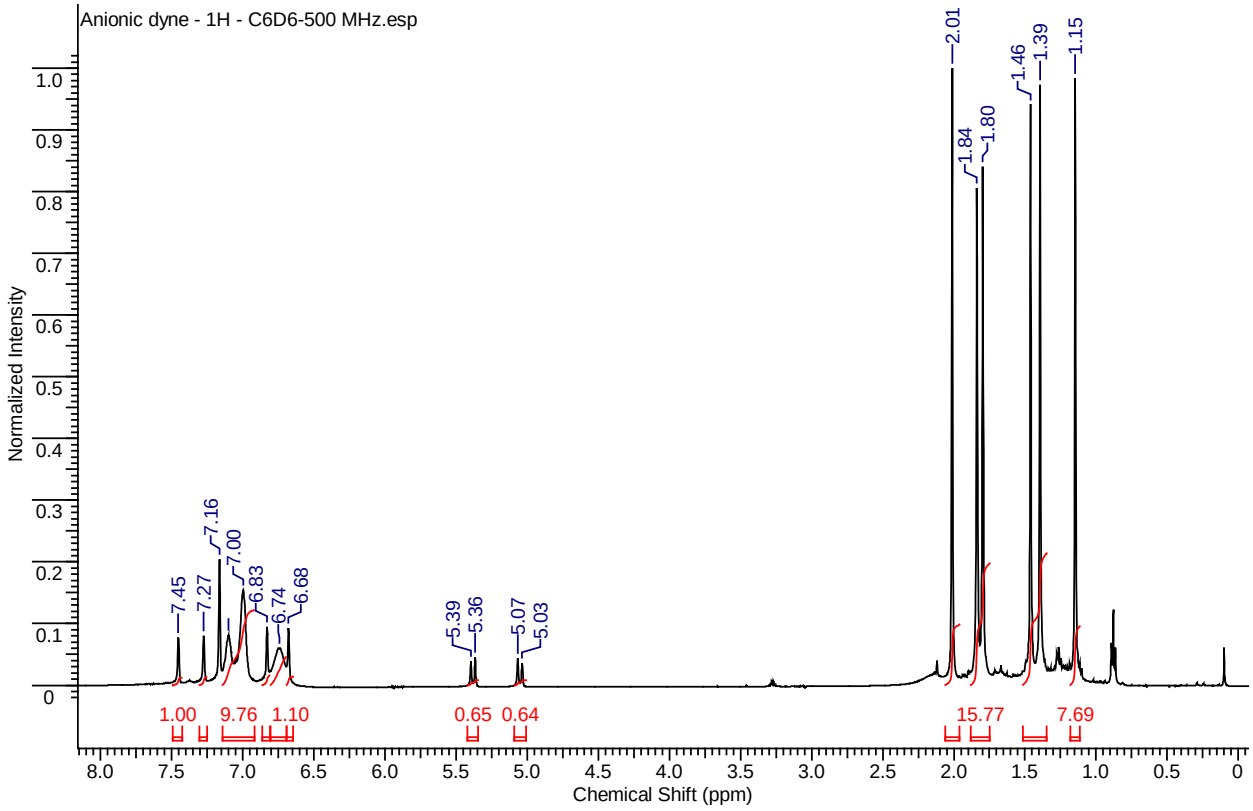

Figure S35. ^{1}H NMR spectrum of **4** (C_6D_6, 500 MHz, 25 °C)

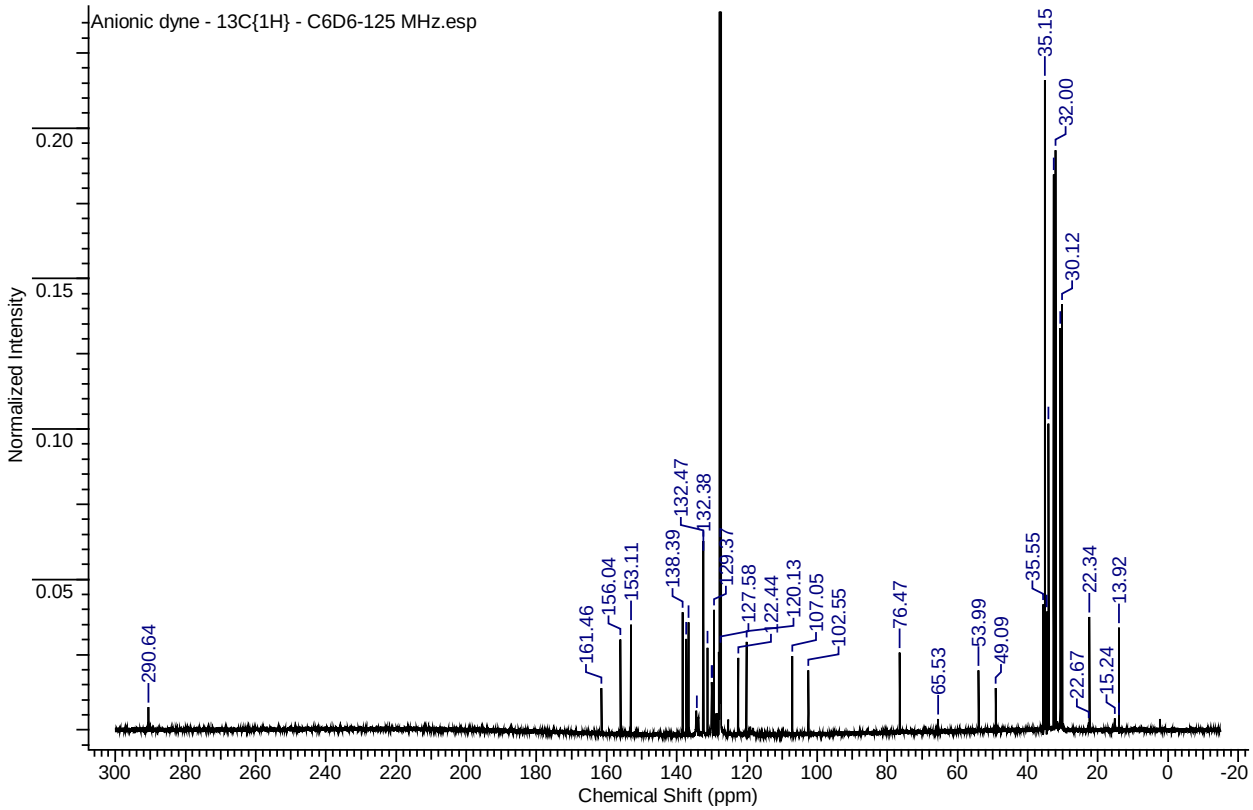

Figure S36. $^{13}C\{^{1}H\}$ NMR spectrum of **4** (C_6D_6, 125 MHz, 25 °C)

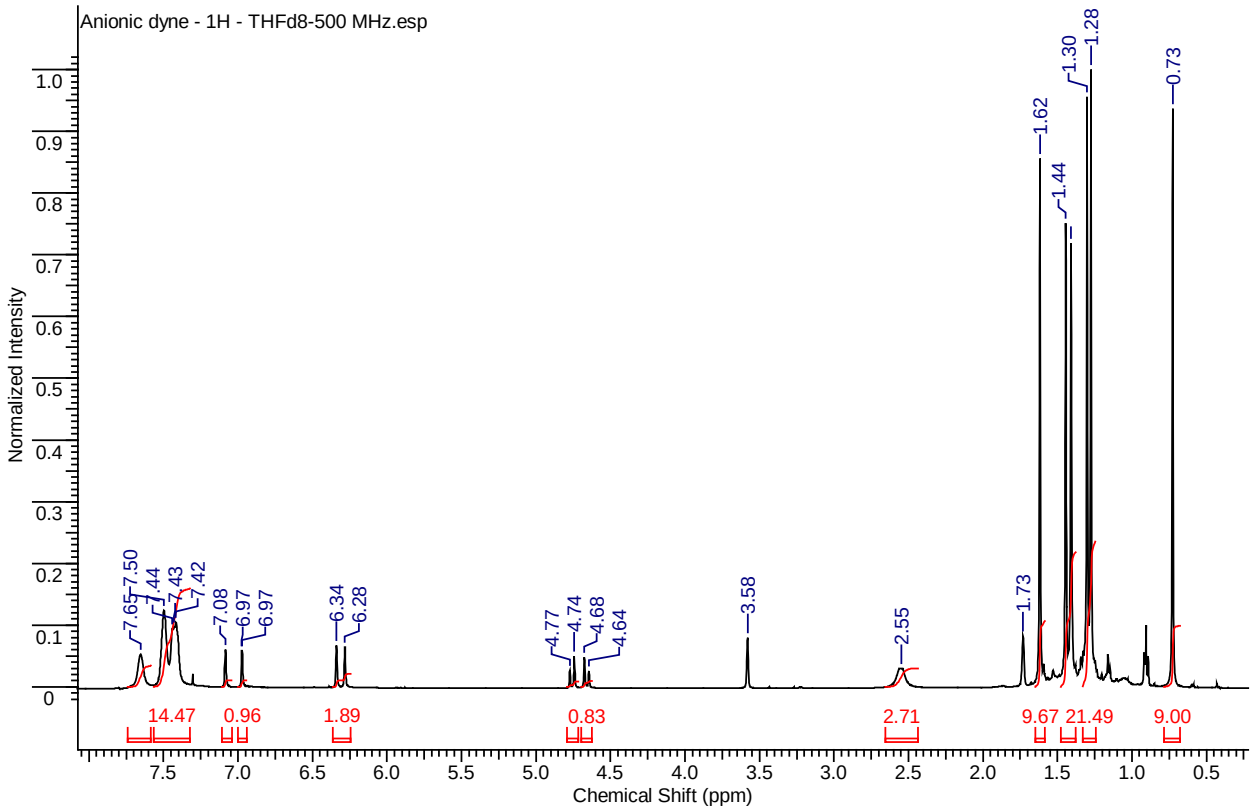

Figure S37. ^{1}H NMR spectrum of **4** (THF-d_8, 500 MHz, 25 °C)

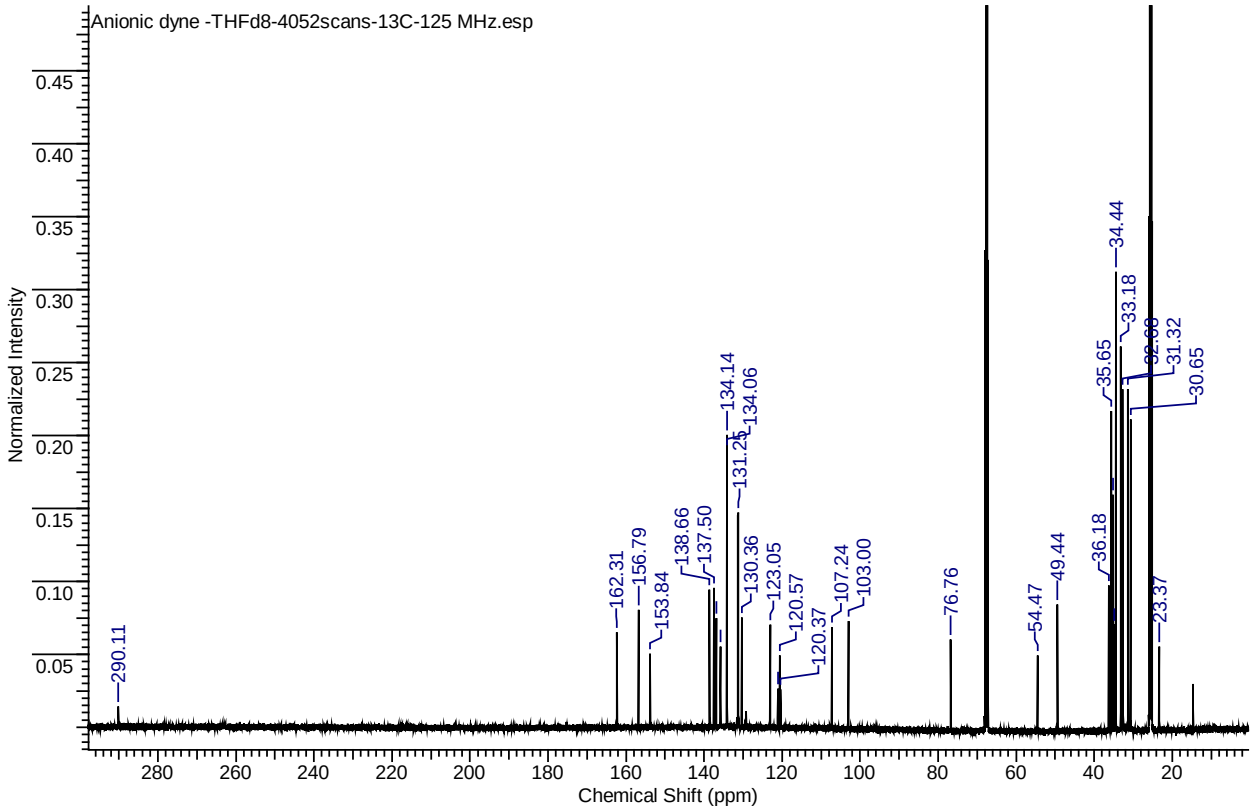

Figure S38. $^{13}C\{^{1}H\}$ NMR spectrum of **4** (THF-d_8, 125 MHz, 25 °C)

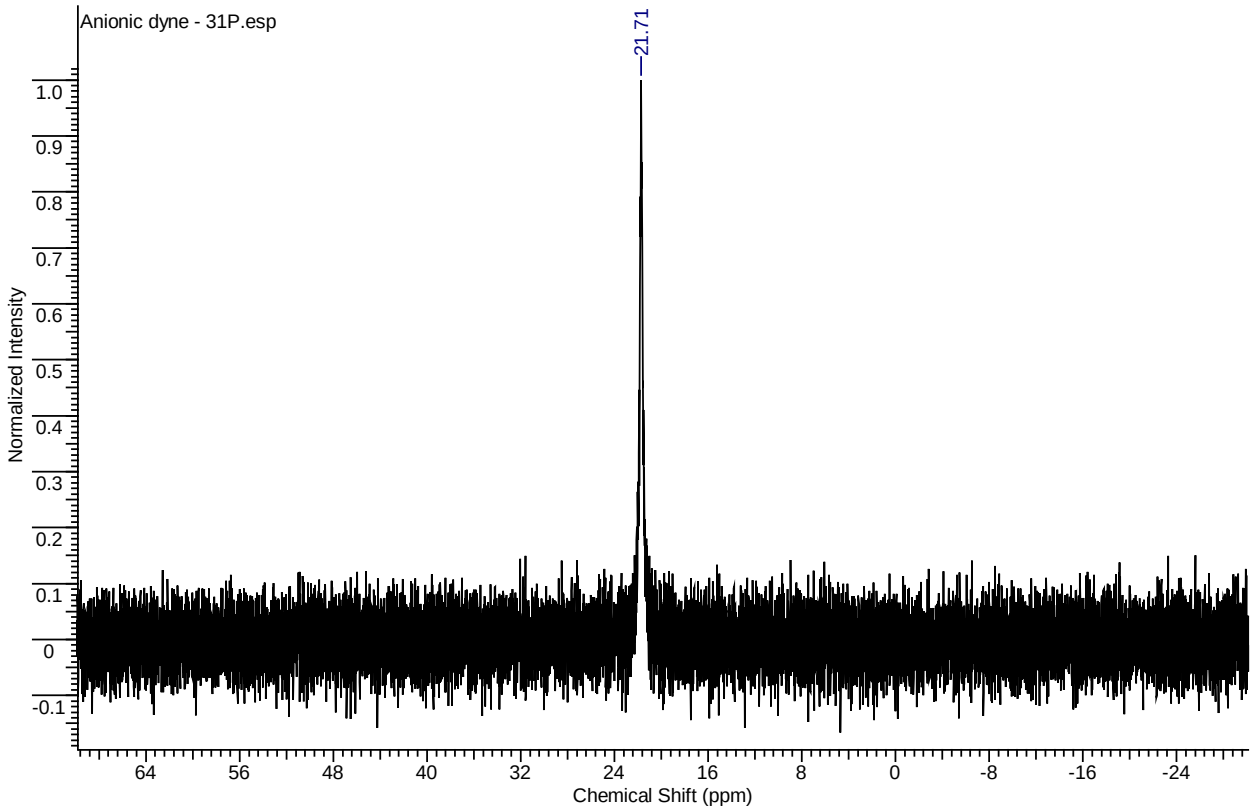

Figure S39. $^{31}P\{^{1}H\}$ NMR spectrum of **4** (THF-d_8, 121.5 MHz, 25 °C)

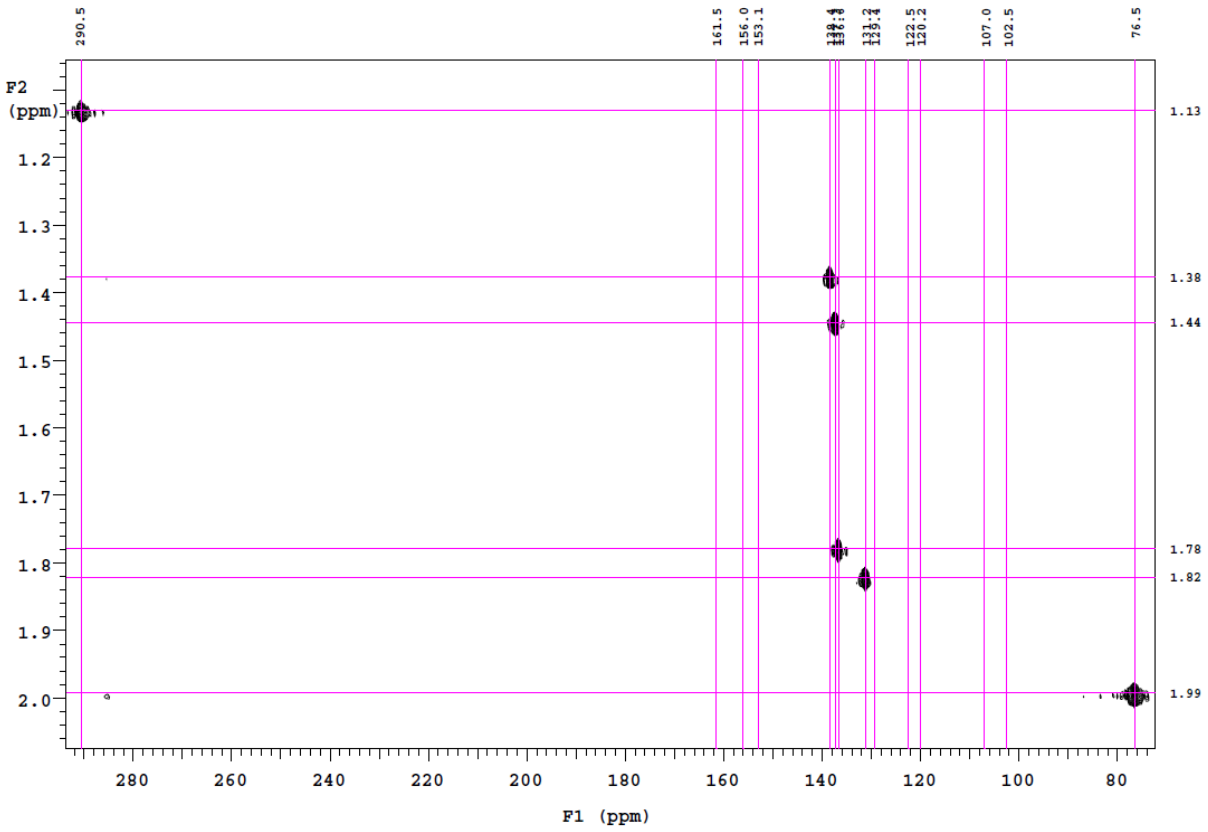

Figure S40. ^{1}H – ^{13}C *g*HMBC spectrum of **4** (500 MHz, C_6D_6, 25 °C)

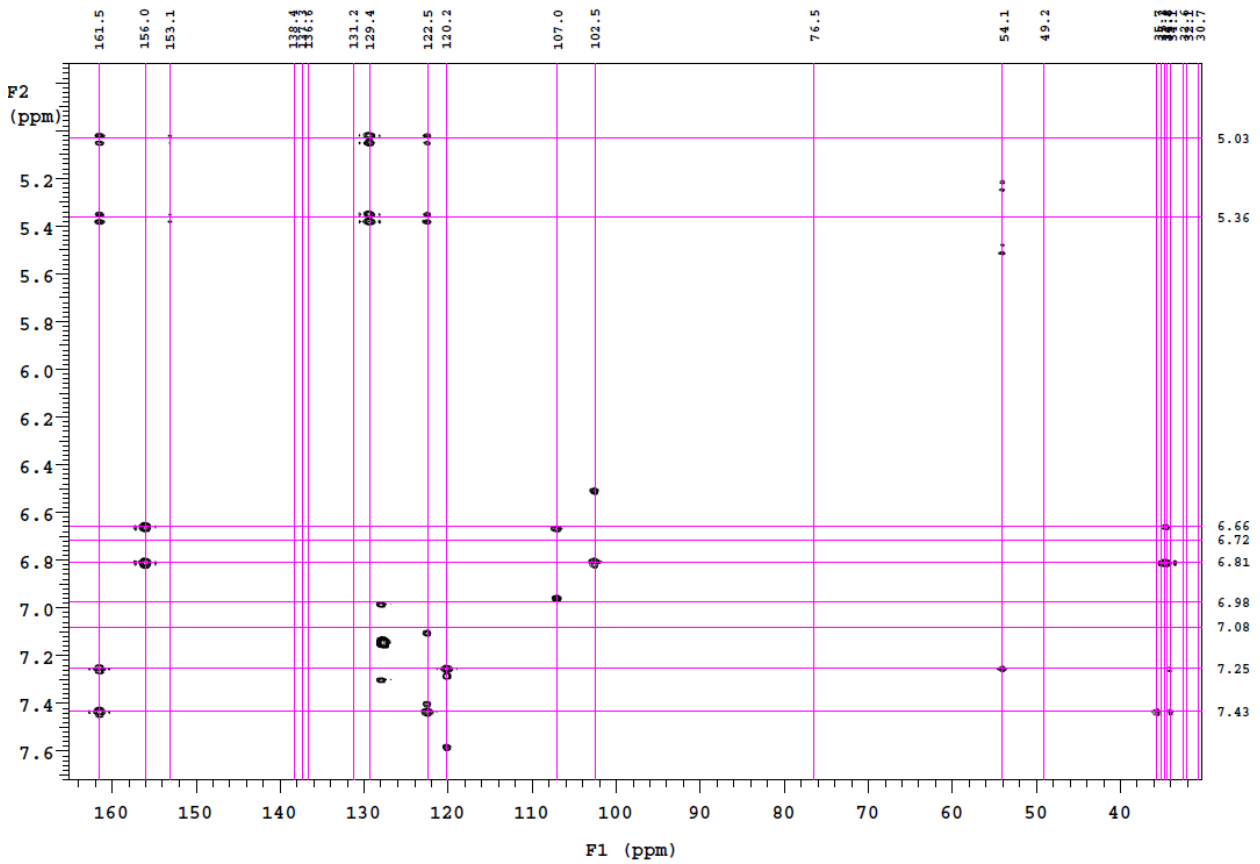

Figure S41. ^{1}H – ^{13}C *g*HMBC spectrum of **4** (500 MHz, C_6D_6, 25 °C)

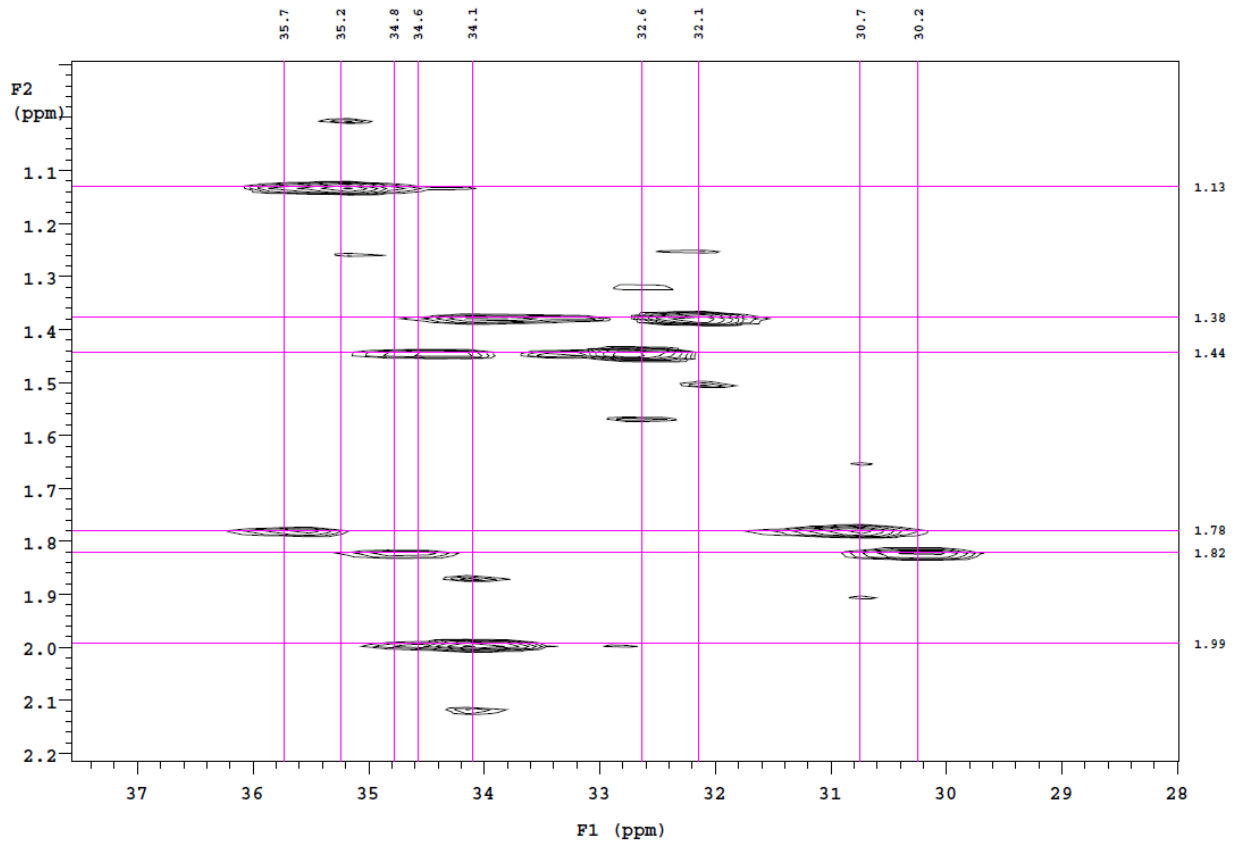

Figure S42. ^{1}H – ^{13}C *g*HMBC spectrum of **4** (500 MHz, C_6D_6, 25 °C)

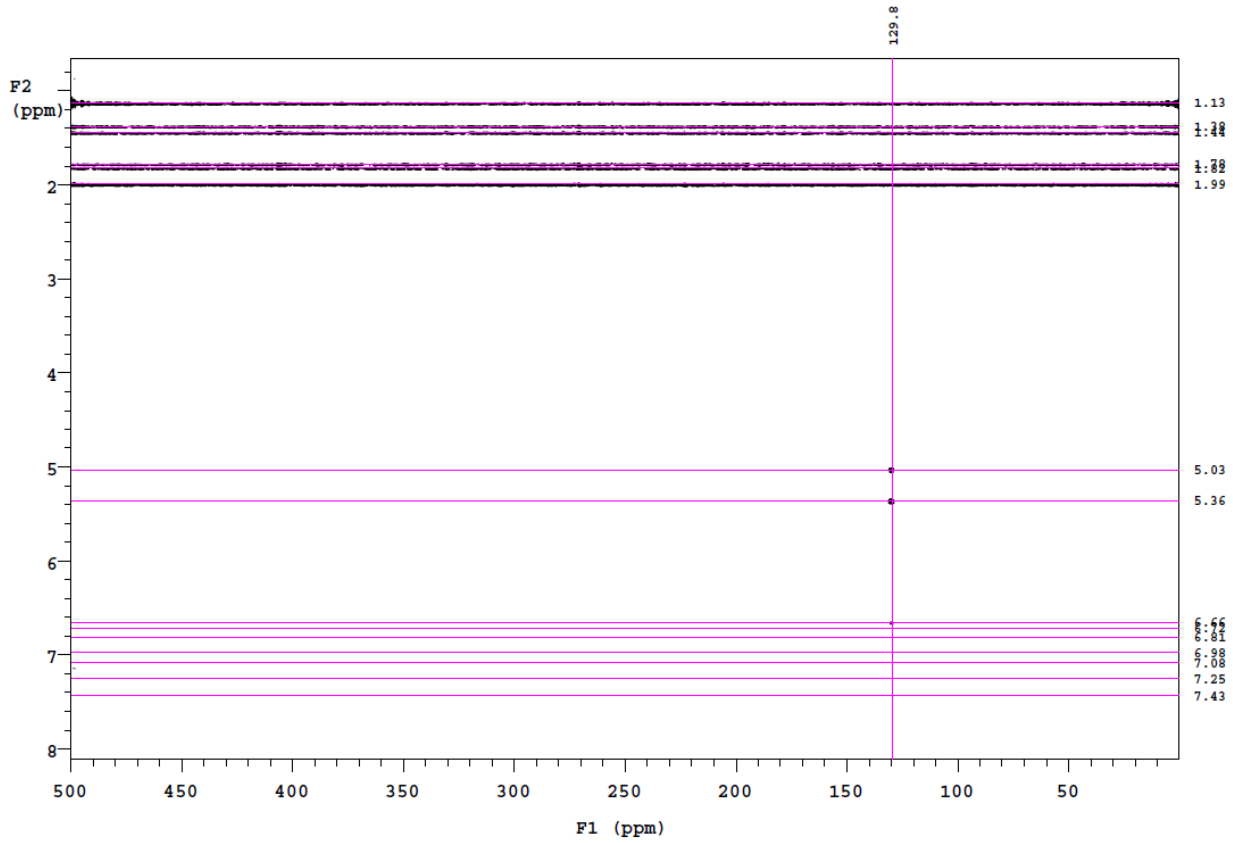

Figure S43. ^{1}H – ^{15}N *g*HMBC spectrum of **4** (500 MHz, C_6D_6, 25 °C)

Synthesis of [ON^{CH2}O]W($CH_2C(CH_3)_3$)(O^tBu)Cl (5)

In the glove-box, (^{t}BuO)$_3$W≡C^{t}Bu (163 mg, 0.345 mmol) in 2 mL C_6H_6 was added in drops to a C_6H_6 suspension of **1·HCl** (161 mg, 0.338 mmol) and mixed well with a pipette. The deep brown-red suspension becomes homogeneous within fifteen minutes of stirring at ambient temperature. After the reaction mixture was stirred for 15 h, all volatiles were removed in vacuo leaving behind a deep brown residue. Pentane trituration (3x) and extensive drying yields **5**. (Yield = 220 mg, 80.9%). Crystals suitable for X-ray interrogation can be grown by the slow evaporation of a concentrated diethyl ether solution of **5** at ambient temperature.

Complex **5** can also be accessed through addition of 2 equiv of HCl in Et_2O to **4**.

^{1}H NMR (300 MHz, C_6D_6, 25 °C): δ = 7.49 (d, 1H, $^4J_{HH}$ = 2.3 Hz, Ar-*H*), 7.22 (d, 1H, $^4J_{HH}$ = 2.3 Hz, Ar-*H*), 6.75 (d, 1H, $^4J_{HH}$ = 1.8 Hz, Ar-*H*), 6.65 (d, 1H, $^4J_{HH}$ = 1.8 Hz, Ar-*H*), 6.64 (d, 1H, $^2J_{HH}$ = 20.4 Hz, NC*H*$_2$), 6.29 (d, 1H, $^2J_{HH}$ = 20.4 Hz, NC*H*$_2$), 2.41 (d, 1H, $^2J_{HH}$ = 14.1 Hz, WC*H*$_2$^{t}Bu), 2.20 (d, 1H, $^2J_{HH}$ = 14.1 Hz, WC*H*$_2$^{t}Bu), 1.75 (s, 9H, OC(C*H*$_3$)$_3$), 1.62 (s, 9H, Ar-C(C*H*$_3$)$_3$), 1.56 (s, 9H, Ar-C(C*H*$_3$)$_3$), 1.26 (s, 9H, Ar-C(C*H*$_3$)$_3$), 1.24 (s, 9H, Ar-C(C*H*$_3$)$_3$), 0.96 (s, 9H, WCH$_2$(C(C*H*$_3$)$_3$)) ppm.

^{13}C{^{1}H} NMR (125 MHz, C_6D_6, 25 °C): δ = 155.5 (s, Ar-*C*), 150.9 (s, Ar-*C*), 149.8 (s, Ar-*C*), 147.1 (s, Ar-*C*), 146.2 (s, Ar-*C*), 137.4 (s, Ar-*C*), 135.2 (s, Ar-*C*), 128.3 (s, Ar-*C*), 123.2 (s, Ar-*C*), 123.2 (s, Ar-*C*), 123.0 (s, Ar-*C*), 109.4 (s, Ar-*C*), 93.5 (s, W*C*H$_2$^{t}Bu), 90.1 (s, O*C*(CH$_3$)$_3$), 52.7 (s, N*C*H$_2$), 37.4 (s, WCH$_2$(*C*(CH$_3$)$_3$)), 35.5 (s, Ar(*C*(CH$_3$)$_3$)), 34.9 (s, Ar(*C*(CH$_3$)$_3$)), 34.8 (s, Ar(*C*(CH$_3$)$_3$)), 34.7 (s, WCH$_2$(C(*C*H$_3$)$_3$)), 32.0 (s, Ar(C(*C*H$_3$)$_3$)), 31.6 (s, Ar(C(*C*H$_3$)$_3$)), 30.8 (s, Ar(C(*C*H$_3$)$_3$)), 30.2 (s, OC(*C*H$_3$)$_3$), 30.0 ppm (s, Ar(C(*C*H$_3$)$_3$)) ppm.

^{15}N NMR (From ^{1}H-^{15}N *g*HMBC, 500 MHz, C_6D_6, 25 °C): δ = 299.8 ppm

Anal. Calcd. for $C_{38}H_{62}ClNO_3W$: C, 57.04%; H, 7.81%; N, 1.75%. Found: C, 56.99%; H, 7.94%; N, 2.01%.

NMR Characterization of 5

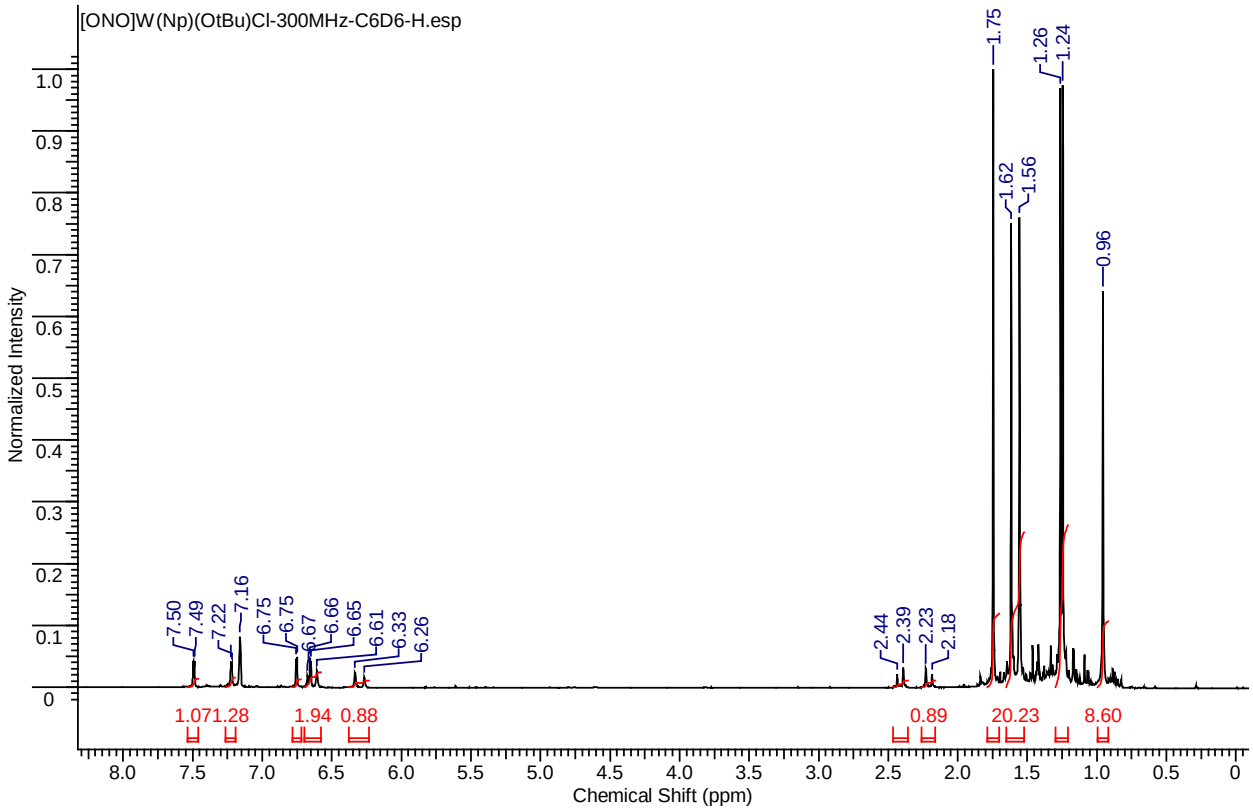

Figure S44. ^{1}H NMR spectrum of **5** (300 MHz, C_6D_6, 25 °C)

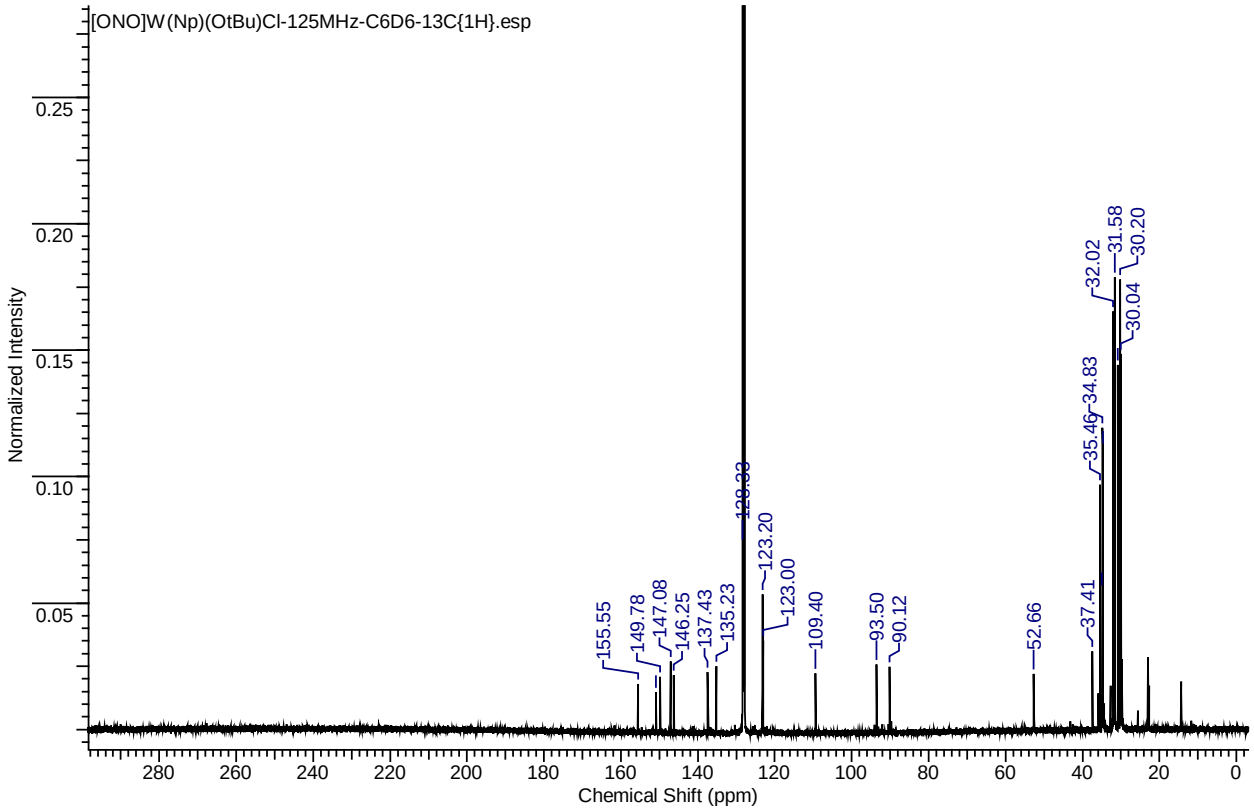

Figure S45. $^{13}C\{^{1}H\}$ NMR spectrum of **5** (125 MHz, C_6D_6, 25 °C)

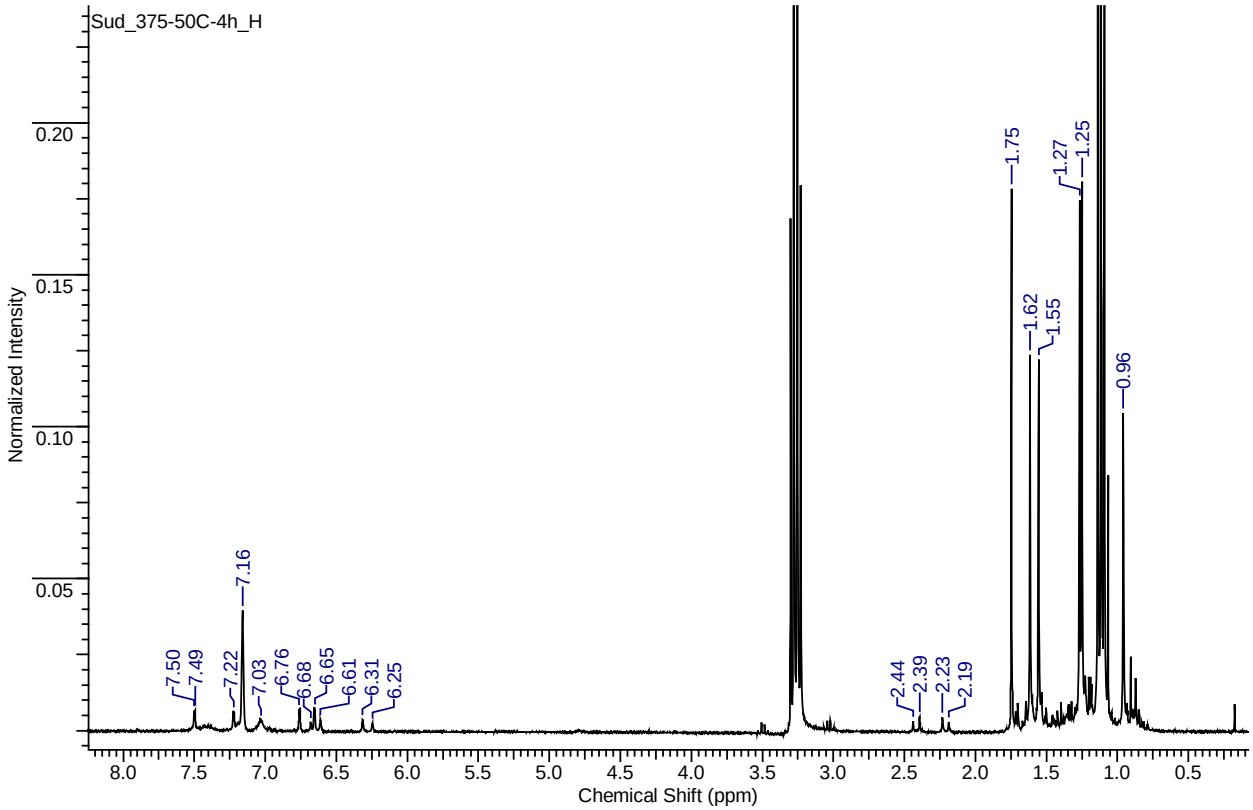

Figure S46. Synthesis of complex **5** through addition of 2 equiv HCl (as an Et_2O solution) to **4.**

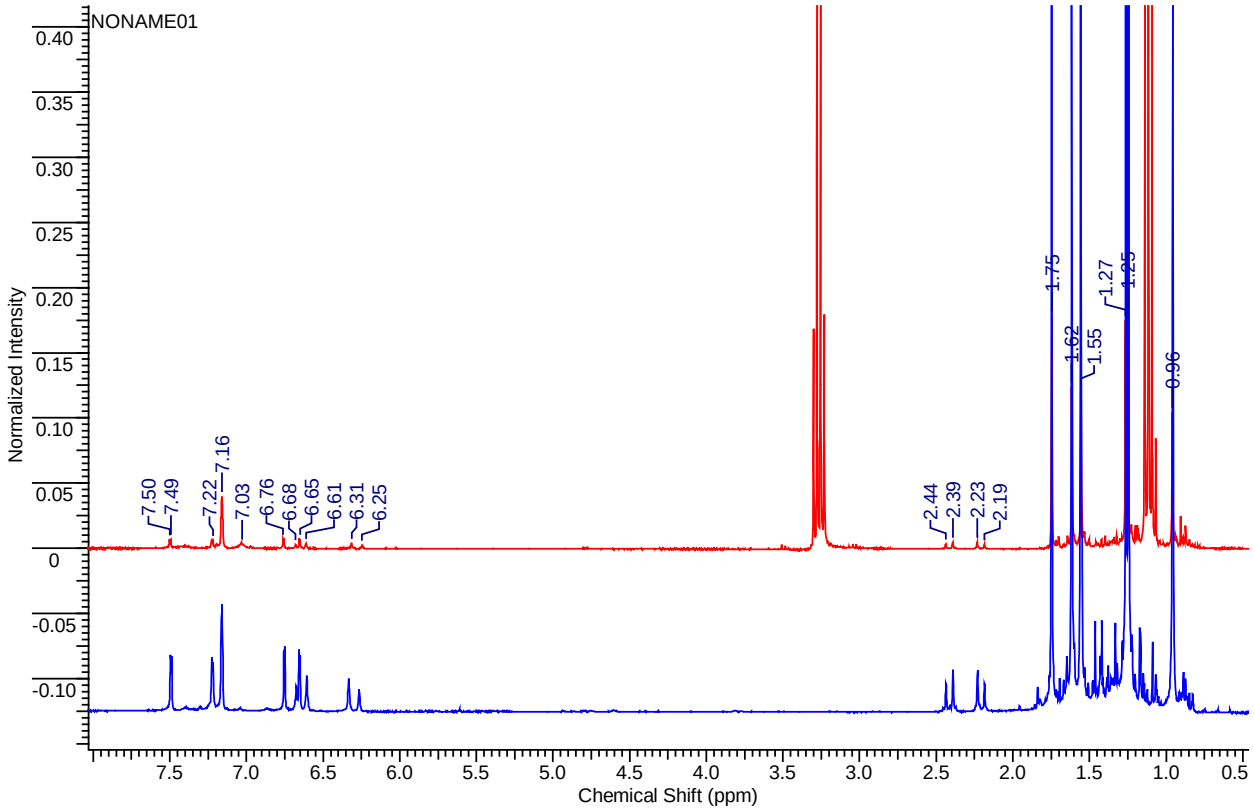

Figure S47. Comparison of methods: (BLUE) Synthesis of complex **5** through addition of **1·HCl** to (^{t}BuO)$_3$W≡C^{t}Bu; (RED) addition of 2 equiv HCl (as an Et_2O solution) to **4.**

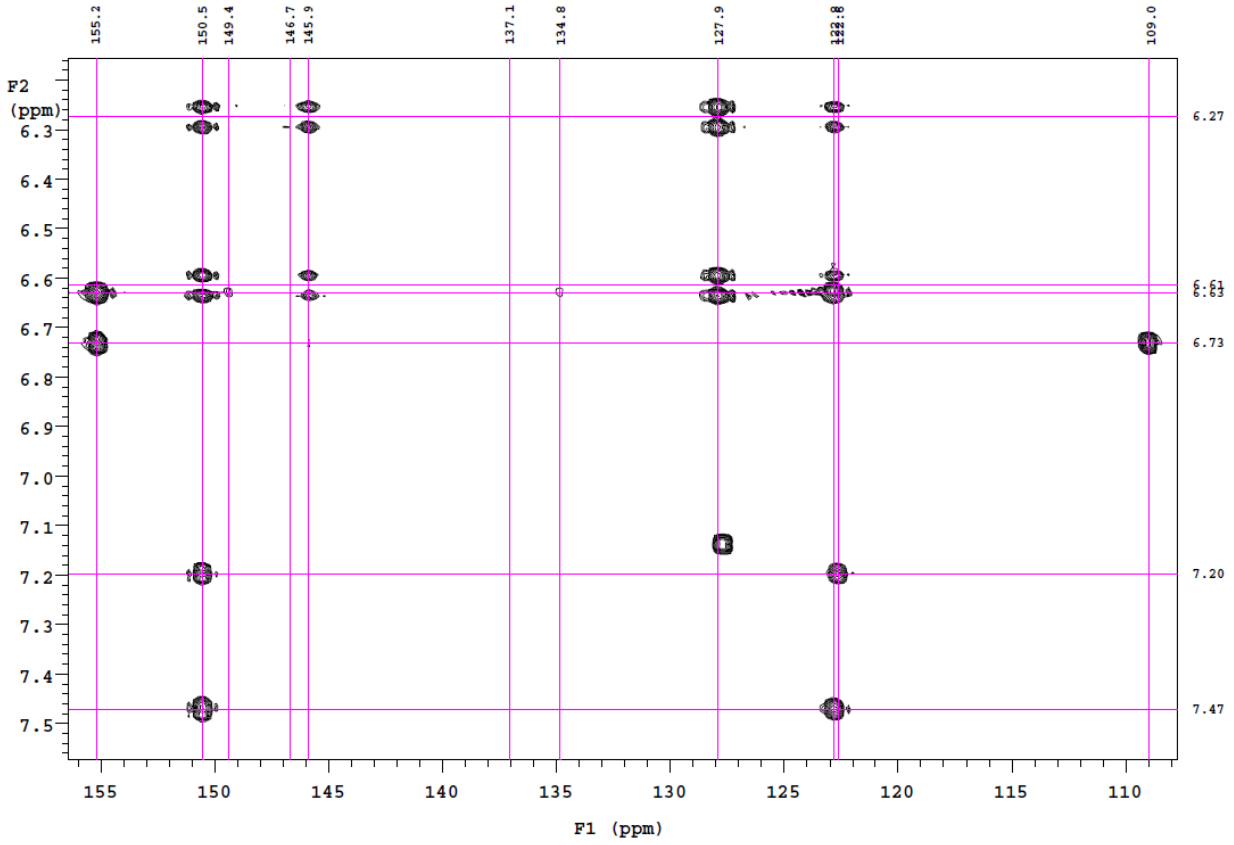

Figure S48. ^{1}H-^{13}C NMR *g*HMBC spectrum of **5** (500 MHz, C_6D_6, 25 °C)

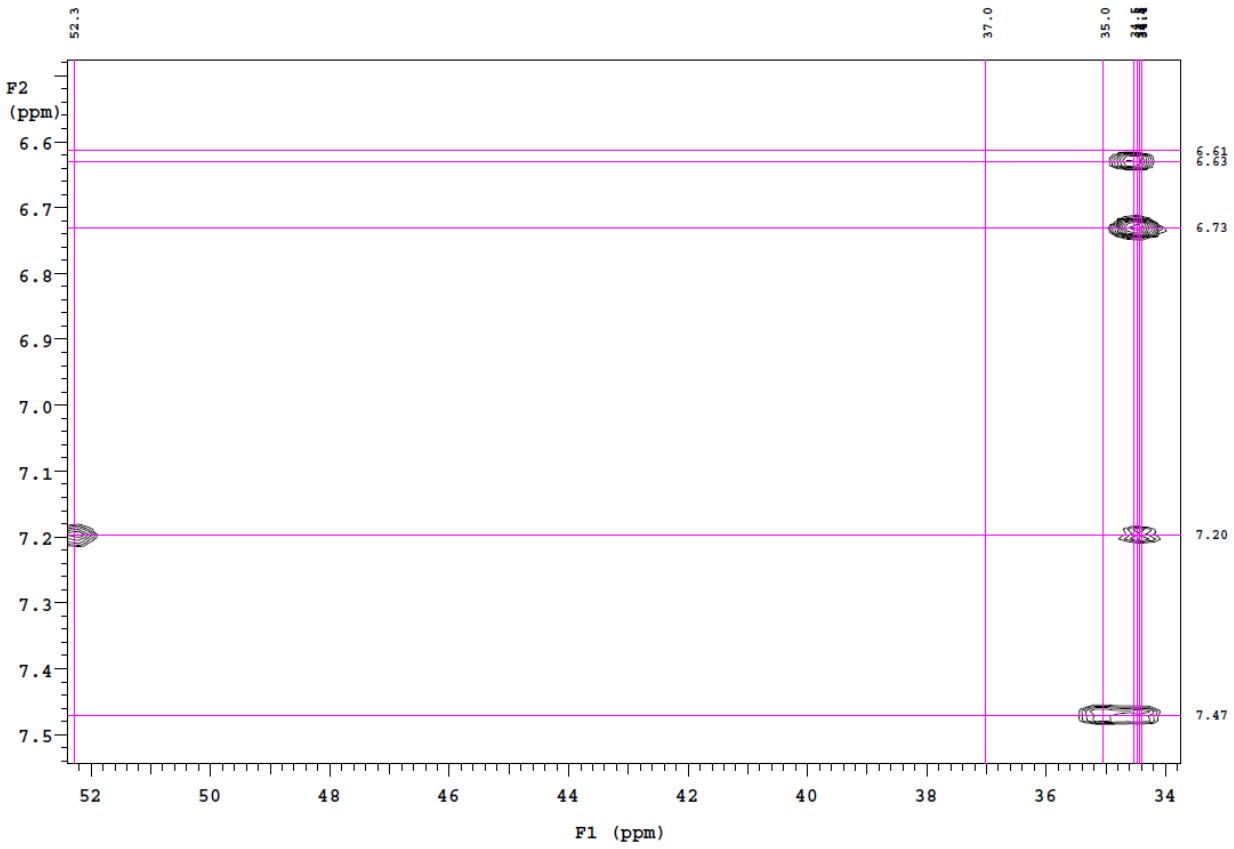

Figure S49. ^{1}H-^{13}C NMR *g*HMBC spectrum of **5** (500 MHz, C_6D_6, 25 °C)

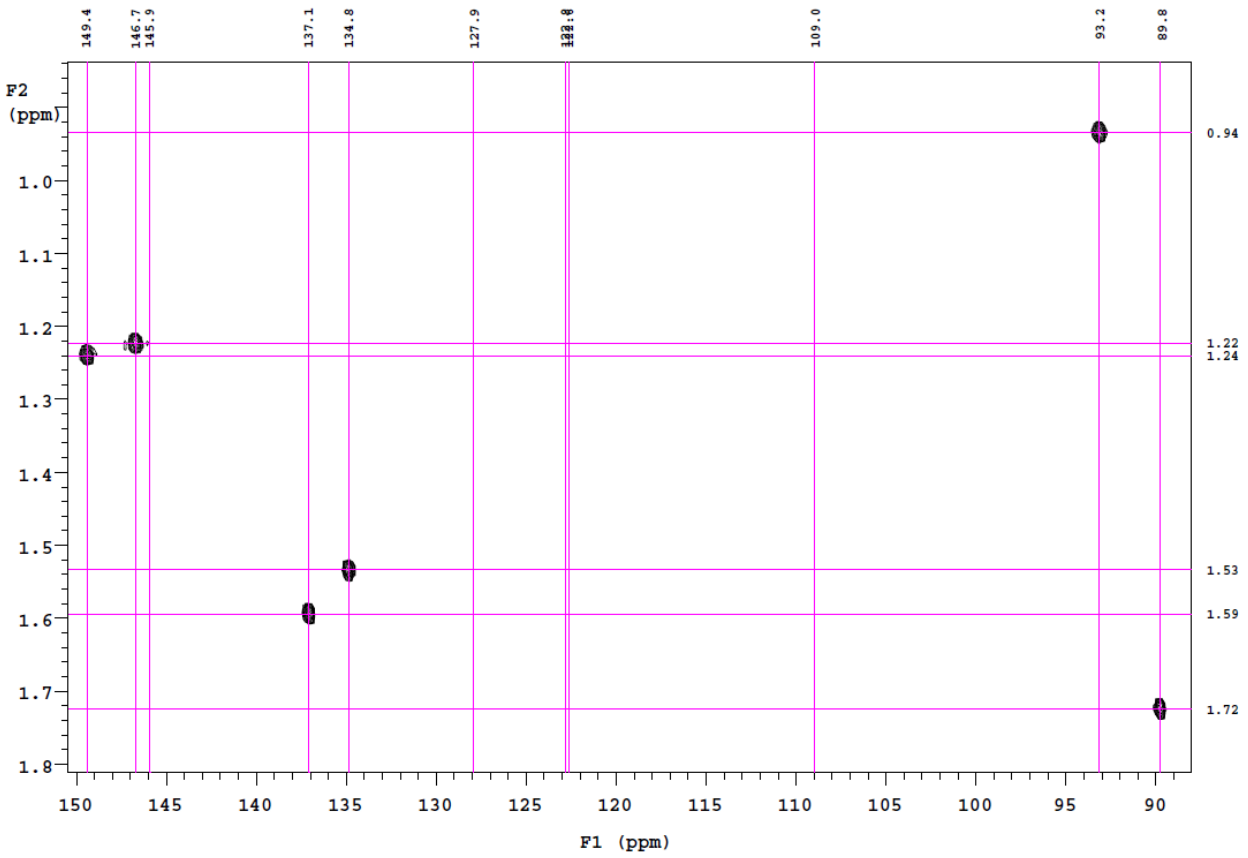

Figure S50. ^{1}H-^{13}C NMR *g*HMBC spectrum of **5** (500 MHz, C_6D_6, 25 °C)

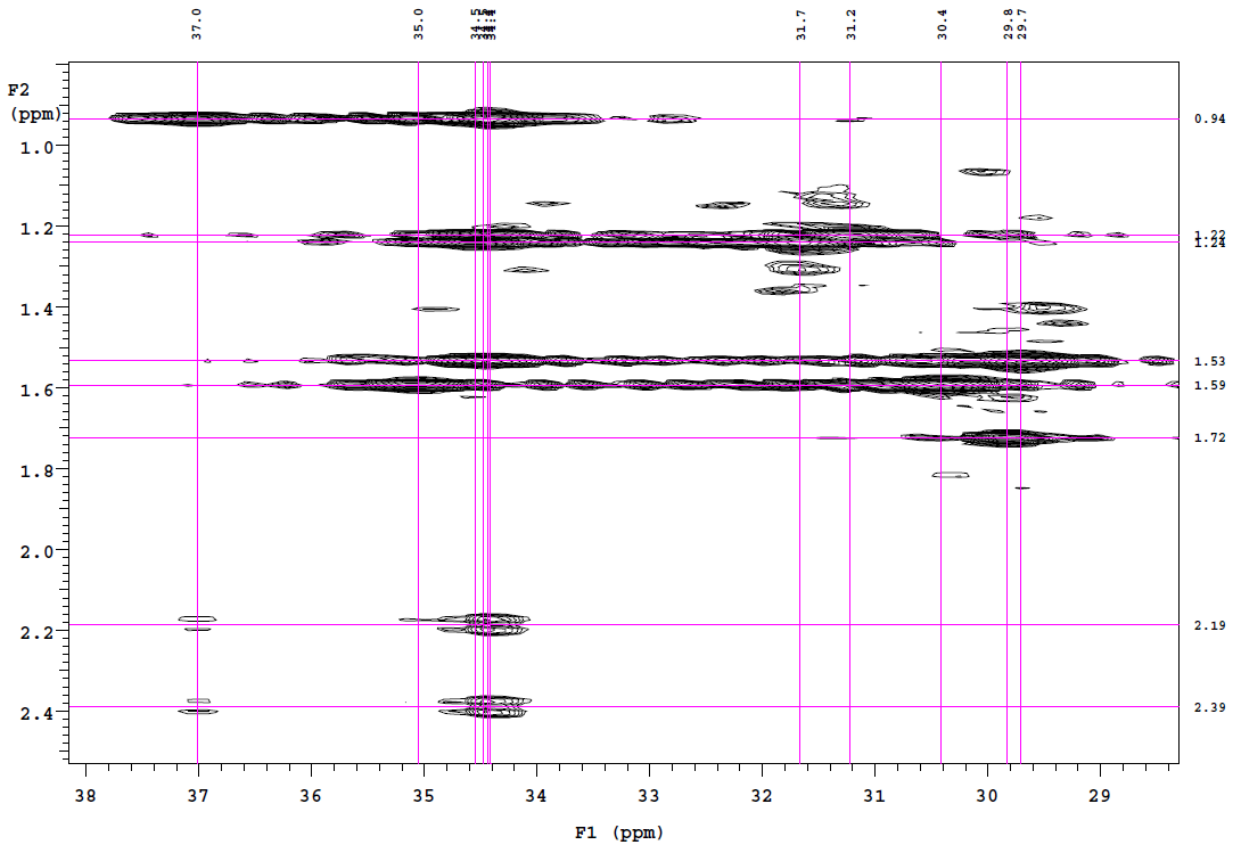

Figure S51. ^{1}H-^{13}C NMR *g*HMBC spectrum of **5** (500 MHz, C_6D_6, 25 °C)

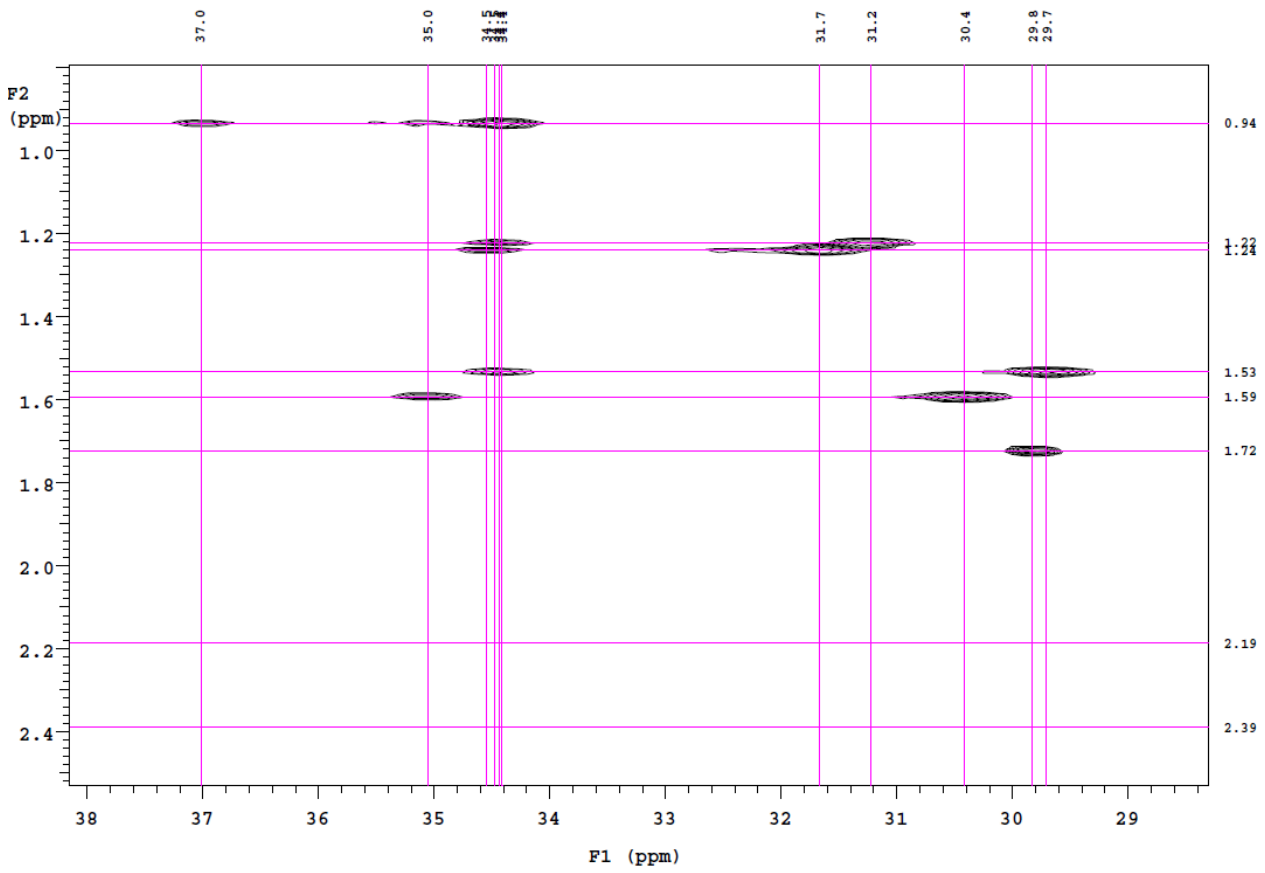

Figure S52. ^{1}H-^{13}C NMR *g*HMBC spectrum of **5** (500 MHz, C_6D_6, 25 °C)

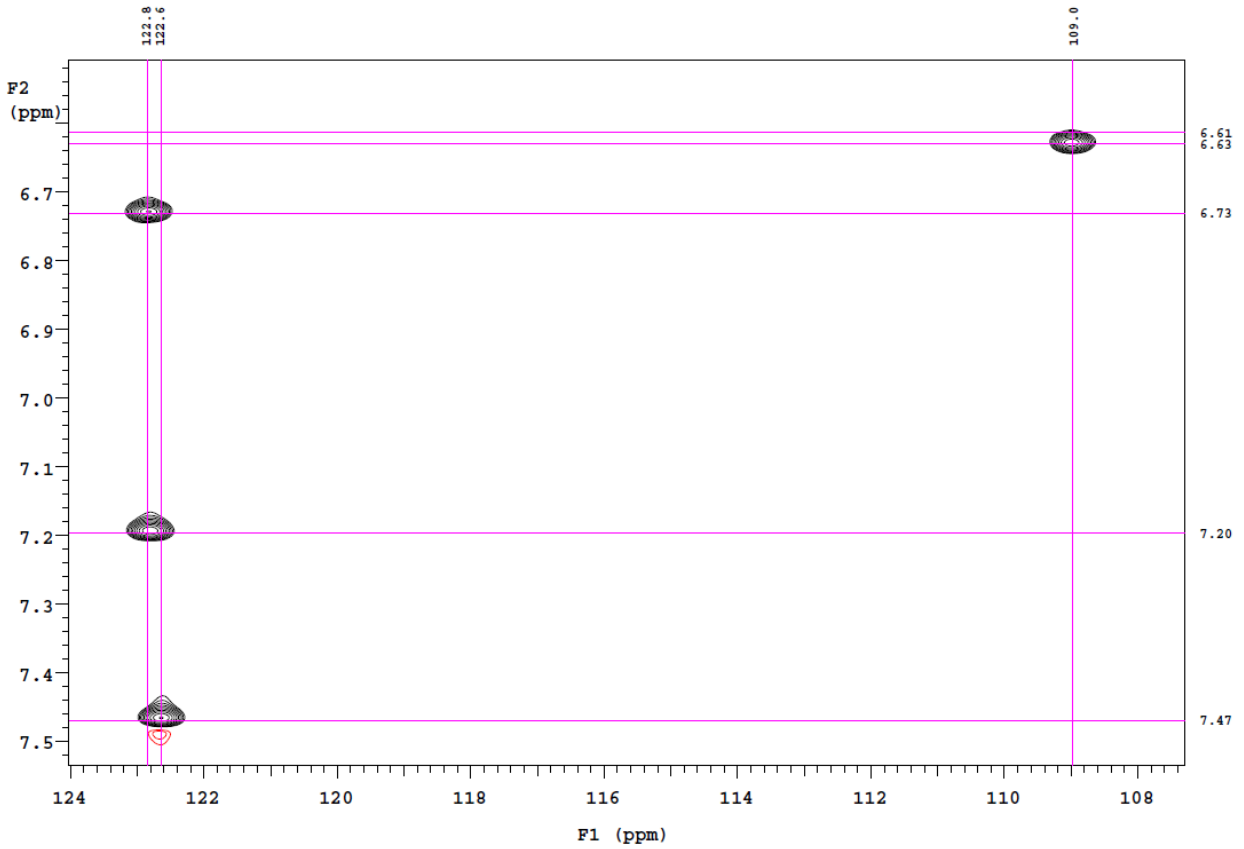

Figure S53. ^{1}H-^{13}C NMR *g*HSQC spectrum of **5** (500 MHz, C_6D_6, 25 °C)

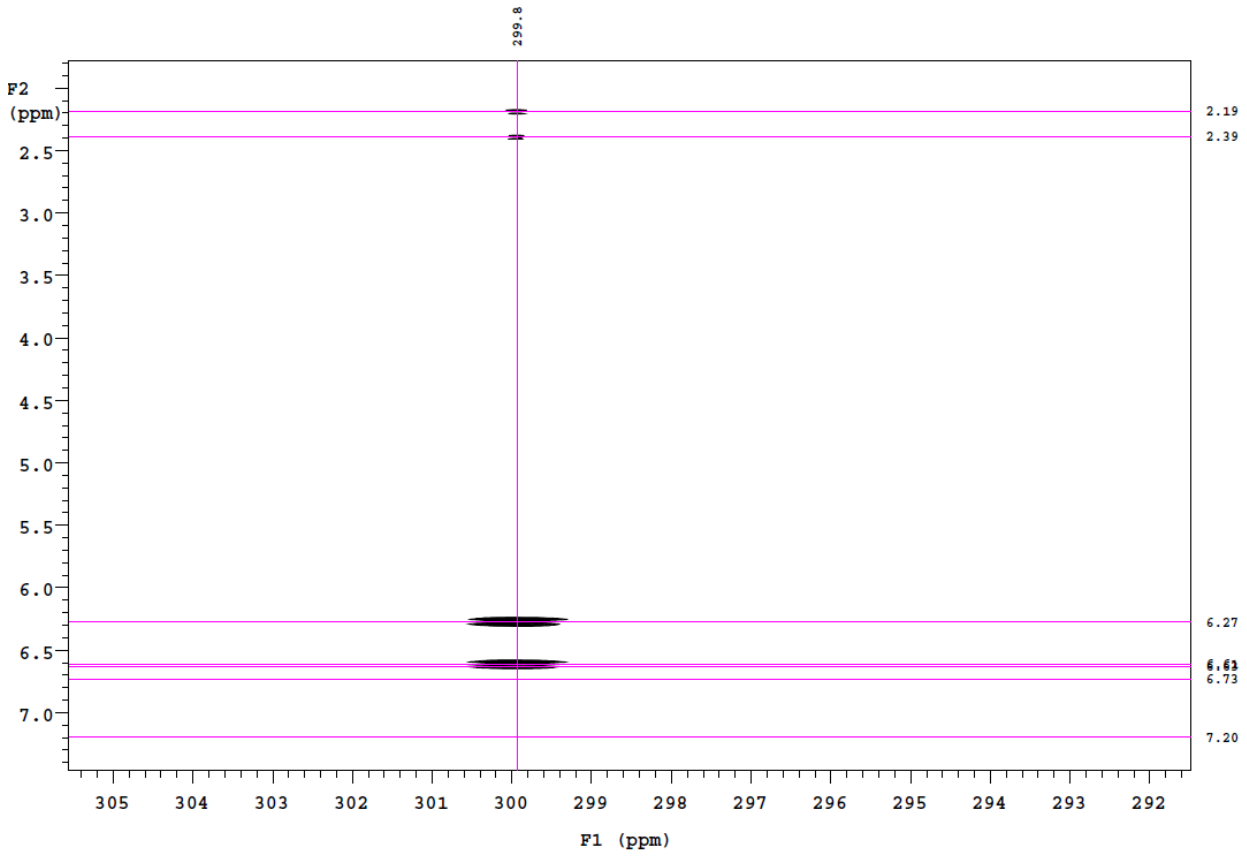

Figure S54. ^{1}H-^{15}N NMR *g*HMBC spectrum of **5** (500 MHz, C_6D_6, 25 °C)

In situ solution phase experiments: Synthesis of 6-Me

To a C_6D_6 solution (0.8 mL) of **4** (120 mg, 0.115 mmol) in a vial, cold MeOTf (12.7 µL, 0.115 mmol) was added in two portions (2 x 6.3 µL). The reaction mixture showed no appreciable color change. The reaction mixture was stirred for 4 h and then filtered into a J-Young NMR tube for 2D-NMR interrogation.

The same reaction can be performed in pentane. In pentane, an immediate color change from orange to brown was observed upon addition of MeOTf with the formation of a precipitate. After 2 h of stirring, the reaction mixture was filtered, and the volatiles were removed in vacuo to afford a brown residue identified as **6-Me**.

Note: Use of a fresh batch of MeOTf is advised. Older batches yield a variable percentage of the alkylidene, **3** from an adventitious protic impurity (perhaps from triflic acid). Extended reaction time leads to undesirable, inseparable impurities.

^{1}H NMR (C_6D_6, 500 MHz): δ = 7.58 (d, 1H, $^4J_{HH}$ =3.0 Hz, Ar-*H*), 7.40 (d, 1H, $^4J_{HH}$ = 3.0 Hz, Ar-*H*), 7.20 (d, 1H, $^4J_{HH}$ = 3.0 Hz, Ar-*H*), 7.14 (d, 1H, $^4J_{HH}$ = 3.0 Hz, Ar-*H*), 5.49 (d, 1H, $^2J_{HH}$ = 14.0 Hz, C*H*$_2$), 4.78 (d, 1H, $^2J_{HH}$ = 14.0 Hz, C*H*$_2$), 2.05 (s, 3H, NC*H*$_3$), 1.75 (s, 9H, Ar-C(C*H*$_3$)$_3$), 1.75 (s, 9H, OC(C*H*$_3$)$_3$), 1.73 (s, 9H, Ar-C(C*H*$_3$)$_3$), 1.36 (s, 9H, Ar-C(C*H*$_3$)$_3$), 1.33 (s, 9H, Ar-C(C*H*$_3$)$_3$), 0.80 (s, 9H, W≡C(C*H*$_3$)$_3$) ppm.

^{13}C NMR (From ^{1}H-^{13}C *g*HMBC NMR spectrum, C_6D_6, 500 MHz): δ = 288.7 (s, W≡*C*C(CH$_3$)$_3$), 159.1 (s, Ar-*C*), 158.3 (s, Ar-*C*), 144.6 (s, Ar-*C*), 141.7 (s, Ar-*C*), 140.5 (s, Ar-*C*), 138.3 (s, Ar-*C*), 136.8 (s, Ar-*C*), 123.0 (s, Ar-*C*), 122.7 (s, Ar-*C*), 121.6 (s, Ar-*C*), 121.2 (s, Ar-*C*), 111.1 (s, Ar-*C*), 80.0 (s, -O*C*(CH$_3$)$_3$), 64.1 (s, *C*H$_2$), 50.3 (s, W≡C*C*(CH$_3$)$_3$), 47.1 (s, N*C*H$_3$). 35.4 (s, Ar-*C*(CH$_3$)$_3$), 35.2 (s, Ar-*C*(CH$_3$)$_3$), 34.4 (s, Ar-*C*(CH$_3$)$_3$), 34.1 (s, Ar-*C*(CH$_3$)$_3$), 33.0 (s, OC(*C*H$_3$)$_3$),

32.9 (s, W≡CC(CH$_3$)$_3$), 31.7 (s, Ar-C(CH$_3$)$_3$), 31.6 (s, Ar-C(CH$_3$)$_3$), 30.1 (s, Ar-C(CH$_3$)$_3$), 29.5 (s, Ar-C(CH$_3$)$_3$) ppm.

^{15}N NMR: (From ^{1}H-^{15}N *g*HMBC, 500 MHz, C_6D_6): δ = 48.9 ppm

NMR Characterization of 6-Me

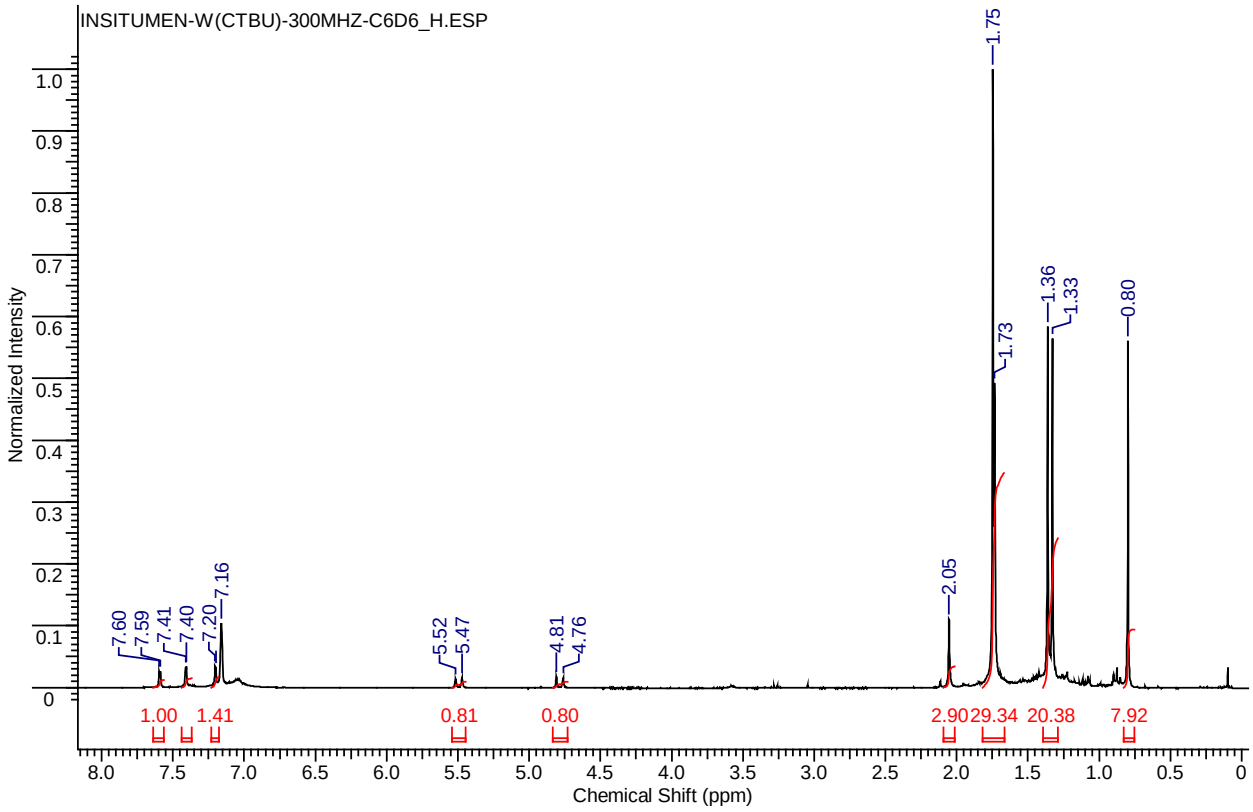

Figure S55. ^{1}H NMR spectrum of **6-Me** (C_6D_6, 300 MHz, 25 °C)

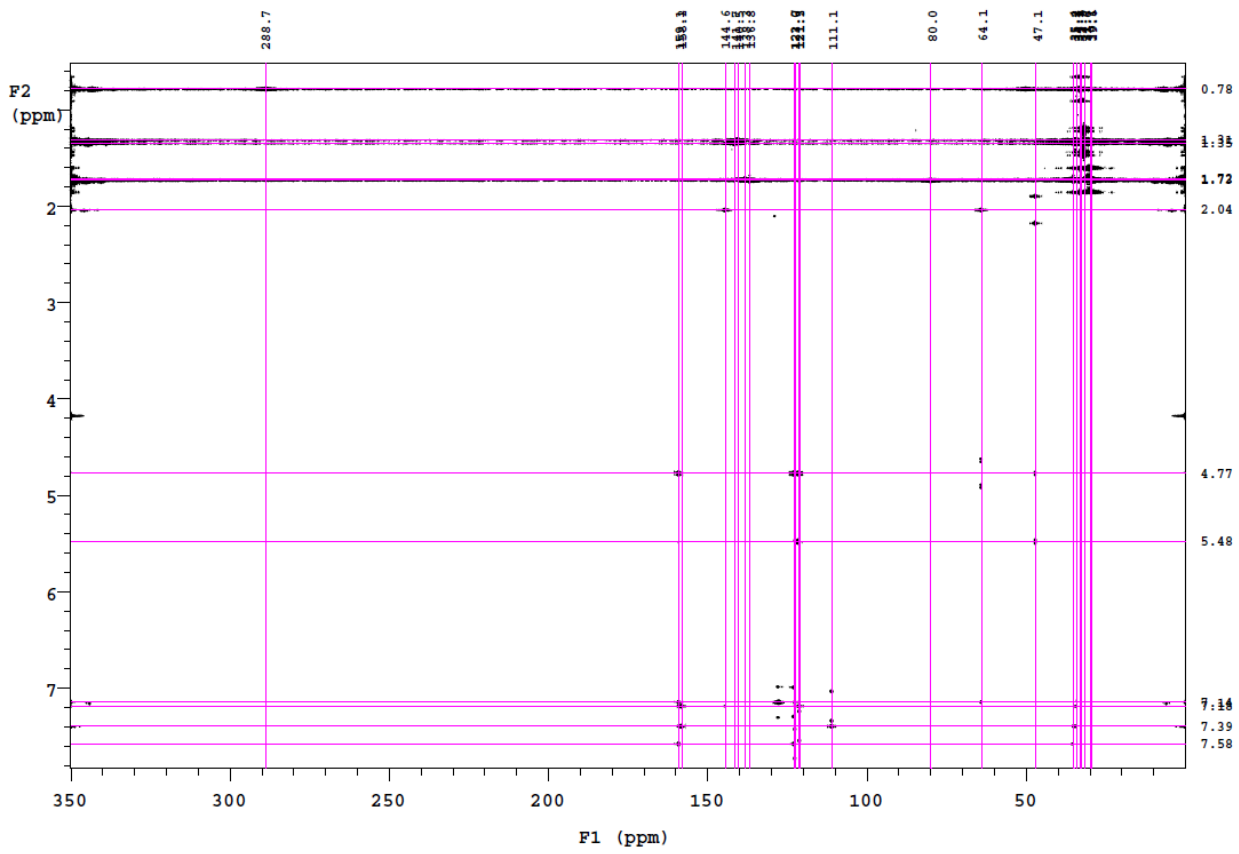

Figure S56. ^{1}H – ^{13}C *g*HMBC NMR spectrum of **6-Me** (C_6D_6, 300 MHz, 25 °C)

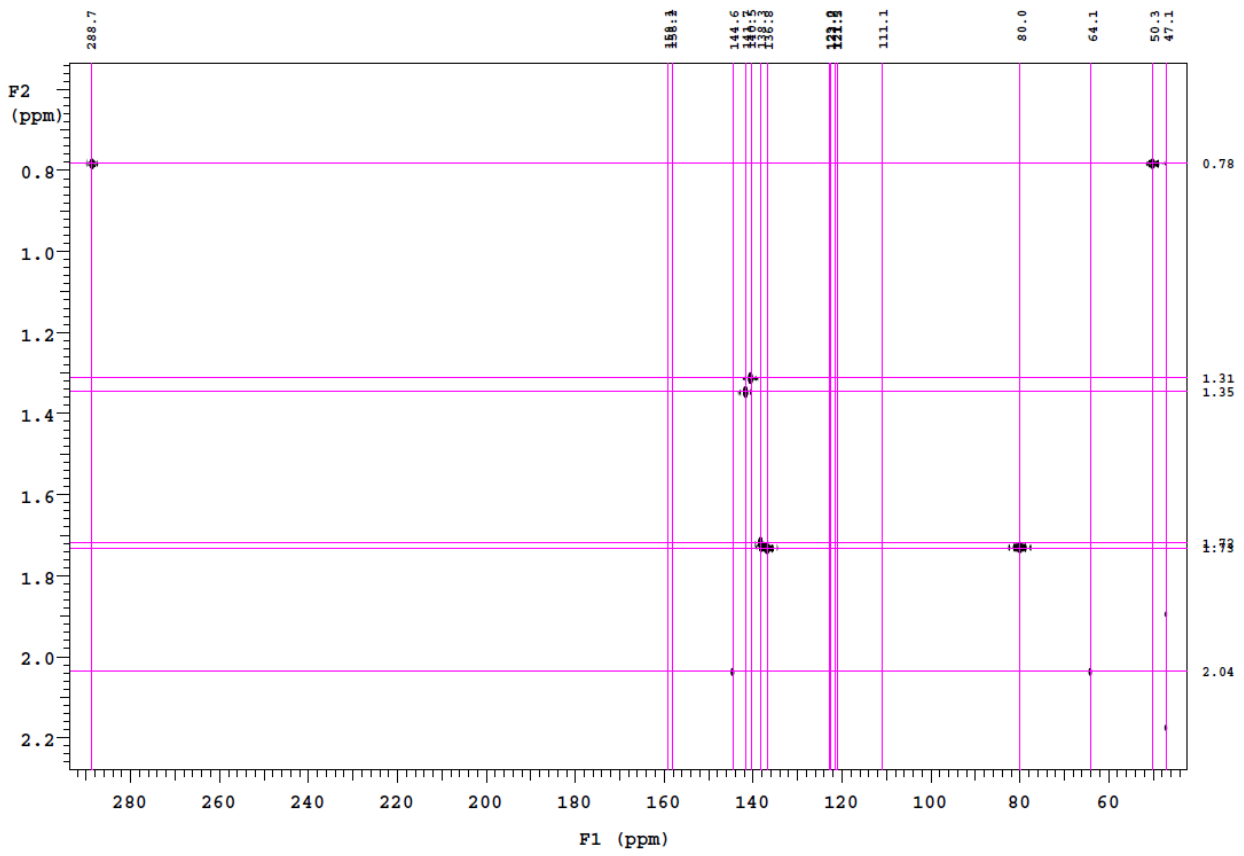

Figure S57. ^{1}H – ^{13}C *g*HMBC NMR spectrum of **6-Me** (C_6D_6, 300 MHz, 25 °C)

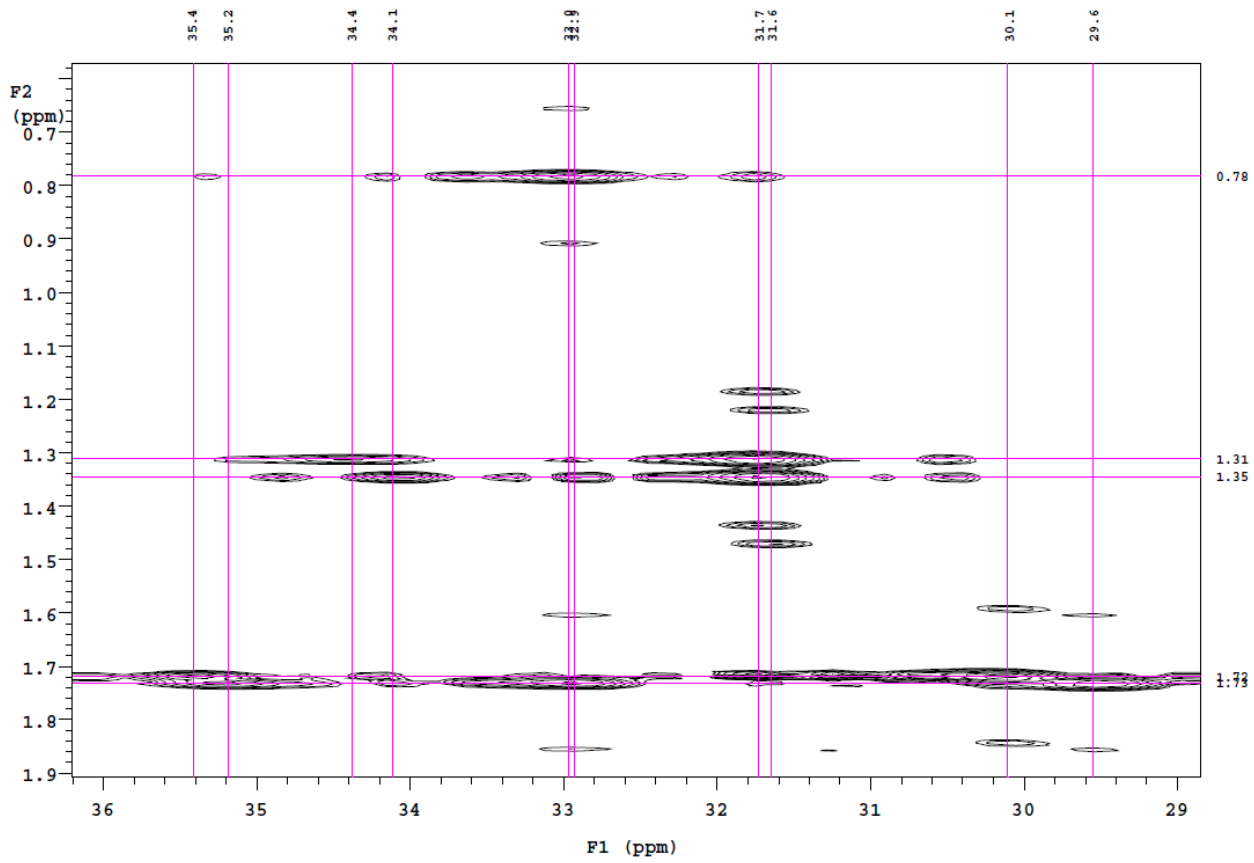

Figure S58. ^{1}H – ^{13}C *g*HMBC NMR spectrum of **6-Me** (C_6D_6, 300 MHz, 25 °C)

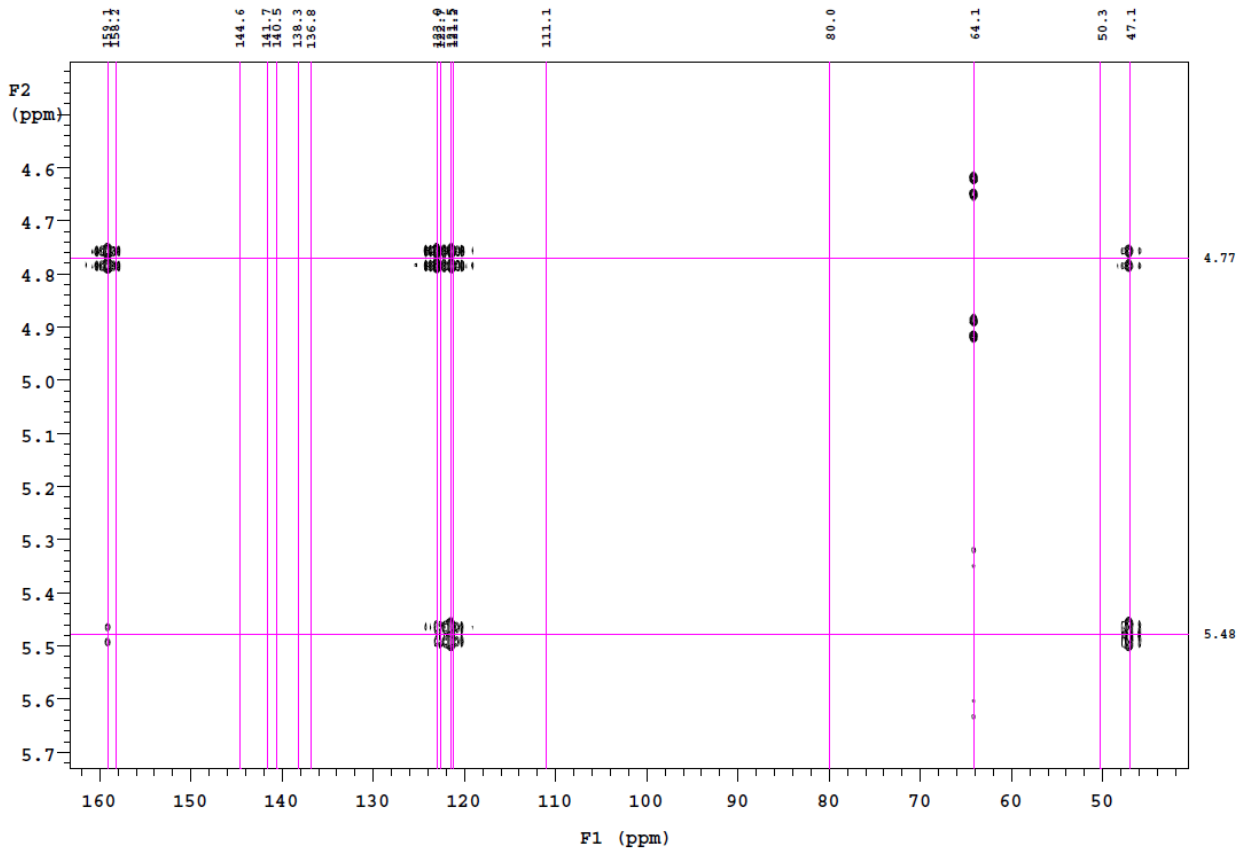

Figure S59. ^{1}H – ^{13}C *g*HMBC NMR spectrum of **6-Me** (C_6D_6, 300 MHz, 25 °C)

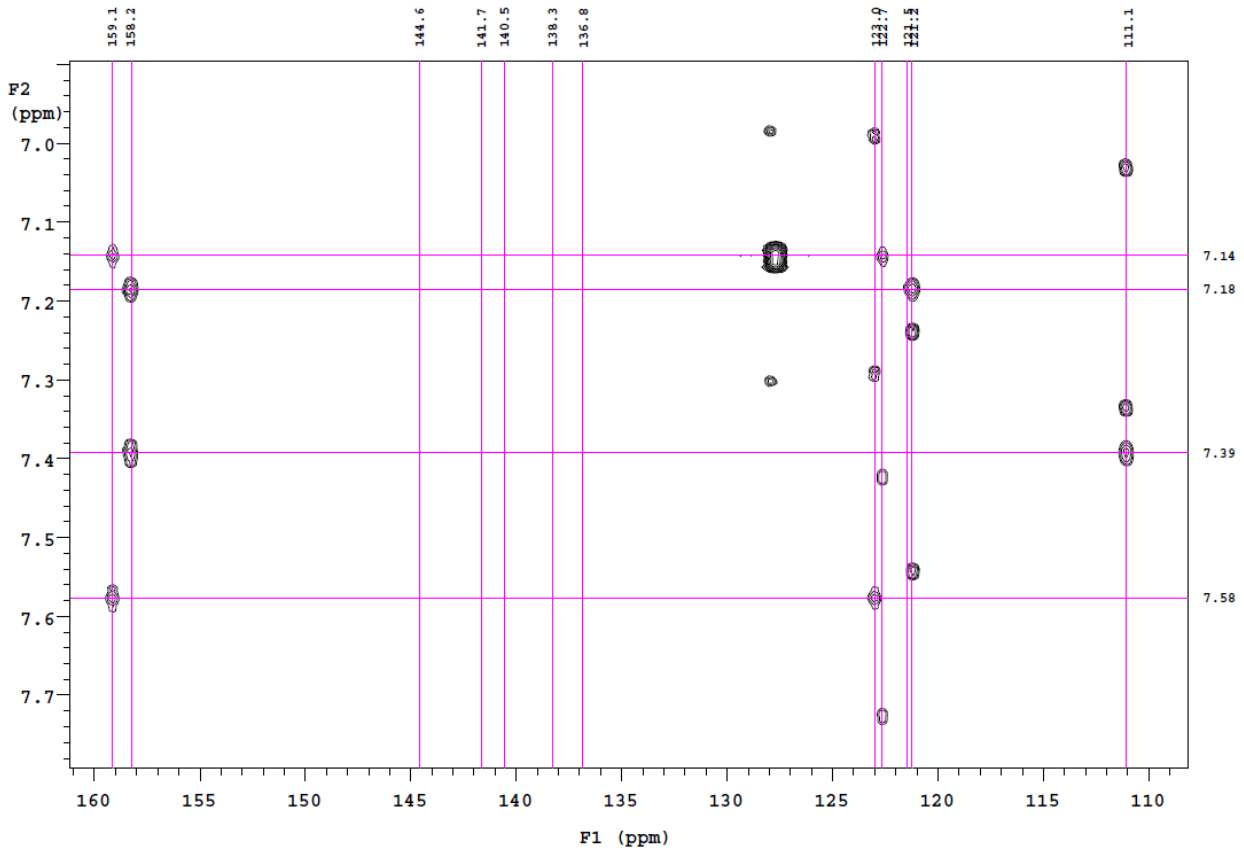

Figure S60. ^{1}H – ^{13}C *g*HMBC NMR spectrum of **6-Me** (C_6D_6, 300 MHz, 25 °C)

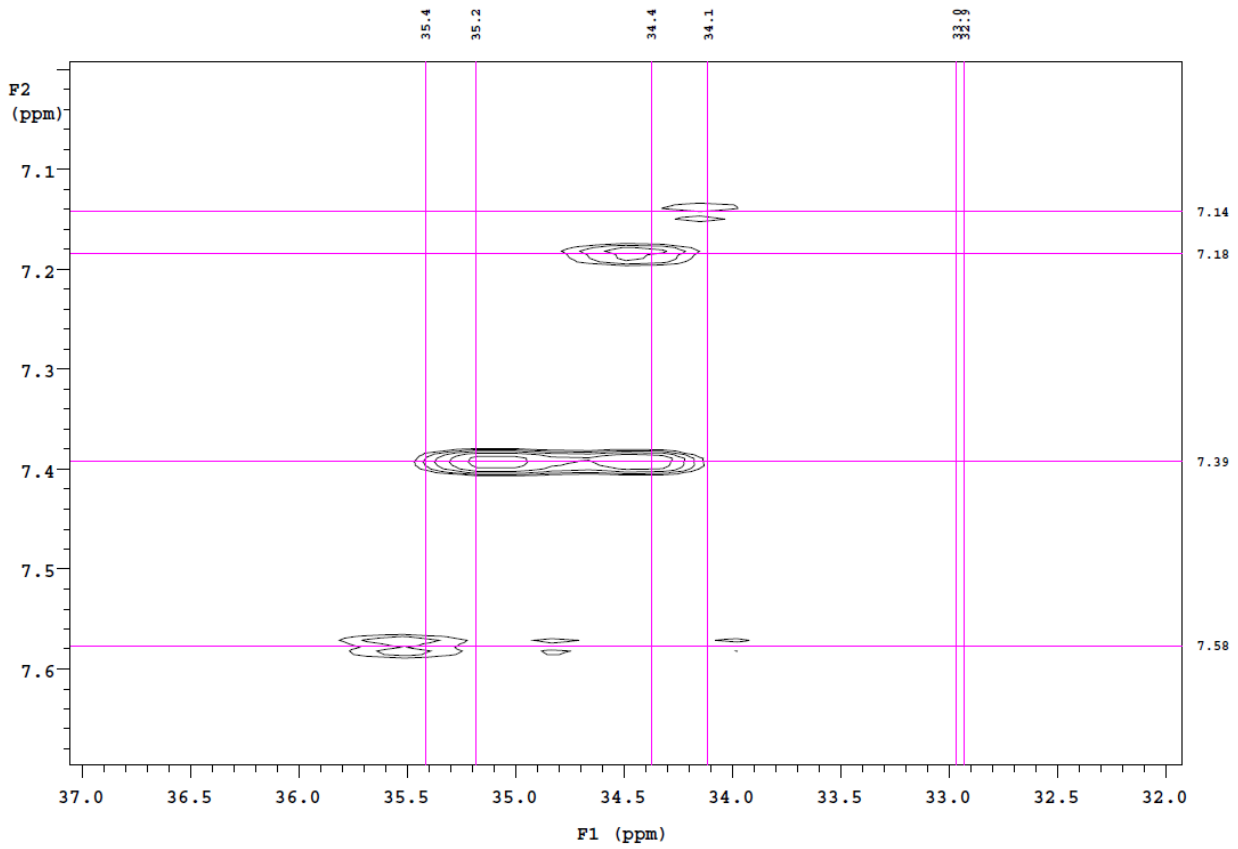

Figure S61. ^{1}H – ^{13}C *g*HMBC NMR spectrum of **6-Me** (C_6D_6, 300 MHz, 25 °C)

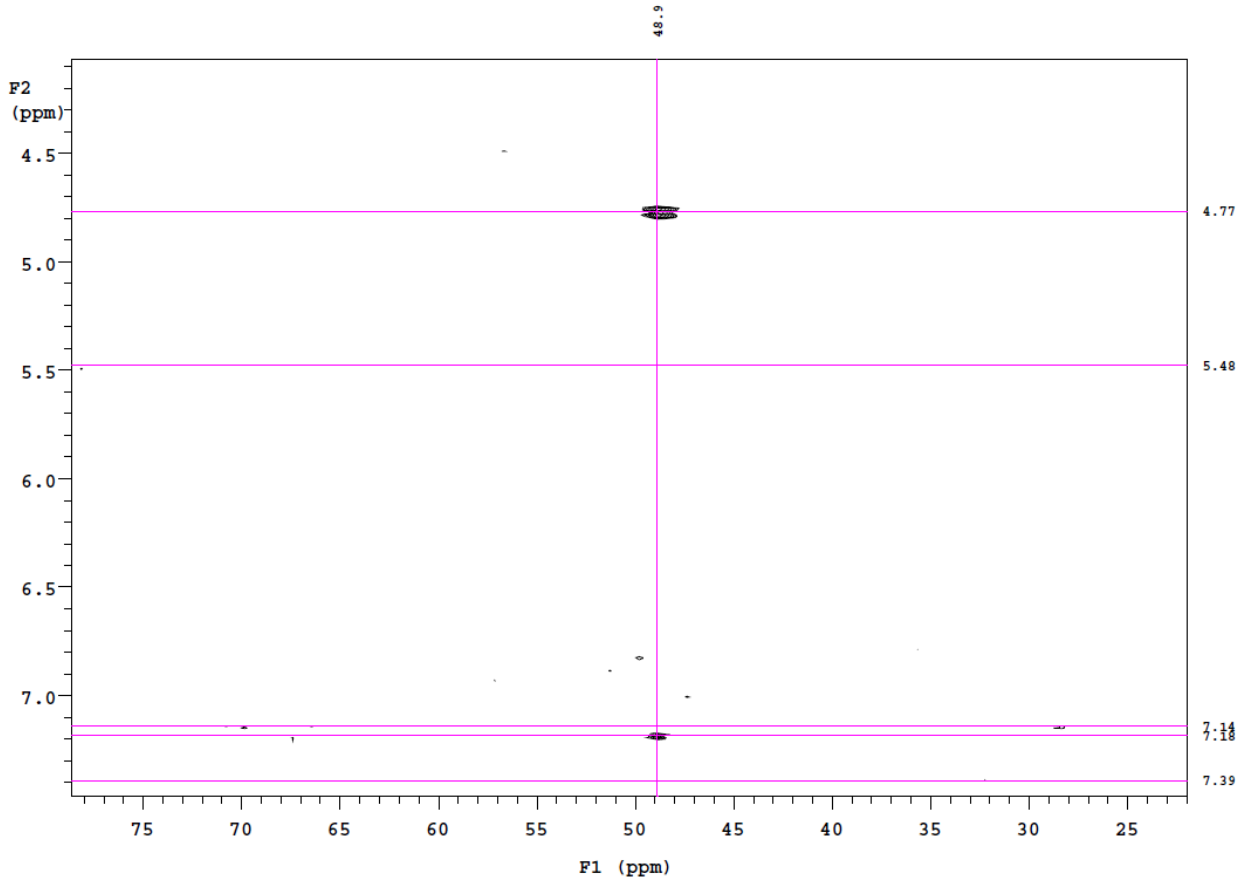

Figure S62. ^{1}H – ^{15}N *g*HMBC NMR spectrum of **6-Me** (C_6D_6, 300 MHz, 25 °C)

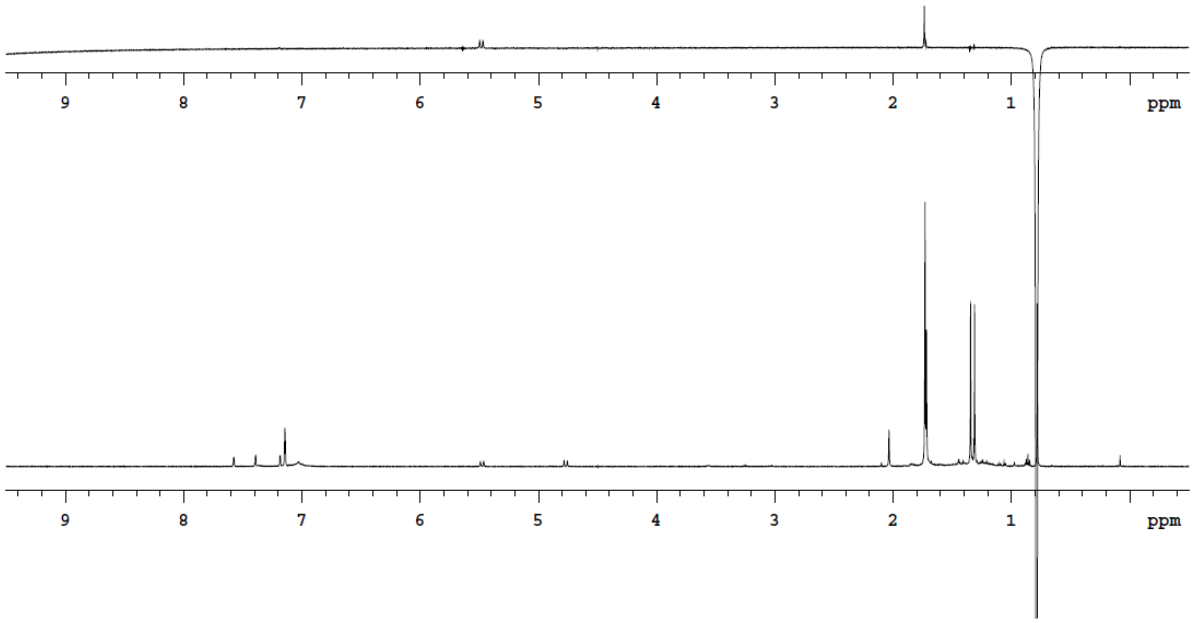

Figure S63. (Top) NOESY-1D spectrum of **6-Me** with selective excitation at 0.78 ppm (C_6D_6, 500 MHz, 25 °C); ^{1}H NMR spectrum of **4** (C_6D_6, 500 MHz, 25 °C) (bottom). A nOe from 0.78 ppm to 5.48 ppm demonstrates that the N-CH_3 and the alkylidyne-^{t}Bu groups are disposed *anti* relative to one another.

In situ solution phase experiments: Synthesis of 6-TMS

To a pentane suspension (2.0 mL) of **4** (52 mg, 0.055 mmol), TMSOTf (10 µL, 0.055 mmol) was added in drops. The orange suspension turned brown upon addition of TMSOTf with copious precipitation. The reaction mixture was stirred for an hour, filtered, and the volatiles were removed in vacuo to yield **6-TMS**.

Note: Use of a fresh batch of TMSOTf is advised. Older batches yield a variable percentage of the alkylidene, **3** from an adventitious protic impurity (perhaps from triflic acid). **6-TMS**, in solution, is relatively more unstable than **6-Me**, decomposing into a number of unidentifiable species.

^{1}H NMR (C_6D_6, 500 MHz): δ = 7.53 (d, 1H, $^4J_{HH}$ =2.2 Hz, Ar-*H*), 7.33 (d, 1H, $^4J_{HH}$ = 2.2 Hz, Ar-*H*), 7.18 (d, 1H, $^4J_{HH}$ = 2.2 Hz, Ar-*H*), 7.14 (d, 1H, $^4J_{HH}$ = 2.2 Hz, Ar-*H*), 5.53 (d, 1H, $^2J_{HH}$ =

14.4 Hz, CH_2), 5.29 (d, 1H, $^2J_{HH}$ = 14.4 Hz, CH_2), 1.73 (s, 9H, OC(CH_3)$_3$), 1.72 (s, 18H, Ar-C(CH_3)$_3$), 1.36 (s, 9H, Ar-C(CH_3)$_3$), 1.35 (s, 9H, Ar-C(CH_3)$_3$), 0.81 (s, 9H, W≡C(CH_3)$_3$), 0.01 (s, 9H, NSi(CH_3)$_3$) ppm.

^{13}C{^{1}H} NMR (C_6D_6, 125 MHz): δ = 289.0 (s, W≡*C*C(CH$_3$)$_3$), 161.6 (s, Ar-*C*), 159.2 (s, Ar-*C*), 141.5 (s, Ar-*C*), 141.4 (s, Ar-*C*), 139.5 (s, Ar-*C*), 137.5 (s, Ar-*C*), 135.9 (s, Ar-*C*), 124.5 (s, Ar-*C*), 122.0 (s, Ar-*C*), 121.9 (s, Ar-*C*), 119.7 (s, Ar-*C*), 114.9 (s, Ar-*C*), 79.9 (s, -O*C*(CH$_3$)$_3$), 60.8 (s, *C*H$_2$), 50.1 (s, W≡C*C*(CH$_3$)$_3$), 35.3 (s, Ar-*C*(CH$_3$)$_3$), 34.9 (s, Ar-*C*(CH$_3$)$_3$), 34.2 (s, Ar-*C*(CH$_3$)$_3$), 34.1 (s, Ar-*C*(CH$_3$)$_3$), 33.1 (s, W≡CC(*C*H$_3$)$_3$), 32.9 (s, OC(*C*H$_3$)$_3$), 31.6 (s, Ar-C(*C*H$_3$)$_3$), 31.6 (s, Ar-C(*C*H$_3$)$_3$), 30.1 (s, Ar-C(*C*H$_3$)$_3$), 29.4 (s, Ar-C(*C*H$_3$)$_3$), -0.6 (s, NSi(*C*H$_3$)$_3$) ppm.

^{15}N NMR: δ = not measured

NMR Characterization of 6-TMS

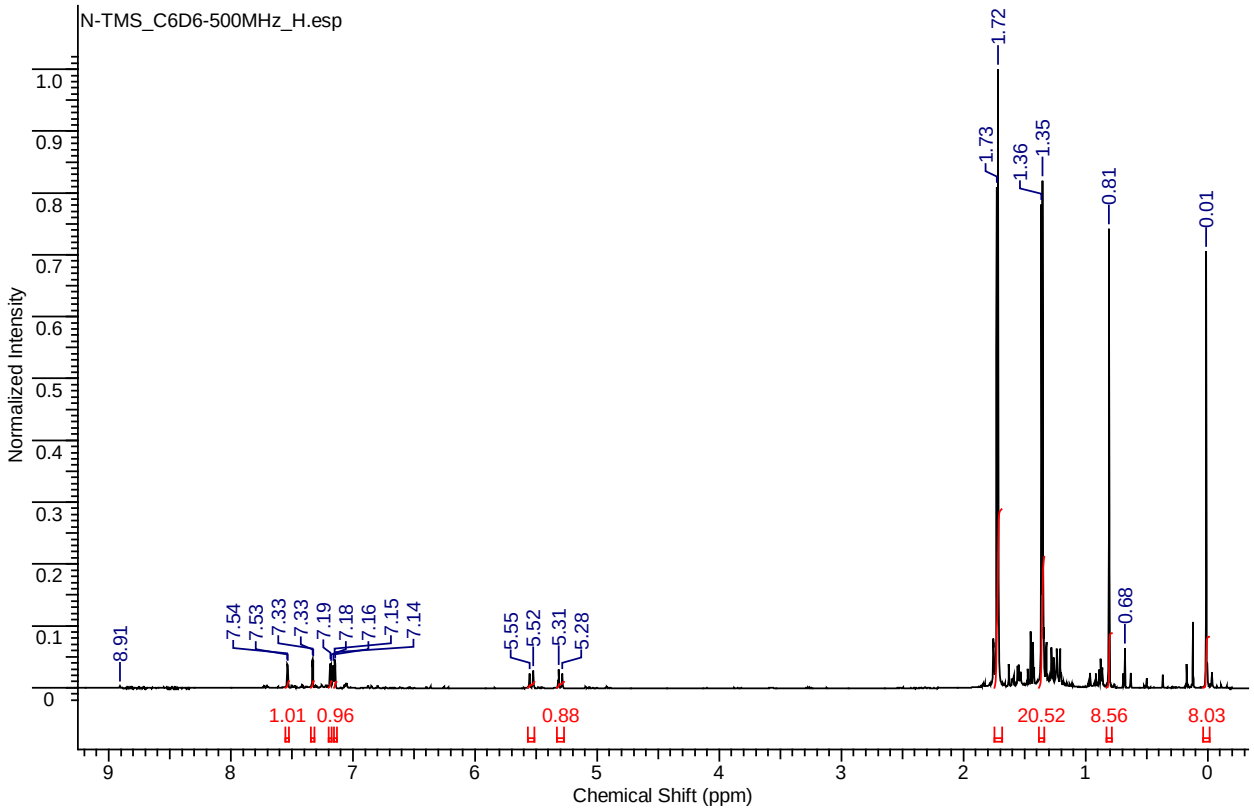

Figure S64. ^{1}H NMR spectrum of **6-TMS** (C_6D_6, 500 MHz, 25 °C) [Note: A small amount (~ 8%) of alkylidene **3** is found in this sample; resonances at 8.91 ppm (W=C*H*^{t}Bu) and 0.68 ppm (W=CH^{t}*Bu*) are indicative of the same. Refer **Figure S26** for ^{1}H NMR spectrum of **3**]

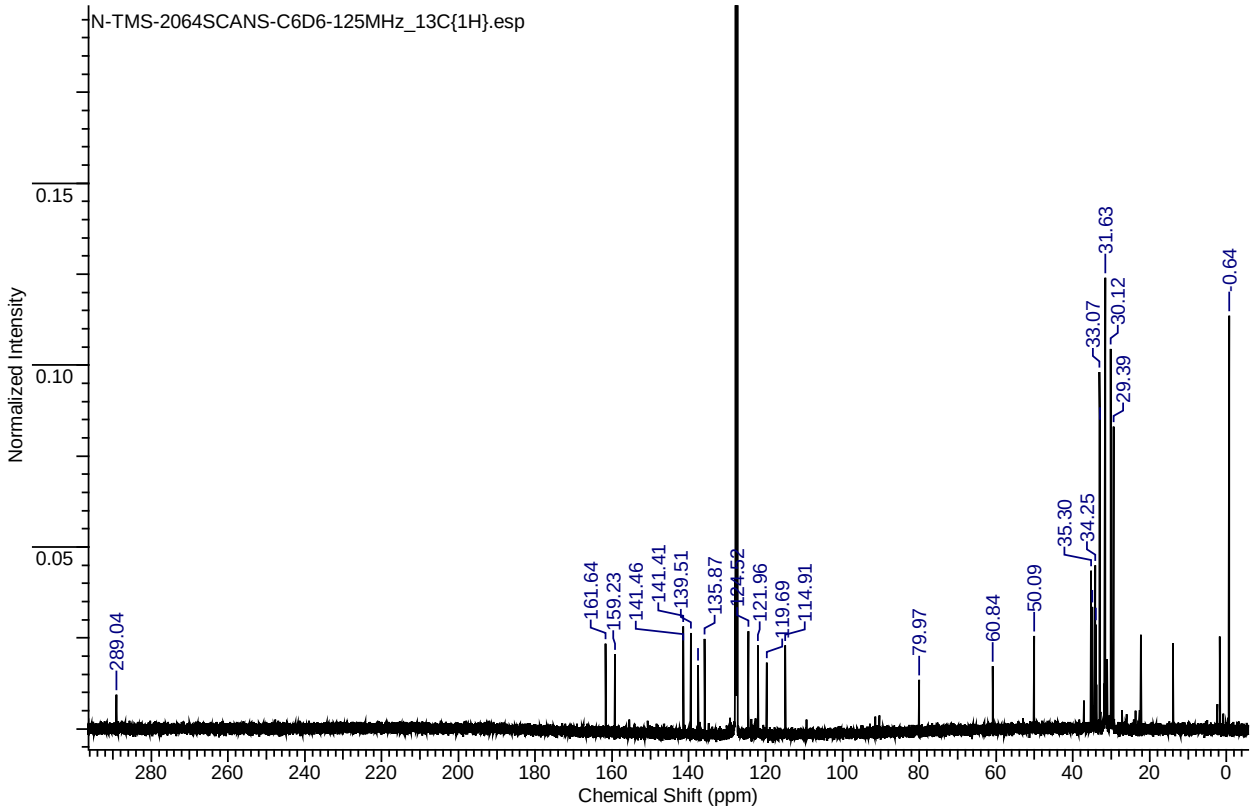

Figure S65. $^{13}C\{^{1}H\}$ NMR spectrum of **6-TMS** (C_6D_6, 125 MHz, 25 °C)

In the sample used for 2D NMR assignment of **6-TMS**, there was a higher percentage of **3**. Nevertheless, knowledge of the resonances pertaining to **3** rendered assignment of resonances for **6-TMS** possible. The authenticity of the procedure for the N-silylation of **4** to afford **6-TMS** was confirmed using a fresh batch of TMSOTf employing the synthetic procedure provided in page **S76**. A fresh batch of TMSOTf was used to minimize protic impurities; the solution-phase characterization **6-TMS** (Refer **Figure S49** and **Figure S50**) matched with the 2D-assignments provided below.

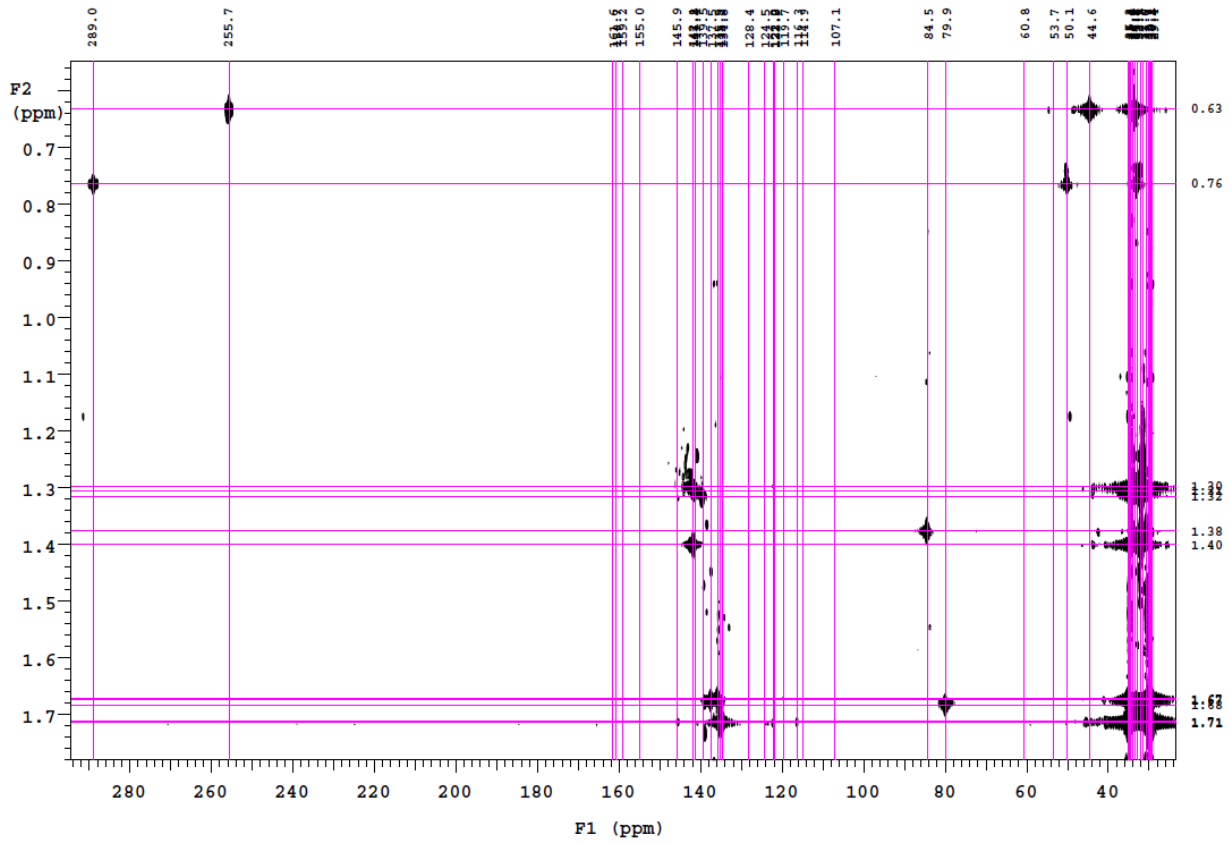

Figure S66. ^{1}H-^{13}C *g*HMBC NMR spectrum of **6-TMS** (C_6D_6, 500 MHz, 25 °C)

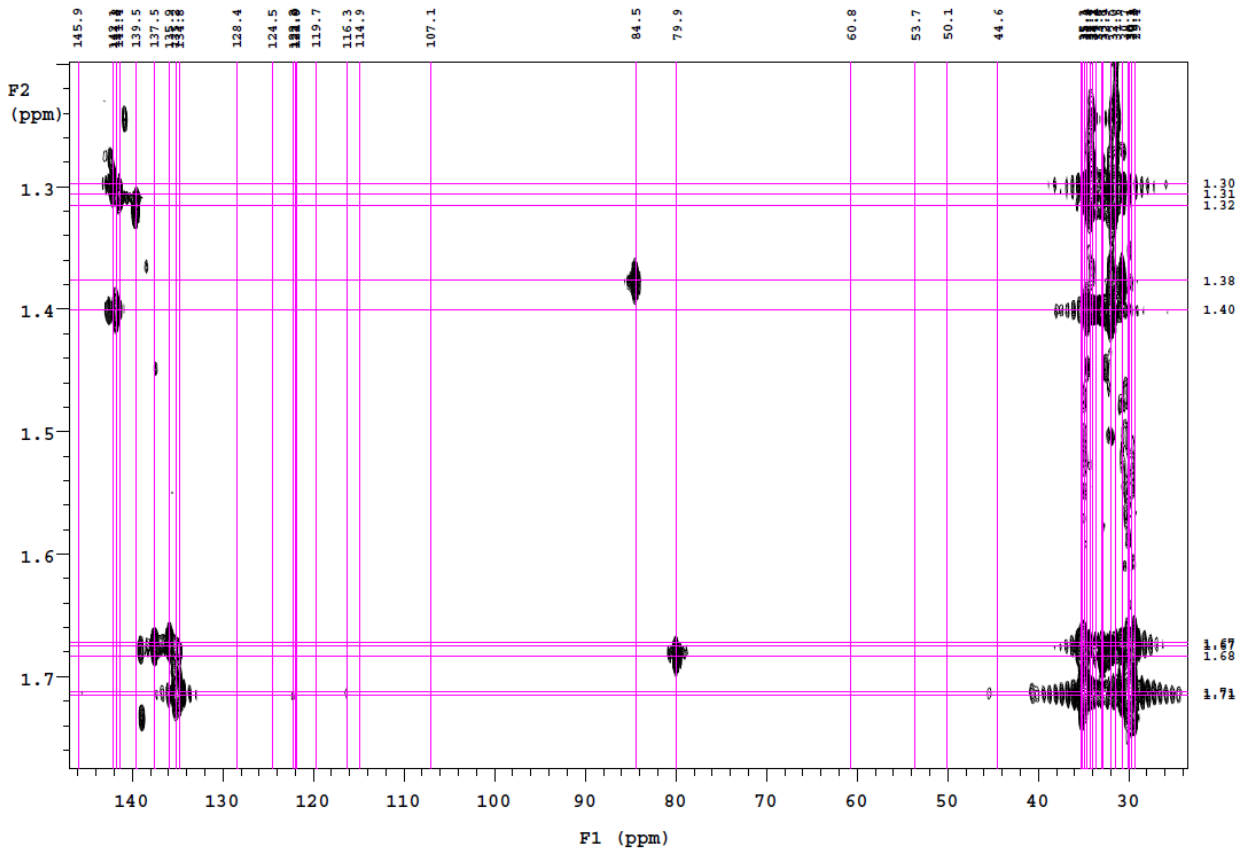

Figure S67. ^{1}H-^{13}C *g*HMBC NMR spectrum of **6-TMS** (C_6D_6, 500 MHz, 25 °C)

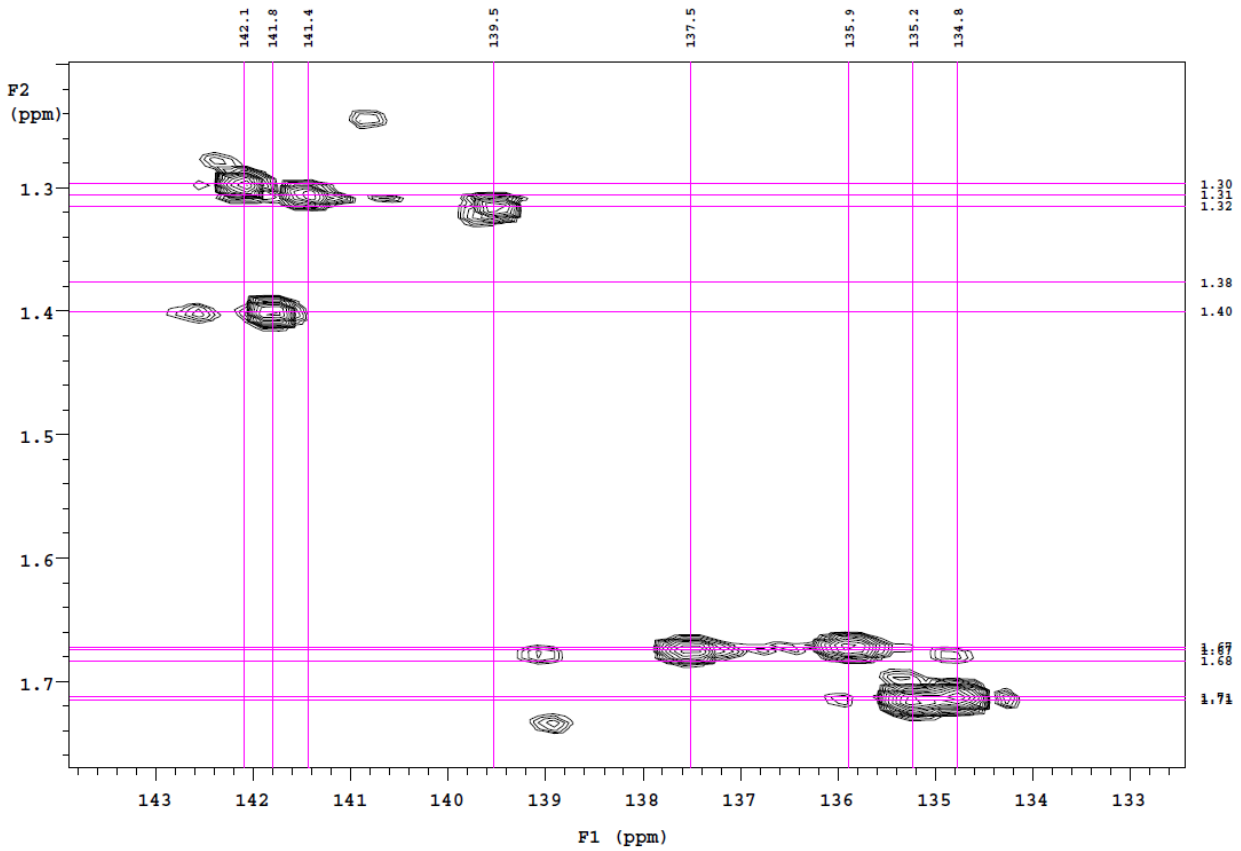

Figure S68. ^{1}H-^{13}C *g*HMBC NMR spectrum of **6-TMS** (C_6D_6, 500 MHz, 25 °C)

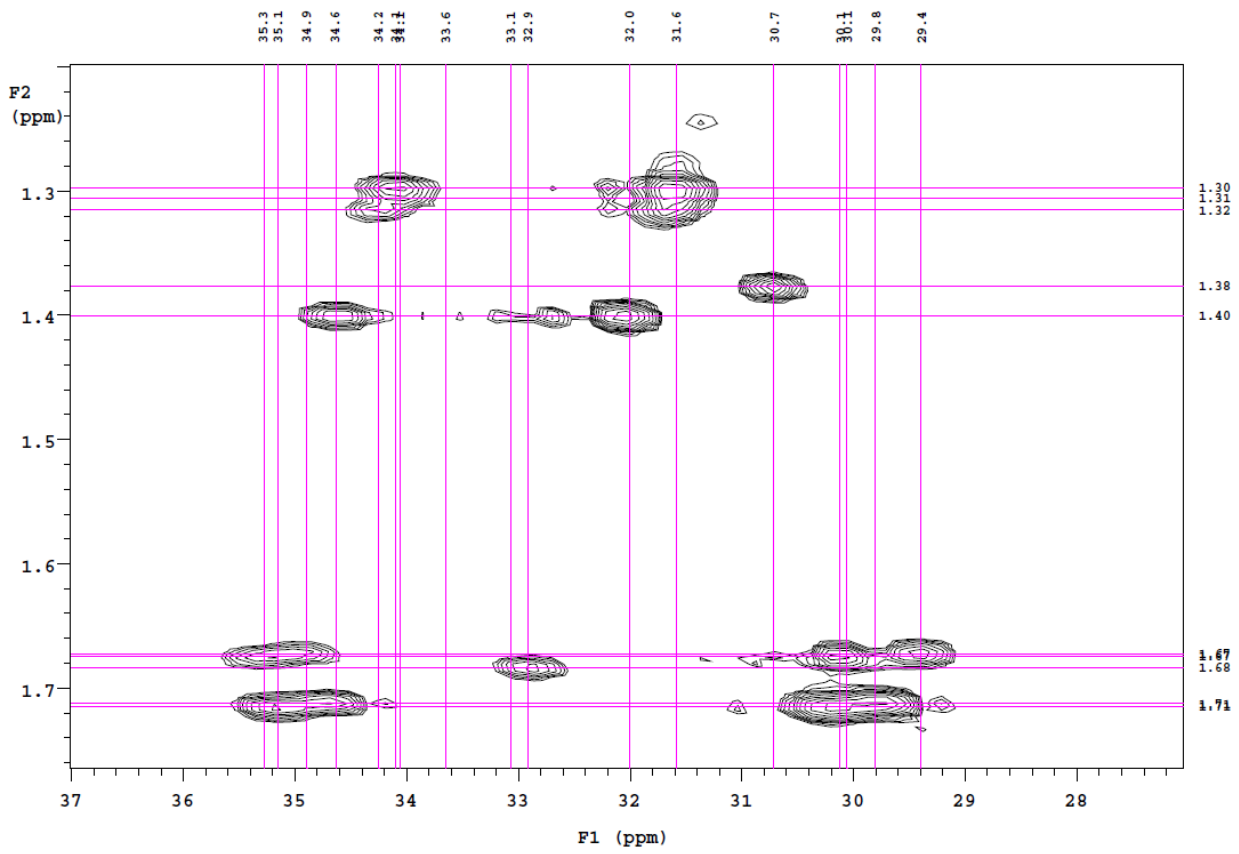

Figure S69. ^{1}H-^{13}C *g*HMBC NMR spectrum of **6-TMS** (C_6D_6, 500 MHz, 25 °C)

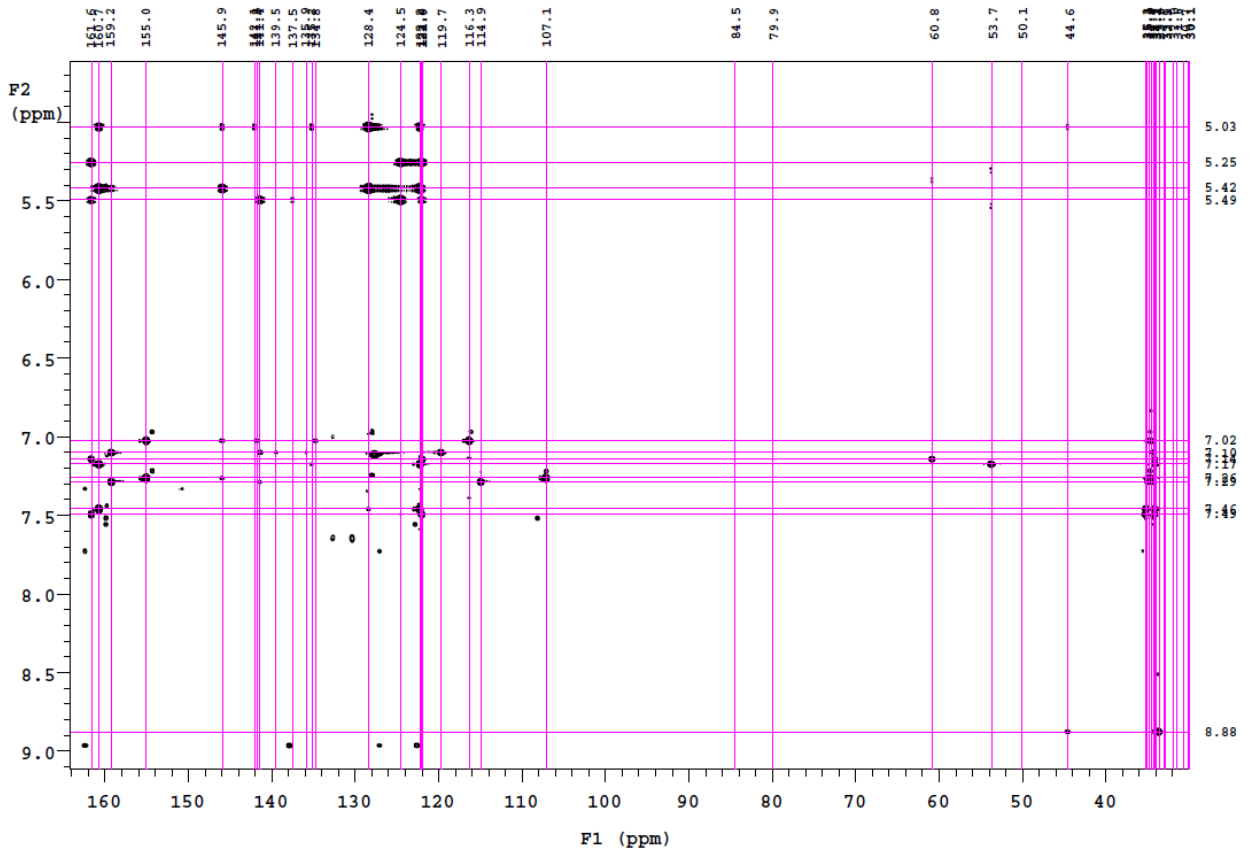

Figure S70. ^{1}H-^{13}C *g*HMBC NMR spectrum of **6-TMS** (C_6D_6, 500 MHz, 25 °C)

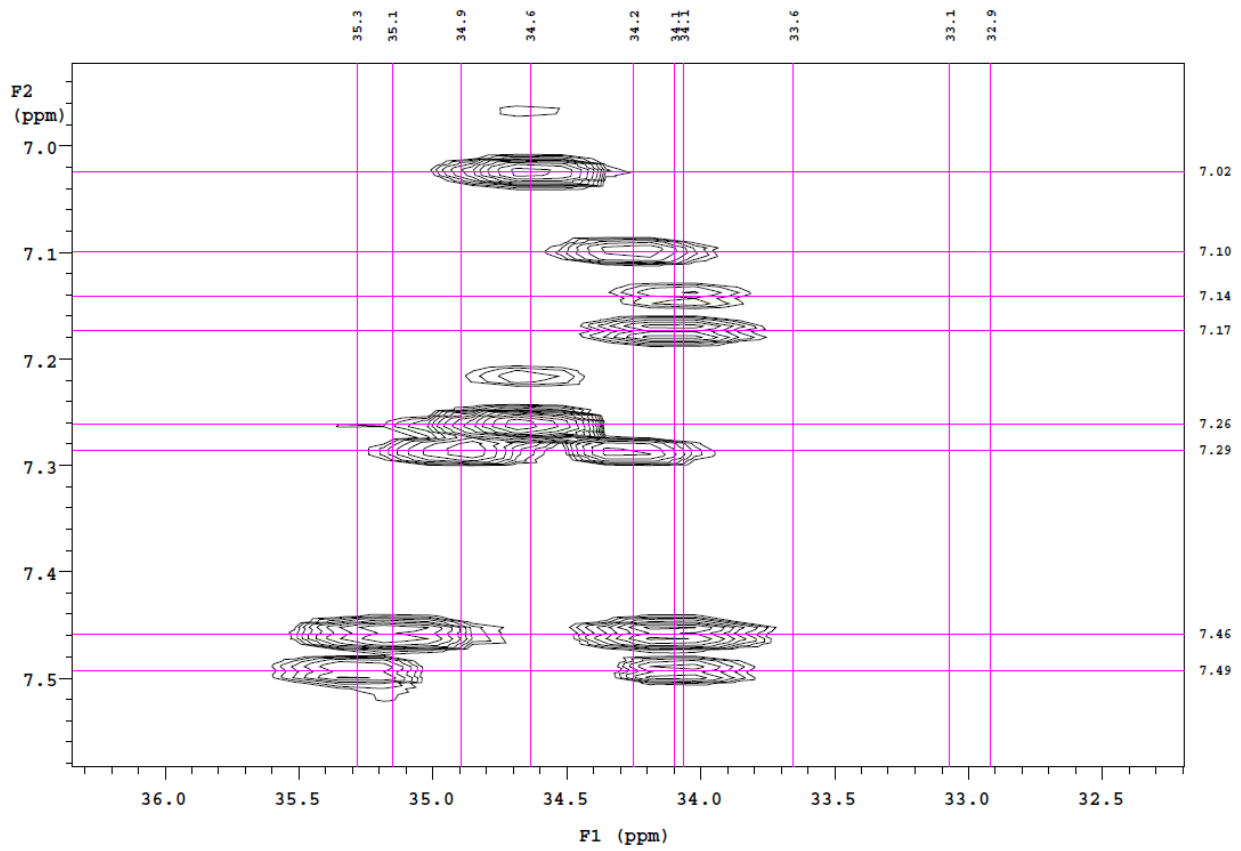

Figure S71. ^{1}H-^{13}C *g*HMBC NMR spectrum of **6-TMS** (C_6D_6, 500 MHz, 25 °C)

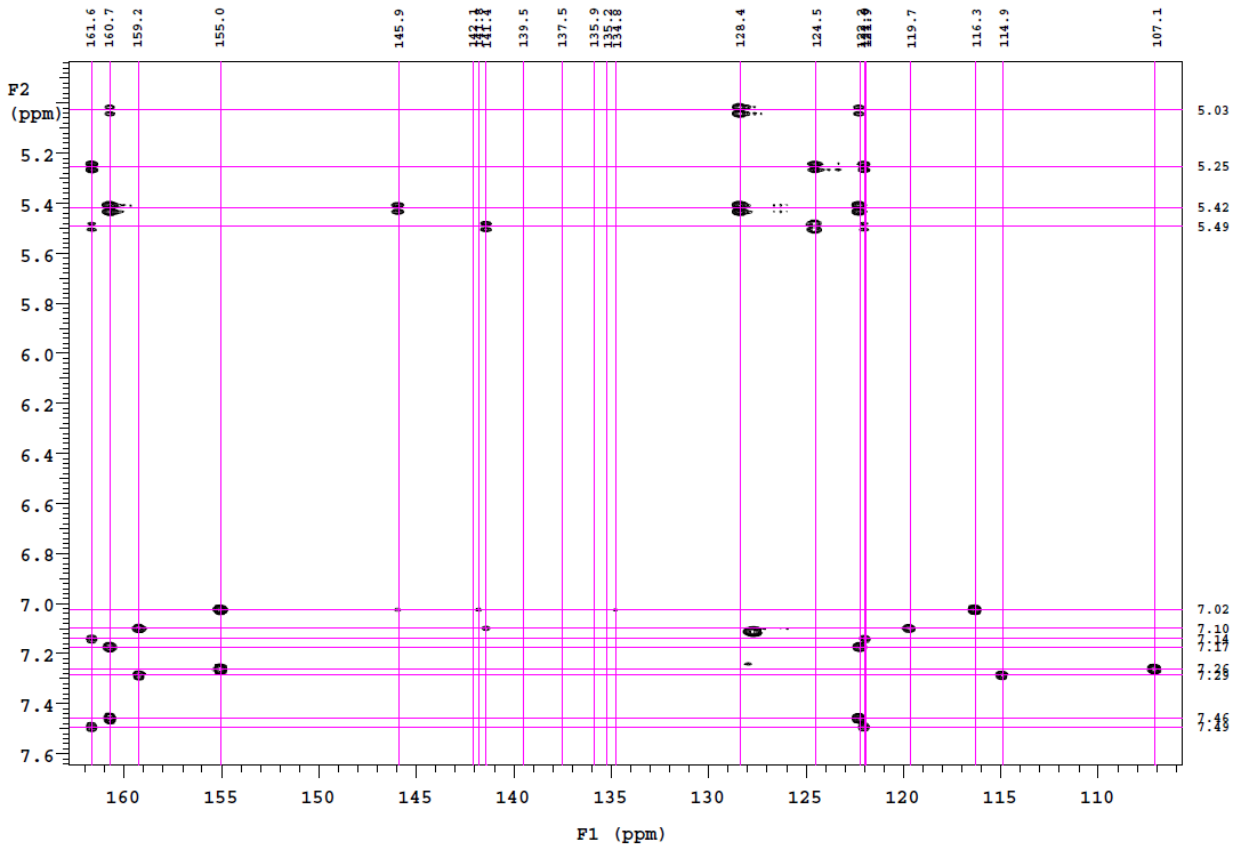

Figure S72. ^{1}H-^{13}C *g*HMBC NMR spectrum of **6-TMS** (C_6D_6, 500 MHz, 25 °C)

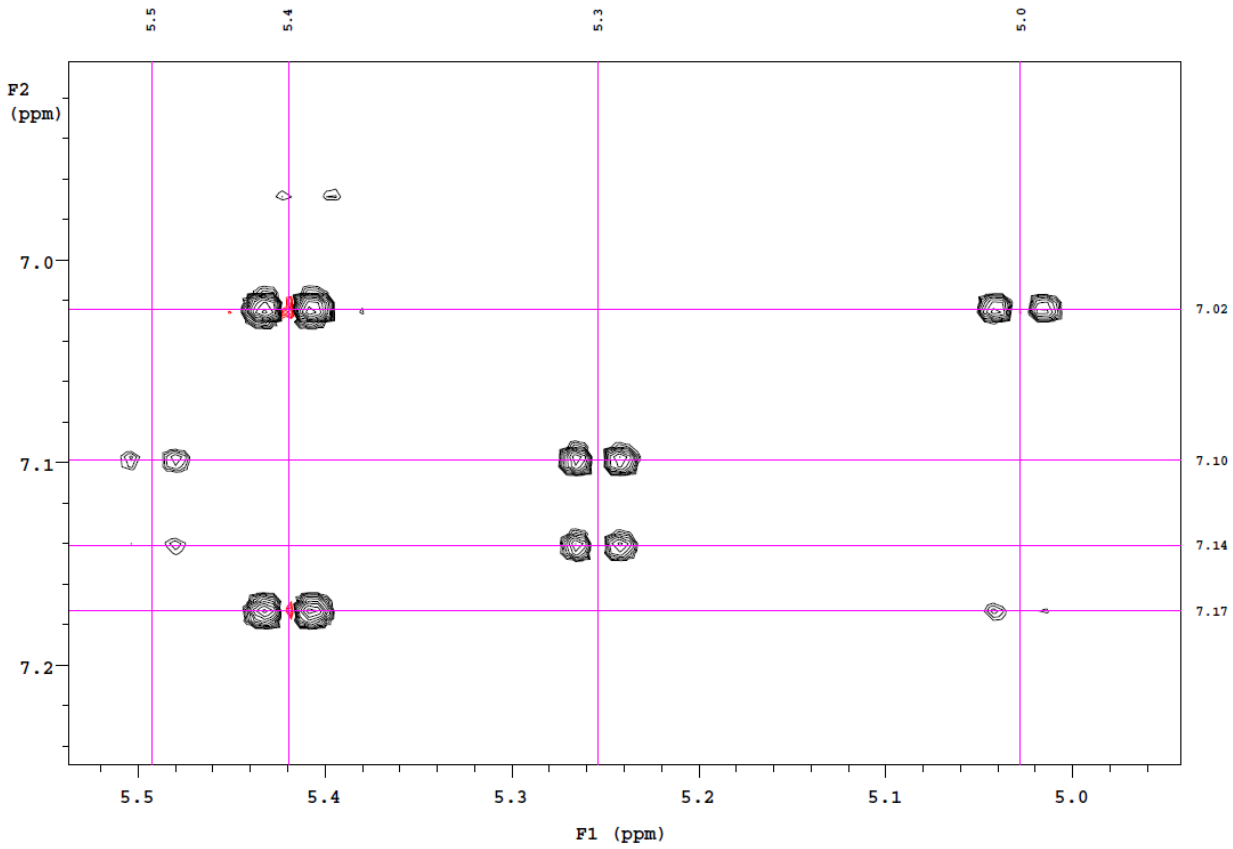

Figure S73. ^{1}H-^{1}H ROESY NMR spectrum of **6-TMS** (C_6D_6, 500 MHz, 25 °C)

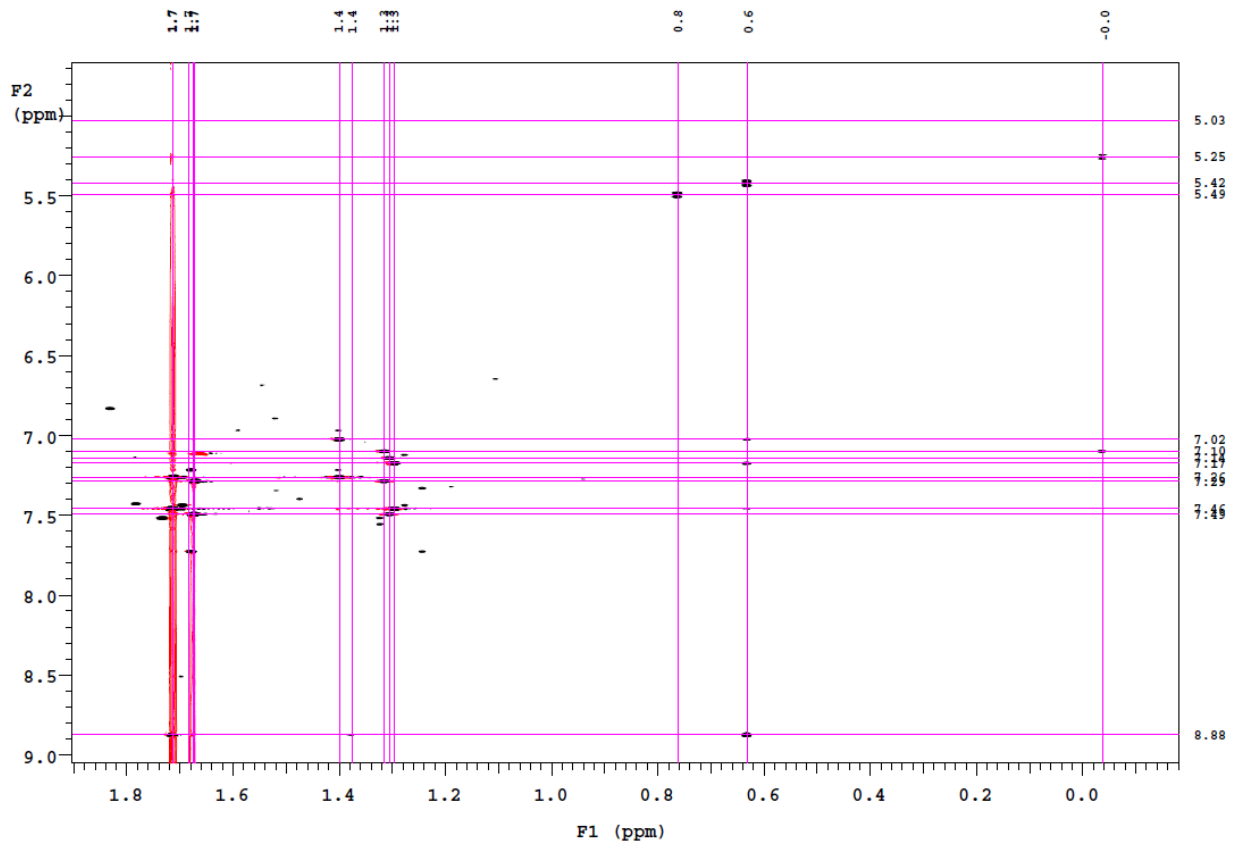

Figure S74. ^{1}H-^{1}H ROESY NMR spectrum of **6-TMS** (C_6D_6, 500 MHz, 25 °C)

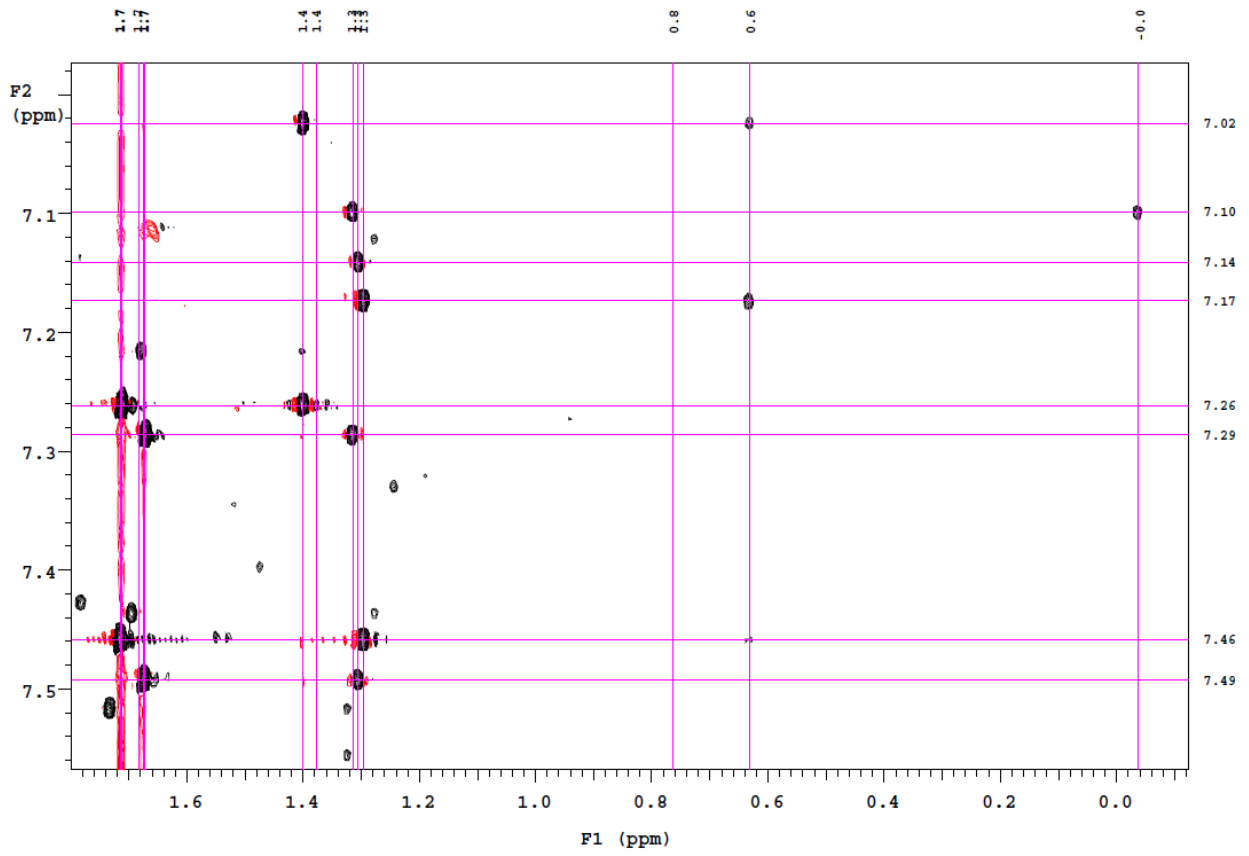

Figure S75. ^{1}H-^{1}H ROESY NMR spectrum of **6-TMS** (C_6D_6, 500 MHz, 25 °C)

X-ray crystallography of 4

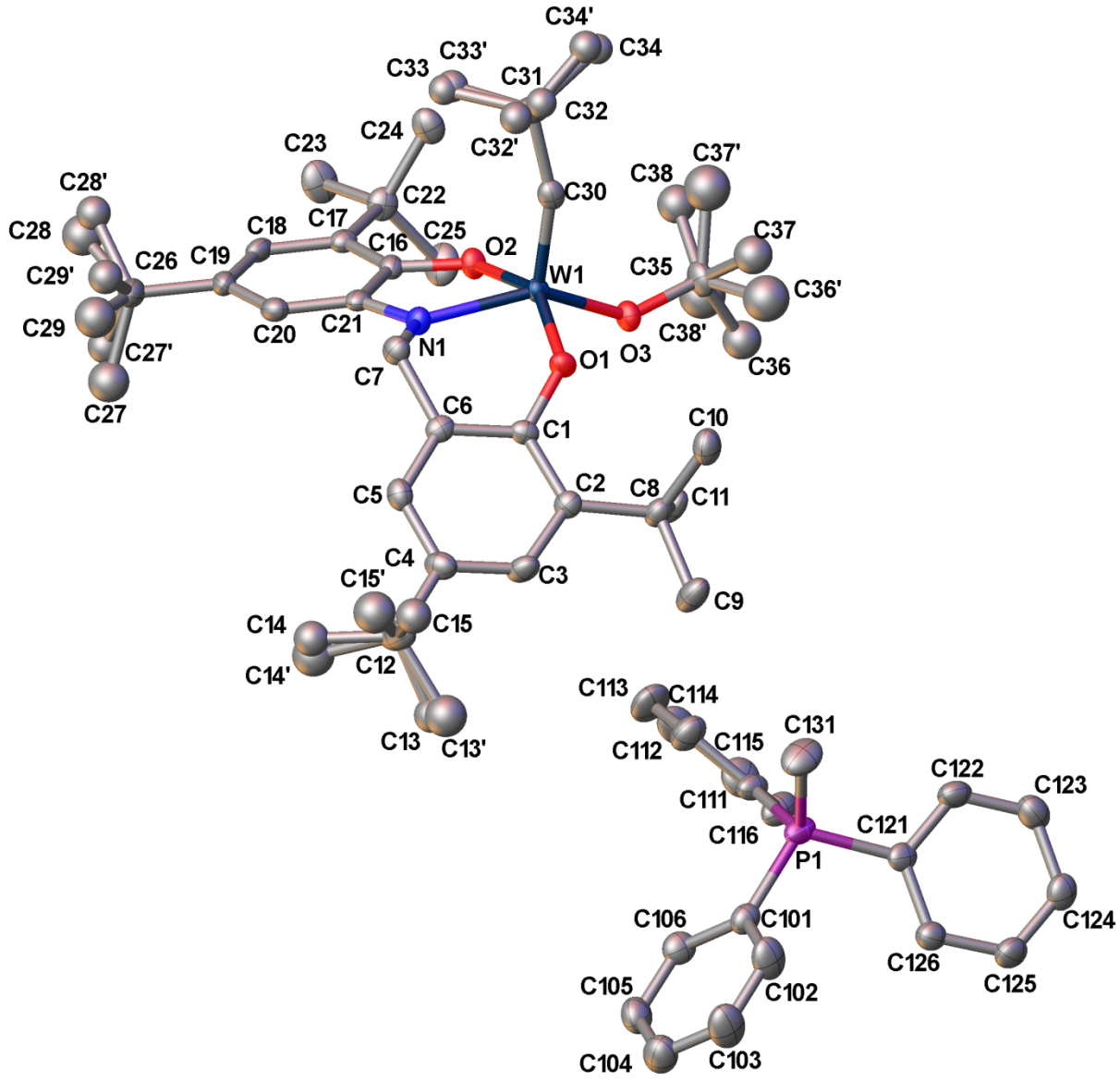

Figure S76. Molecular structure of **4** at 40% probability (all hydrogen atoms removed for clarity)

X-ray experimental: X-Ray Intensity data were collected at 100 K on a Bruker SMART diffractometer using Mo K_α radiation (λ = 0.71073 Å) and an APEXII CCD area detector. Raw data frames were read by program SAINT and integrated using 3D profiling algorithms. The resulting data were reduced to produce hkl reflections and their intensities and estimated

standard deviations. The data were corrected for Lorentz and polarization effects and numerical absorption corrections were applied based on indexed and measured faces. The structure was solved and refined in SHELXTL2013[20], using full-matrix least-squares refinement. The non-H atoms were refined with anisotropic thermal parameters and all of the H atoms were calculated in idealized positions and refined riding on their parent atoms. The half pentane solvent molecule (located on an inversion center) was disordered and could not be modeled properly, thus program SQUEEZE, a part of the PLATON[21-23] package of crystallographic software, was used to calculate the solvent disorder area and remove its contribution to the overall intensity data. In studying the fine structure, the C7 and C131 protons were obtained from a Difference Fourier maps and refined freely. Additionally, each of the three methyl groups on C12, C26, C31 and C35 are disordered and refined in two parts each with their site occupation parameters dependently refined. Additionally, the Ueq of each set of three carbon atoms were constrained to be equivalent using EADP in SHELX2013. The absence of any electron density near C30, and the short distance of W1-C30 indicate the bond is a triple bond. In the final cycle of refinement, 12808 reflections (of which 10167 are observed with $I > 2\sigma(I)$) were used to refine 570 parameters and the resulting R_1, wR_2 and S (goodness of fit) were 2.84%, 6.52% and 0.984, respectively. The refinement was carried out by minimizing the wR_2 function using F^2 rather than F values. R_1 is calculated to provide a reference to the conventional R value but its function is not minimized.

Table S2. Crystal data and structure refinement for **4**

Identification code	sud13	
Empirical formula	$C_{57}H_{78}NO_3PW$	
Formula weight	1040.02	
Temperature	100(2) K	
Wavelength	0.71073 Å	
Crystal system	Monoclinic	
Space group	P 21/n	
Unit cell dimensions	a = 14.1363(3) Å	α = 90°
	b = 17.4732(4) Å	β = 99.3665(11)°
	c = 22.8371(4) Å	γ = 90°
Volume	5565.7(2) $Å^3$	
Z	4	
Density (calculated)	1.241 Mg/m^3	
Absorption coefficient	2.144 mm^{-1}	
F(000)	2160	
Crystal size	0.267 x 0.178 x 0.064 mm^3	
Theta range for data collection.	1.587 to 27.500°	
Index ranges	$-18\leq h\leq 18$, $-22\leq k\leq 22$, $-29\leq l\leq 29$	
Reflections collected	126389	
Independent reflections	12808 [R(int) = 0.0624]	
Completeness to theta = 25.242°	100.00%	
Absorption correction	Analytical	
Max. and min. transmission	based on measured indexed crystal faces, Bruker SHELXTL v6.14 (Bruker 2008) and 0.7239	
Refinement method	Full-matrix least-squares on F^2	
Data / restraints / parameters	12808 / 30 / 570 [10167]	
Goodness-of-fit on F^2	0.984	
Final R indices [I>2sigma(I)]	R1 = 0.0284, wR2 = 0.0652	
R indices (all data)	R1 = 0.0404, wR2 = 0.0678	
Extinction coefficient	n/a	
Largest diff. peak and hole	1.366 and -0.502 $e.Å^{-3}$	

$R_1 = \Sigma(||F_o| - |F_c||) / \Sigma|F_o|$

$wR_2 = [\Sigma[w(F_o^2 - F_c^2)^2] / \Sigma[w(F_o^2)^2]]^{1/2}$

$S = [\Sigma[w(F_o^2 - F_c^2)^2] / (n - p)]^{1/2}$

$w= 1/[\sigma^2(F_o^2) + (m*p)^2 + n*p]$, $p = [\max(F_o^2,0) + 2* F_c^2]/3$, m & n are constants

X-ray crystallography for 5

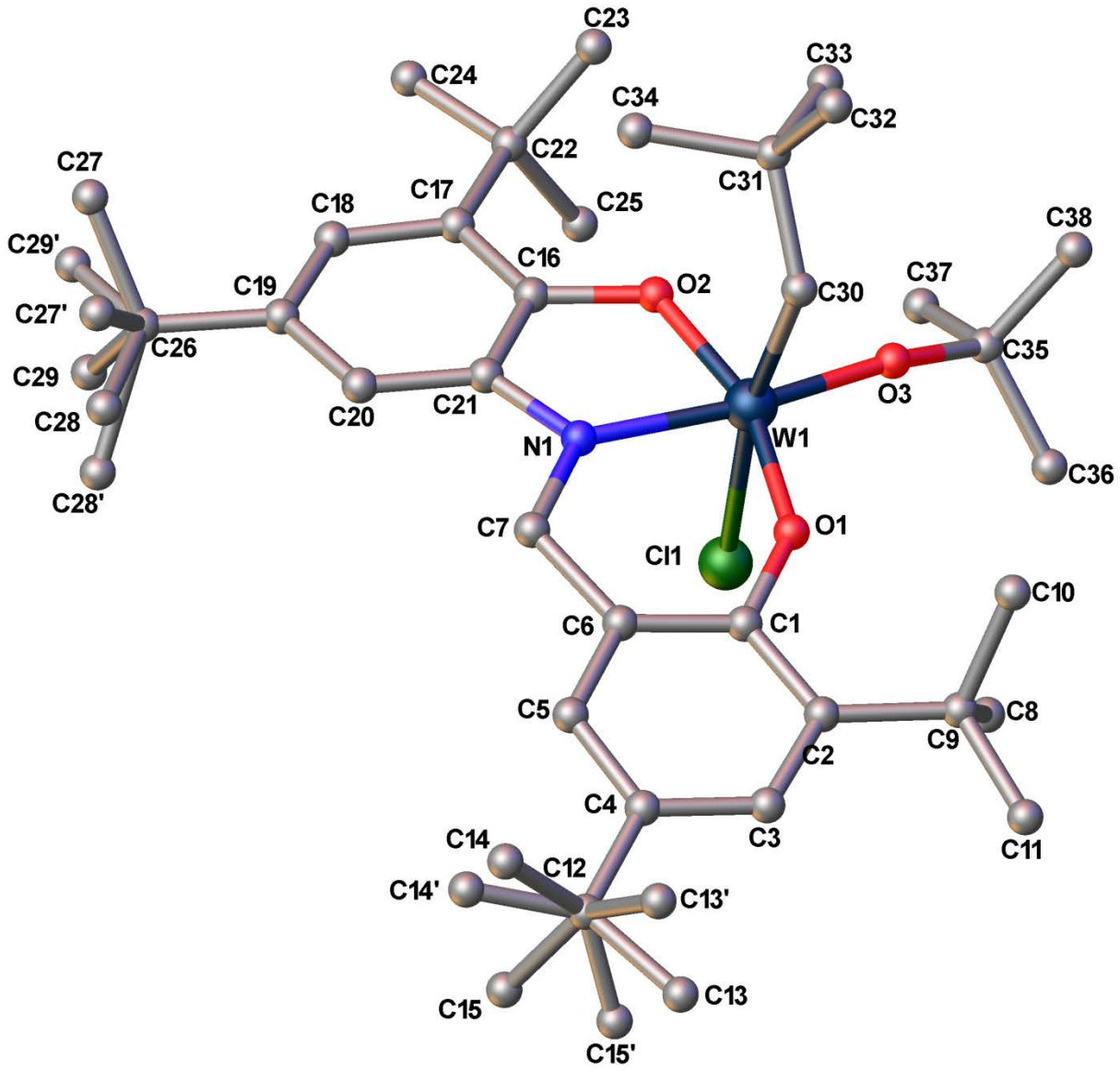

Figure S77. Molecular structure of **5** at 40% probability (all hydrogen atoms removed for clarity)

X-ray experimental: X-Ray Intensity data were collected at 100 K on a Bruker **DUO** diffractometer using Mo K_α radiation (λ = 0.71073 Å) and an APEXII CCD area detector. Raw data frames were read by program SAINT and integrated using 3D profiling algorithms. The resulting data were reduced to produce hkl reflections and their intensities and estimated

standard deviations. The data were corrected for Lorentz and polarization effects and numerical absorption corrections were applied based on indexed and measured faces. The structure was solved and refined in SHELXTL2013[20], using full-matrix least-squares refinement. The non-H atoms were refined with anisotropic thermal parameters and all of the H atoms were calculated in idealized positions and refined riding on their parent atoms. The two protons on C30 were obtained from a Difference Fourier and refined freely. The structure has two disordered regions in two sets of methyl groups on C12 and C26 which were refined in two parts with their site occupation factors dependently refined. In the final cycle of refinement, 8954 reflections (of which 8263 are observed with $I > 2\sigma(I)$) were used to refine 413 parameters and the resulting R_1, wR_2 and S (goodness of fit) were 2.66%, 6.22% and 1.128, respectively. The refinement was carried out by minimizing the wR_2 function using F^2 rather than F values. R_1 is calculated to provide a reference to the conventional R value but its function is not minimized.

Table S3. Crystal data and structure refinement for **5**

Identification code	sud12	
Empirical formula	$C_{38}H_{62}ClNO_3W$	
Formula weight	800.18	
Temperature	100(2) K	
Wavelength	0.71073 Å	
Crystal system	Monoclinic	
Space group	C 2/c	
Unit cell dimensions	a = 26.8944(19) Å	α = 90°
	b = 14.716(1) Å	β = 101.8459(13)°
	c = 20.1230(14) Å	γ = 90°
Volume	7794.6(9) $Å^3$	
Z	8	
Density (calculated)	1.364 Mg/m^3	
Absorption coefficient	3.066 mm^{-1}	
F(000)	3296	
Crystal size	0.227 x 0.127 x 0.043 mm^3	
Theta range for data collection.	1.547 to 27.495°	
Index ranges	$-34\leq h\leq 34$, $-19\leq k\leq 19$, $-25\leq l\leq 26$	
Reflections collected	91255	
Independent reflections	8954 [R(int) = 0.0318]	
Completeness to theta = 25.242°	100.00%	
Absorption correction	Analytical	
Max. and min. transmission	0.8882 and 0.5561	
Refinement method	Full-matrix least-squares on F^2	
Data / restraints / parameters	8954 / 0 / 413	
Goodness-of-fit on F^2	1.128	
Final R indices [I>2sigma(I)]	R_1 = 0.0266, wR_2 = 0.0622 [8263]	
R indices (all data)	R_1 = 0.0297, wR_2 = 0.0632	
Extinction coefficient	n/a	
Largest diff. peak and hole	1.336 and - 0.932 $e.Å^{-3}$	

$R_1 = \Sigma(||F_o| - |F_c||) / \Sigma|F_o|$

$wR_2 = [\Sigma[w(F_o^2 - F_c^2)^2] / \Sigma[w(F_o^2)^2]]^{1/2}$

$S = [\Sigma[w(F_o^2 - F_c^2)^2] / (n - p)]^{1/2}$

$w= 1/[\sigma^2(F_o^2) + (m*p)^2 + n*p]$, $p = [\max(F_o^2,0) + 2* F_c^2]/3$, m & n are constants

DFT Geometry optimization of 4a

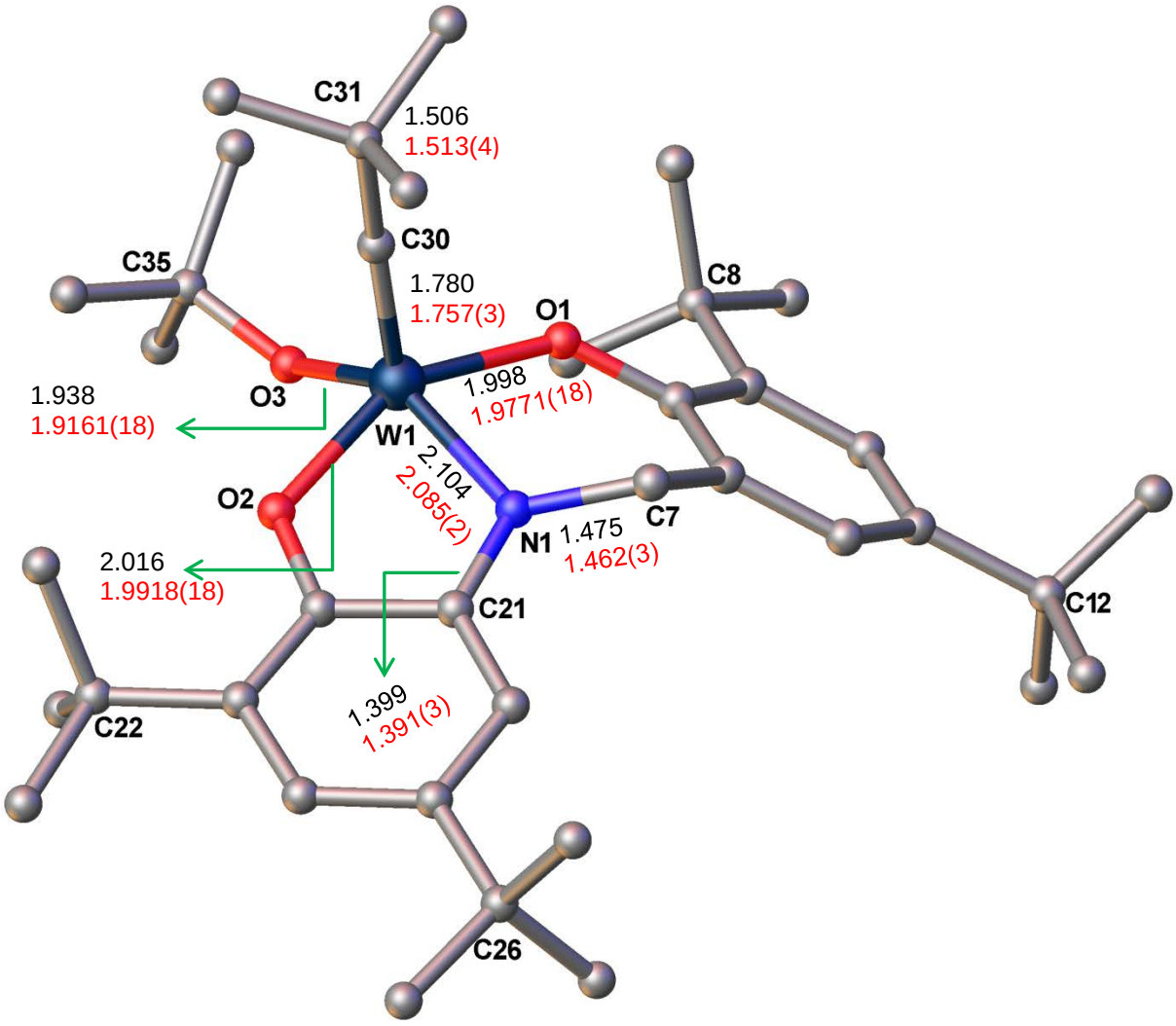

Figure S78. Geometry optimized structure of $\{[ON^{CH2}O]W{\equiv}C^{t}Bu(O^{t}Bu)\}^{1-}$ (**4a**) using B3LYP / LANL2DZ level theory. Values in BLACK represent computed bond lengths; values in RED correspond to experimentally observed bond lengths.

Table 1. Atomic coordinates for the geometry optimized structure of **4a**

Atom	X	Y	Z
W	0.2637680000	-1.2908740000	0.1583170000
O	-1.7066910000	-1.0002890000	0.3124360000
O	2.0761430000	-0.6854840000	-0.4845240000
O	0.1923370000	-2.6414500000	-1.2302340000
N	0.3142850000	0.7796120000	0.5283510000
C	-2.5547220000	0.0640990000	0.1839430000

C	-3.8623820000	-0.0945540000	-0.3718420000
C	-4.6740130010	1.0553070000	-0.4458640000
C	-4.2656340010	2.3364960000	-0.0055070000
C	-2.9742690000	2.4430320000	0.5470850000
C	-2.1248900000	1.3295370000	0.6532580000
C	-0.7525990000	1.4415040000	1.3027300000
C	-4.3568110010	-1.4745420000	-0.8668580000
C	-5.8135090010	-1.4258180000	-1.3996250000
C	-4.3171930010	-2.4984600000	0.3066810000
C	-3.4458400000	-1.9746610000	-2.0272010000
C	-5.2258480010	3.5413960000	-0.1484730000
C	-5.5880300010	3.7513810000	-1.6490230000
C	-4.6014630010	4.8586460010	0.3780140000
C	-6.5330320010	3.2758200000	0.6560030000
C	2.4833900000	0.6240570000	-0.3650490000
C	3.7415820000	1.1074020000	-0.7671490000
C	3.9862860000	2.4973690000	-0.5925730000
C	3.0302920000	3.3716710000	-0.0386460000
C	1.7757380000	2.8469430000	0.3620580000
C	1.4845100000	1.4760950000	0.2058090000
C	4.7924170010	0.1502030000	-1.3746360000
C	6.1150060010	0.8720140000	-1.7394330000
C	5.1236970010	-0.9742600000	-0.3490170000
C	4.2206120010	-0.4934100000	-2.6730100000
C	3.3013720000	4.8862650010	0.1482310000
C	2.2481830000	5.7143490010	-0.6470090000
C	4.7064750010	5.3106020010	-0.3505600000
C	3.2011870000	5.2577570010	1.6578720000
C	0.6114110000	-2.0988790000	1.7055760000
C	0.9865020000	-2.6038360000	3.0736550000
C	-0.2751410000	-3.1751640000	3.7861260000
C	1.5651540000	-1.4313560000	3.9211970000
C	2.0632590000	-3.7224340000	2.9590840000
C	0.4398900000	-4.0516090000	-1.5063030000
C	0.0509070000	-4.2769560010	-2.9829480000
C	-0.4306180000	-4.9112920010	-0.5635840000
C	1.9422440000	-4.3377070010	-1.2848360000
H	-5.6680740010	0.9520330000	-0.8692800000
H	-2.6048390000	3.4003620000	0.9056860000
H	-0.7963100000	0.9820330000	2.3070390000
H	-0.5301510000	2.5036360000	1.4562560000

H	-6.5229650010	-1.1015130000	-0.6257800000
H	-6.1102670010	-2.4327580000	-1.7240000000
H	-5.9124130010	-0.7552020000	-2.2643570000
H	-4.9974590010	-2.1876540000	1.1126380000
H	-3.3063490000	-2.5729250000	0.7147910000
H	-4.6332140010	-3.4917070000	-0.0464240000
H	-2.4069700000	-2.0722510000	-1.7033730000
H	-3.4808730000	-1.2737490000	-2.8733260000
H	-3.7940140000	-2.9570020000	-2.3822790000
H	-6.0708510010	2.8622190000	-2.0722580000
H	-6.2763180010	4.6018250010	-1.7678130000
H	-4.6839330010	3.9512600000	-2.2386370000
H	-4.3494080010	4.7874600010	1.4442130000
H	-3.6880230000	5.1192880010	-0.1720120000
H	-5.3161230010	5.6846290010	0.2551370000
H	-7.0381910010	2.3664380000	0.3087130000
H	-6.3088360010	3.1459000000	1.7229820000
H	-7.2337760010	4.1174370000	0.5478260000
H	4.9461960010	2.8918650000	-0.8993850000
H	1.0271680000	3.5126990000	0.7826800000
H	5.9566020010	1.6576540000	-2.4907570000
H	6.8229390010	0.1429860000	-2.1586290000
H	6.5851480010	1.3290540000	-0.8579690000
H	4.2121650010	-1.5126440000	-0.0744710000
H	5.5648130010	-0.5468920000	0.5625190000
H	5.8434380010	-1.6872700000	-0.7803420000
H	3.2906730000	-1.0259330000	-2.4535700000
H	4.9461150010	-1.2025170000	-3.1013320000
H	4.0081610000	0.2795370000	-3.4251530000
H	1.2279380000	5.4910290010	-0.3135010000
H	2.4221420000	6.7935390010	-0.5162600000
H	2.3049950000	5.4794910010	-1.7180100000
H	4.8443150010	6.3902030010	-0.1942800000
H	5.5030630010	4.7863480010	0.1932750000
H	4.8315980010	5.1050630010	-1.4216430000
H	3.3735070000	6.3348100010	1.8069660000
H	2.2134140000	5.0100240010	2.0637440000
H	3.9477460000	4.7013870010	2.2398490000
H	-0.0264620000	-3.5310570000	4.7989120010
H	-1.0505660000	-2.4031550000	3.8654430000
H	-0.6942900000	-4.0127730000	3.2137900000

H	2.4419110000	-0.9978450000	3.4249820000
H	0.8174920000	-0.6361490000	4.0336570000
H	1.8608100000	-1.7803090000	4.9239460010
H	2.9575330000	-3.3390800000	2.4519090000
H	2.3549610000	-4.0887010000	3.9562740000
H	1.6794470000	-4.5702730010	2.3767830000
H	0.1965920000	-5.3266230010	-3.2772700000
H	-1.0011240000	-4.0076070000	-3.1357150000
H	0.6646810000	-3.6377550000	-3.6292160000
H	-0.2253420000	-5.9826040010	-0.7025650000
H	-0.2197880000	-4.6351900010	0.4759410000
H	-1.4948290000	-4.7262060010	-0.7559580000
H	2.1840670000	-5.3815760010	-1.5330340000
H	2.5455680000	-3.6715860000	-1.9127330000
H	2.2087210000	-4.1485450000	-0.2390320000

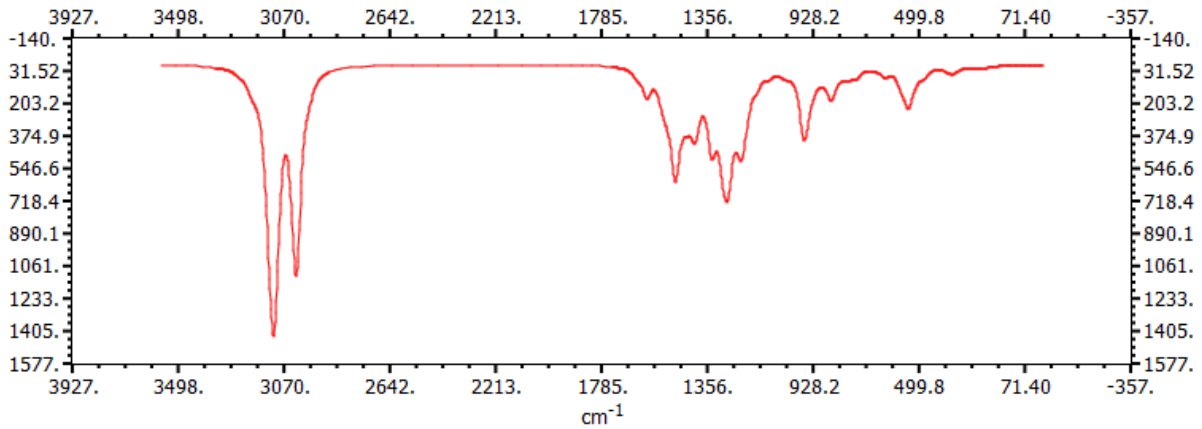

Figure S79. IR spectrum for the geometry optimized structure of **4a** (B3LYP / LANL2DZ level of theory)

References

1. M. L. Listemann and R. R. Schrock, *Organometallics*, 1985, **4**, 74-83.
2. F. Dulong, O. Bathily, P. Thuery, M. Ephritikhine and T. Cantat, *Dalton Transactions*, 2012, **41**, 11980-11983.
3. T. M. Khomenko, O. V. Salomatina, S. Y. Kurbakova, I. V. Il'ina, K. P. Volcho, N. I. Komarova, D. V. Korchagina, N. F. Salakhutdinov and A. G. Tolstikov, *Russian Journal of Organic Chemistry*, 2006, **42**, 1653-1661.

4. V. I. Lodyato, I. L. Yurkova, V. L. Sorokina, O. I. Shadyro, V. I. Dolgopalets and M. A. Kisel, *Bioorganic & Medicinal Chemistry Letters*, 2003, **13**, 1179-1182.
5. J. Vinsova, K. Cermakova, A. Tomeckova, M. Ceckova, J. Jampilek, P. Cermak, J. Kunes, M. Dolezal and F. Staud, *Bioorganic & Medicinal Chemistry*, 2006, **14**, 5850-5865.
6. N. U. Hofslokken and L. Skattebol, *Acta Chemica Scandinavica*, 1999, **53**, 258-262.
7. J. F. Larrow and E. N. Jacobsen, *Organic Syntheses, Vol 75*, 1998, **75**, 1-11.
8. G. F. Moore, J. D. Megiatto, Jr., M. Hambourger, M. Gervaldo, G. Kodis, T. A. Moore, D. Gust and A. L. Moore, *Photochemical & Photobiological Sciences*, 2012, **11**, 1018-1025.
9. A. Abreu, S. J. Alas, H. I. Beltran, R. Santillan and N. Farfan, *Journal of Organometallic Chemistry*, 2006, **691**, 337-348.
10. V. V. Lukov, A. A. Knysh, S. N. Lyubchenko, Y. P. Tupolova and V. A. Kogan, *Russian Journal of Coordination Chemistry*, 2002, **28**, 874-876.
11. T. Tanaka, S. Ikegami, M. Koyama and M. Koga, *Bulletin of the Chemical Society of Japan*, 1972, **45**, 630-+.
12. S. Y. S. Wang, J. M. Boncella and K. A. Abboud, *Acta Crystallographica Section C-Crystal Structure Communications*, 1997, **53**, 436-438.
13. T. Xu, J. Liu, G.-P. Wu and X.-B. Lu, *Inorganic Chemistry*, 2011, **50**, 10884-10892.
14. H. J. Bestmann, W. Stransky and O. Vostrowsky, *Chemische Berichte-Recueil*, 1976, **109**, 1694-1700.
15. A. D. Becke, *Journal of Chemical Physics*, 1993, **98**, 5648-5652.
16. C. T. Lee, W. T. Yang and R. G. Parr, *Physical Review B*, 1988, **37**, 785-789.
17. P. J. Hay and W. R. Wadt, *Journal of Chemical Physics*, 1985, **82**, 270-283.
18. M. J. Frisch, G. W. Trucks, H. B. Schlegel, G. E. Scuseria, M. A. Robb, J. R. Cheeseman, G. Scalmani, V. Barone, B. Mennucci, G. A. Petersson, H. Nakatsuji, M. Caricato, X. Li, H. P. Hratchian, A. F. Izmaylov, J. Bloino, G. Zheng, J. L. Sonnenberg, M. Hada, M. Ehara, K. Toyota, R. Fukuda, J. Hasegawa, M. Ishida, T. Nakajima, Y. Honda, O. Kitao, H. Nakai, T. Vreven, J. A. Montgomery Jr., J. E. Peralta, F. Ogliaro, M. J. Bearpark, J. Heyd, E. N. Brothers, K. N. Kudin, V. N. Staroverov, R. Kobayashi, J. Normand, K. Raghavachari, A. P. Rendell, J. C. Burant, S. S. Iyengar, J. Tomasi, M. Cossi, N. Rega, N. J. Millam, M. Klene, J. E. Knox, J. B. Cross, V. Bakken, C. Adamo, J. Jaramillo, R. Gomperts, R. E. Stratmann, O. Yazyev, A. J. Austin, R. Cammi, C. Pomelli, J. W. Ochterski, R. L. Martin, K. Morokuma, V. G. Zakrzewski, G. A. Voth, P. Salvador, J. J. Dannenberg, S. Dapprich, A. D. Daniels, Ö. Farkas, J. B. Foresman, J. V. Ortiz, J. Cioslowski and D. J. Fox, *Journal*, 2009.
19. A.-R. Allouche, *Journal of Computational Chemistry*, 2011, **32**, 174-182.
20. G. M. Sheldrick, *Acta Crystallographica Section A*, 2008, **64**, 112-122.
21. P. van der Sluis and A. L. Spek, *Acta Crystallographica Section A*, 1990, **46**, 194-201.
22. A. Spek, *Journal of Applied Crystallography*, 2003, **36**, 7-13.
23. A. Spek, *Acta Crystallographica Section D*, 2009, **65**, 148-155.